university of groningen / faculty of science and engineering

Optimizing the bidding strategy of agents owning a battery in the day-ahead energy market under price uncertainty

Research Project

Msc. Industrial Engineering & Management

Author:
Wendy van den Berg
S3801780

First supervisor:
Prof. N. Monshizadeh

Second supervisor:
Dr. A.K Cherukuri

1 Abstract

The deregulation of electricity markets has led to an increased demand for optimizing market bidding strategies. Consequently, this research focuses on the optimization of bidding strategies for an agent owning a Battery Energy Storage System (BESS), participating in the day-ahead Local Electricity Market (LEM). It investigates both stochastic and robust optimization domains to navigate the uncertainty inherent in LEM day-ahead prices. Consequently, this research develops two stochastic optimization (SO) models and one robust optimization (RO) model aimed at maximizing the agent's bidding schedule's profitability.

Scenario-based modeling is employed within the framework of stochastic optimization to generate a set of scenarios forecasting the day-ahead LEM prices. On the other hand, the robust optimization model uses a polyhedral box interval uncertainty set to represent the stochastic day-ahead LEM prices. In this research, SO model 1 serves as a benchmark, allowing for the submission of a single price-quantity point per time step, while the RO model also permits a single price-quantity point submission per time step. Conversely, SO model 2 enables the submission of multiple price-quantity points per time step, resulting in the construction of a monotonic bidding curve for both demand and supply bids. Furthermore, risk management is integrated into all models. Robust optimization adjusts the size of the uncertainty set using the budget of uncertainty, thereby adapting the risk attitude of the agent. In the stochastic optimization models, risk management is implemented through the utilization of the Conditional Value at Risk (CVaR) risk measure.

Evaluation of the developed models is conducted through a series of case studies, evaluating the pre-clearance and post-clearance performance metrics. SO model 2 outperforms SO model 1 and the RO model in terms of expected profit, for all risk attitudes of the agent. However, for all models, a tradeoff arises between expected profit and risk aversion. Moreover, SO model 2 exhibits superior post-clearance performance metrics, particularly in terms of bid clearance percentages, indicating its effectiveness in the LEM day-ahead market. Overall, this research contributes to the existing knowledge base of developing optimal bidding strategies for an agent in the (local) day-ahead market, while incorporating the risk attitude of the agent. Moreover, the incorporation of post-clearance performance evaluation in addition to pre-clearance performance assessment represents a novel approach utilized in this research.

This research was made possible with the support of the Dutch Topsector Energy-subsidy of the Ministry of Economic Affairs and Climate.

Contents

1 Abstract **2**

2 List of Abbreviations **6**

3 Introduction **7**
3.1 Contribution and research organization . . . 8

4 Scenario-based modeling of price uncertainty **9**
4.1 Point forecast model . . . 10
4.1.1 ARMA model . . . 10
4.1.2 ARIMA model . . . 12
4.1.3 SARIMA model . . . 12
4.1.4 ARIMAX model . . . 13
4.1.5 SARIMAX model . . . 13
4.1.6 Box-Jenkins approach . . . 14
4.2 Residual analysis . . . 15
4.3 Scenario generation . . . 15
4.4 Scenario reduction . . . 16

5 Risk management in stochastic optimization **20**
5.1 CVaR derivation . . . 20
5.2 CVaR optimization problem . . . 21

6 Robust modeling of price uncertainty **23**
6.1 Uncertainty set modeling . . . 24
6.2 Uncertainty set construction via risk measures . . . 27
6.2.1 Risk measures . . . 27
6.2.2 Coherent risk measures . . . 28
6.2.3 Comonotonic risk measures . . . 29
6.2.4 Conditional Value at Risk . . . 30

7 Stochastic optimization applied to battery asset modeling **32**
7.1 Model 1: single bid (base model) . . . 32
7.2 Model 1 with risk management . . . 33
7.2.1 SO Model 1 with battery charging risk . . . 34
7.2.2 SO model 1 with battery discharging risk . . . 36
7.2.3 SO model 1 with battery discharging and charging risk . . . 37
7.3 Model 2: multiple bids . . . 38
7.3.1 Battery constraints . . . 38
7.3.2 Monotonicity constraints of bidding curves . . . 39
7.3.3 Non-anticipativity constraints . . . 40
7.3.4 Active price-quantity point constraints . . . 41
7.3.5 State of charge constraint of active price-quantity points . . . 41
7.3.6 SO model 2 mathematical overview . . . 42
7.4 Model 2 with risk management . . . 43
7.4.1 SO model 2 with battery charging risk . . . 43
7.4.2 SO model 2 with battery discharging risk . . . 45
7.4.3 SO model 2 with battery discharging and charging risk . . . 46

8 Robust optimization applied to battery asset modeling **47**
8.1 Charging state of BESS . . . 48
8.2 Discharging state of BESS . . . 48
8.3 Simultaneous charging and discharging state of battery . . . 49

8.3.1 Case: identical budget of uncertainties . . . 50

9 Numerical investigations of the models **52**
9.1 Price scenarios for stochastic optimization . . . 52
9.1.1 Point forecast . . . 52
9.1.2 Scenario generation . . . 53
9.1.3 Scenario reduction . . . 53
9.2 Simulations LEM price forecast . . . 53
9.3 Uncertainty set for robust optimization . . . 53
9.4 Model overview . . . 54
9.5 Case studies . . . 54
9.5.1 Data specifications . . . 54
9.5.2 Performance metrics . . . 55

10 Numerical results **57**
10.1 Price scenarios . . . 57
10.1.1 SARIMA model Example 1 . . . 57
10.1.2 SARIMA$(1,0,1)(1,0,1)_{24}$ model . . . 58
10.2 Simulations LEM price forecast . . . 60
10.3 Case study 1: SO model 1 . . . 61
10.3.1 Analysis case study 1 . . . 64
10.4 Case study 2: SO model 2 . . . 65
10.4.1 Analysis case study 2 . . . 68
10.5 Case study 3: Comparing SO models 1 and 2 . . . 70
10.6 Case study 4: Comparing SO model 1 and RO model . . . 72
10.6.1 RO model results . . . 72
10.6.2 Analysis case study 4 . . . 75

11 Discussion **77**
11.1 Main findings . . . 78
11.2 Future research . . . 79

12 Conclusion **82**

13 Appendix **84**
13.1 Appendix A: Proposed market clearing mechanism . . . 84
13.1.1 Short local market (local demand > local supply) . . . 86
13.1.2 Long local market (local supply > local demand) . . . 87
13.2 Appendix B.1: Example 1 scenarios . . . 89
13.3 Appendix B.2: Example 2 scenarios . . . 90
13.4 Appendix B.3: Example 3 scenarios . . . 91
13.5 Appendix C: Example 3 ACF plot . . . 92
13.6 Appendix D.1: Pre- and post-clearance performance Examples 1, 2, 3, case study 1 92
13.7 Appendix D.2: Pre- and post-clearance performance simulation 1 - 10, case study 1, 4 scenarios . . . 94
13.8 Appendix D.3: Pre- and post-clearance performance simulation 1 - 10, case study 1, 10 scenarios . . . 94
13.9 Appendix E.1: Pre- and post-clearance performance Examples 1, 2, 3, case study 2 95
13.10 Appendix E.2: Pre- and post-clearance performance simulation 1 - 10, case study 2, 4 scenarios . . . 96
13.11 Appendix E.3: Pre- and post-clearance performance simulation 1 - 10, case study 2, 10 scenarios . . . 96
13.12 Appendix F.1: pre- and post-clearance performance Examples 1, 2, 3, case study 4 97

13.13Appendix F.2: pre- and post-clearance performance of simulations 1 - 10, case study 4, 4 scenarios 99
13.14Appendix F.3: pre- and post-clearance performance of simulations 1 - 10, case study 4, 10 scenarios 99

References **100**

2 List of Abbreviations

ACF	Autocorrelation Function
AIC	Akaike Information Criterion
BESS	Battery Energy Storage System
BIC	Bayesian Information Criterion
CVaR	Conditional Value at Risk
GARCH	Generalized Auto-regressive Conditional Heteroskedasticity
LEM	Local Electricity Market
MAPE	Mean Absolute Percentage Error
PACF	Partial Autocorrelation Function
RO	Robust Optimization
(S)AR(I)MA(X)	(Seasonal) Auto-regressive (Integrated) Moving Average with Exogenous variable
SO	Stochastic Optimization
SOC	State of Charge
VaR	Value at Risk
WSM	Wholesale Market

3 Introduction

The energy market is changing rapidly, due to the increase in distributed renewable energy generation [14, 61, 101]. The aforementioned energy consumers in the energy network have become prosumer agents, due to their increasing participation in supplying renewable energy to the grid [14, 67]. Hence, decentralized agents enter the energy market, requiring large adaptations in current electricity market designs [14, 38]. Local Electricity Markets (LEMs) are distributed electricity markets on a communal level, intending to maximize the community's self-sufficiency and reduce the interaction with the wholesale market [101]. The design of LEMs enables managing production uncertainty on a local scale [38]. Due to the unpredictable behavior of wind- and solar power generation, uncertainty arises in the operation and planning of power systems [89]. As a result, Battery Energy Storage Systems (BESS) have been proposed as a sustainable solution in LEMs, to counteract the uncertainty in distributed power generation [89] and to be independent of the main grid [67].

This research focuses on maximizing the profit of an agent owning a BESS asset, participating and bidding in the LEM day-ahead market [61]. Nonetheless, it should be noted that the bidding models developed in this research are generally applicable to other energy markets, besides the LEM day-ahead market. Other markets such as the real-time market [23] are out of the scope of this research. In a day-ahead market, energy is traded on an hourly basis, for the next day (next 24 hours) [101, 92]. Similar to [59, 80], the agent owning the BESS asset acts as a price-taker in the LEM day-ahead market, since the capacity of a battery in the current market cannot dominate the price by itself [80]. Similar to other market designs, the LEM day-ahead market participants exchange energy according to a market clearing mechanism [101], specified in Appendix A.

The BESS asset has the function to both supply and consume electricity, but not at the same time [72]. The goal of the agent is formulated as maximizing the revenue from discharging the battery, meaning that the agent becomes a supplier in the LEM. At the same time, the agent's goal is to minimize the cost attached to charging the battery, meaning that the battery acts as a consumer in the LEM [72]. The agent can exploit the energy arbitrage of the LEM, by charging the battery when the LEM price is low, and discharging the battery when the LEM price is high [59]. Hence, the bidding models developed in this research aim to create the most profitable schedule for supply (discharging) and demand (charging) bids of the BESS asset bidding in the LEM. Throughout this research, supply and discharging bids are used interchangeably, similar to demand and charging bids.

Due to the presence of uncertainty in electricity markets [23], amongst others focused on market prices and power production [66], constructing a profitable bidding schedule for an agent participating in the day-ahead market is challenging. As mentioned above, the agent needs to submit its bids for the entire day-ahead horizon. In this research, the high volatility of (local) electricity market prices [54] is considered the only factor that contributes to the uncertainty in the bidding optimization. The other uncertainties present in the LEM day-ahead market are out of the scope of this research. According to [75, 42, 106], acquiring a good forecast of day-ahead LEM prices contributes to developing a bidding strategy. In addition, incorporating risk management enables the agent to cope with profit volatility caused by (price) uncertainty [25, 20, 86, 23]. Hence, due to the uncertainty present in bidding optimization models, risk management is incorporated in this research [108].

Robust optimization (RO) and stochastic optimization (SO) are two widely used modeling domains to cope with stochasticity in prices [111, 99, 109, 15, 62, 108]. In the application of maximizing the profit of an agent owning a BESS, participating in a day-ahead market, [59, 105] use stochastic programming to maximize the profit of a BESS asset in the day-ahead and real-time market. However, both papers exclude risk management. In [72], SO is used to create a battery arbitrage model that maximizes profit. However, the paper excludes energy price forecasting and risk management. [110] focuses on stochastic optimization of a BESS incorporating risk-aversiveness of the agent. In [25], an optimal bidding strategy is developed for a wind power producer,

incorporating risk management and multiple uncertainties. [102] develops both stochastic and robust optimization models to maximize the revenue of wind-storage systems while minimizing the penalty costs caused by power imbalance. The uncertainty is caused by stochastic wind power production. All papers above focus on single price-quantity point submission per time step. When targeting literature that focuses on allowing the submission of multiple price-quantity points per time step, [50] constructs the bidding schedule of an agent owning multiple assets, amongst others a BESS. However, [50] excludes risk management. Literature is limited in the application of allowing multiple price-quantity points per time steps, in the application of a BESS asset participating in the day-ahead market. For robust optimization, [5] considers a robust self-scheduling optimization model to incorporate price and production stochasticity for a wind power producer owning energy storage. In [54], robust optimization is considered to cope with stochastic prices in multiple markets. The goal of [54] is to maximize the performance of a BESS asset, incorporating risk management.

3.1 Contribution and research organization

The contribution of this research flows out of the state-of-the-art literature on agents participating in the (LEM) day-ahead market. Namely, this research focuses on the development of two stochastic optimization bidding models and one robust optimization bidding model, accounting for LEM price uncertainty [108, 111, 99, 109, 15, 62]. These developed models focus on the participation of a single agent in the LEM day-ahead market, owning a BESS asset. For the stochastic optimization bidding models, scenario-based modeling is employed to obtain a representable set of scenarios. For the robust optimization model, the uncertainty is represented by an uncertainty set. Consequently, real-life data is used to forecast the uncertain day-ahead LEM prices, enabling the development of scenarios for stochastic optimization and generating input for the robust optimization model. The first stochastic optimization model allows for a single price-quantity point submission and acts as a benchmark for this research. The robust optimization model also allows single price-quantity bid submission per time step. However, the second stochastic optimization model allows for the submission of multiple price-quantity points per time step, constructing bidding curves for both selling and buying electricity. This model is an extension of [50], where the focus of this research lies on modeling the BESS asset in the day-ahead market. Then, the two stochastic optimization models are extended to incorporate risk management via the CVaR risk measure [108]. The robust optimization model incorporates risk management via the budget of uncertainty [111, 10]. Lastly, performance is compared between the two stochastic optimization models as well as the performance of the first stochastic optimization model with the robust optimization model.

This research starts by providing the *theoretical background* for both stochastic and robust optimization modeling, addressing the challenge of incorporating uncertainty in LEM prices. First, the theoretical outline is provided for uncertain price modeling, focusing on *scenario generation* in stochastic optimization (Scenario-based modeling of price uncertainty). These scenarios are used to capture the day-ahead LEM price variability in stochastic programming. Then, the theory behind *risk management* modeling in stochastic optimization is outlined in Risk management in stochastic optimization. Shifting the focus to robust optimization, the theoretical framework of constructing a general robust problem with the use of an *uncertainty set* is provided in Robust modeling of price uncertainty. Here, the uncertainty set is used to model the price uncertainty of the LEM day-ahead prices. Next, the theoretical background provided in the first three chapters is used to construct the bidding models of the battery asset, targeting both stochastic and robust optimization. In other words, the provided theory is applied to model the battery asset. First, Stochastic optimization applied to battery asset modeling outlines the two developed stochastic optimization models. This chapter immediately incorporates risk management for both models, by implementing the Conditional Value at Risk. Afterward, Robust optimization applied to battery asset modeling constructs the robust optimization model applied to the battery asset, also accounting for the risk attitude of the agent. Once all bidding models including risk management are introduced, the Numerical investigations of the models outline the specifications of the case studies, followed by the Numerical results. Lastly, the Discussion and Conclusion are provided.

4 Scenario-based modeling of price uncertainty

In this chapter, the theoretical framework of scenario-based modeling in the domain of stochastic optimization is elaborated. The goal of this chapter is to provide an outline of how to obtain a representable set of scenarios to forecast the day-ahead LEM prices. This set of scenarios can be used as input in a stochastic program. This chapter elaborates on existing theories.

Stochastic optimization is a modeling domain to model price uncertainty, which works well under the condition that the probability distribution of the uncertainty is *explicitly* modeled. This introduces the need to attain the probability distribution of the underlying random variable(s) to use as an input for stochastic programming [111, 9, 15, 88, 63].

Within the domain of stochastic optimization, scenario-based modeling is widely adopted in the day-ahead electricity market decision-making to deal with the uncertainty [65, 111, 99, 15, 73]. (Local) Market prices are typically represented by continuous probability distributions, which are complex to attain [111]. As an alternative, scenarios can be created, which represent a discretization of the distribution of the uncertain parameters [53]. Scenarios approximate the true distribution of the uncertainty present, where each scenario stands for a possible realization of the underlying uncertain local market price [64, 99, 85]. Figure 1 represents a visualization of discrete scenarios to approximate the probability distribution [111, 99, 15, 63, 96].

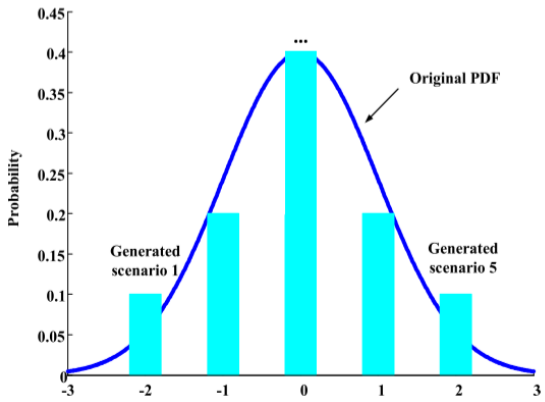

Figure 1: *Scenario discretization of a continuous Probability Density Function [63]*

Suppose the uncertain parameter vector $\mathbf{c}$ represents the local market price. Then, a scenario is represented as $\mathbf{c}_\omega$, where ω represents a scenario. This scenario has occurrence probability π_ω [96]. Lastly, since each scenario represents a possible realization of the uncertainty, it holds that $\sum_\omega \pi_\omega = 1$ [99].

The papers of [59] and [110] both successfully use stochastic programming to incorporate price uncertainty in energy storage decision-making in the electricity market. Both papers include acquiring scenarios via scenario-based modeling to address the stochastic nature of electricity market prices, and aim to derive a discrete probability distribution of the uncertain electricity market price. Overall, scenario generation techniques are successfully used in literature to create accurate forecasts [111, 68, 44, 63].

The goal of scenario-based modeling is to obtain a set of scenarios together with their scenario probabilities. Then, these scenarios are integrated into the scheduling (bidding) optimization problem that maximizes profit for the agent with the battery asset. The local market price determines the expected revenue and costs for the agent with the battery asset by multiplying the forecasted local market price with the (dis)charging bid quantities [72]. The local electricity market price is represented in the form: $\sum_{\omega \in \Omega} \pi_\omega \; c_\omega$. Here, the uncertain market price realization of scenario ω is represented via a discrete scenario price (c_ω) and its corresponding probability (π_ω) [63, 110, 59, 111, 105, 23, 25, 19].

In stochastic programming, a large number of scenarios is generated to create an accurate approximation of the probability distribution [99]. However, the computational requirements grow with the number of scenarios created [99], meaning that a trade-off arises between the accuracy of the forecast and computational performance [111]. To deal with the large numbers of scenarios, scenario reduction techniques are used that select a subset of the scenarios and determine corresponding optimal probabilities [111, 65, 46, 30, 15]. The theoretical framework for obtaining a representable set of scenarios for the day-ahead LEM prices is divided into four stages, depicted in Figure 2 [59, 23]. The remaining of this chapter is divided to elaborate on these four stages.

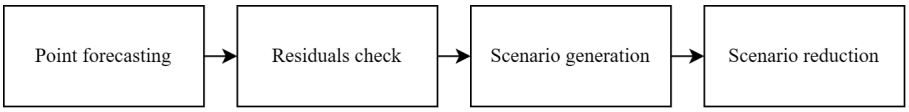

Figure 2: *Framework for price scenario generation via stochastic programming [59]*

4.1 Point forecast model

In this research, the day-ahead LEM price is stochastic, and hourly intervals need to be accurately predicted using a forecasting method [106]. In principle, different elements can be incorporated when forecasting the day-ahead LEM price. First, the local electricity price time series is considered as a base. According to [38], a correlation of the LEM with the WSM is present, meaning that additionally an accurate training and testing set of wholesale electricity prices could be incorporated in the point forecast model. Lastly, to incorporate the dependency of prices on weather conditions, temperature and cloud coverage could be taken into account in the LEM price forecast [91].

As a point forecast model, (Seasonal) Auto-regressive (Integrated) Moving Average model with Exogenous variables type models ((S)AR(I)MA(X)-type) are found to be suitable for predicting the mean local market price variable [48, 76, 6]. The AR(I)MA model types are popular and widely used price forecasting models [40, 84, 27, 48, 81, 82, 93, 21]. Namely, electricity prices exhibit strong auto-regressive behavior and seasonal patterns [60]. Incorporating seasonal patterns in the price forecast is enabled in the SARIMA-type model [23, 78]. Finally, the SARIMAX model is an extension of the (S)AR(I)MA-type models that incorporates an exogenous variable that correlates with the time series to be forecasted (e.g. local electricity price) [48, 56, 82]. Hence, when using the SARIMAX point forecast model, weather conditions and WSM price data can be incorporated to capture the correlation between the time series.

Throughout this section, the (S)AR(I)MA(X)-type model is elaborated to develop a sophisticated price forecast. The following sections build up from the ARMA point forecast model to the SARIMAX point forecast model, to forecast the LEM day-ahead market prices by including daily seasonality and wholesale market price data as exogenous variables. Incorporating weather conditions is out of the scope of this research.

4.1.1 ARMA model

The Auto-Regressive Moving Average model is a linear model that combines auto-regressive and moving average components to forecast data [71, 23, 96, 95, 48].

The auto-regressive term (AR) uses the lagged values of the uncertain variable to estimate the next value. On the other hand, the moving average term (MA) is concerned with modeling the error (residual) term by predicting the error terms based on the realization of previous error terms [27, 24]. Equation 4.1 illustrates the auto-regressive model and Equation 4.2 illustrates the moving average model. In these equations, Z_t represents the stochastic variable denoting the local market price.

$$Z_t = \psi_1 Z_{t-1} + \psi_2 Z_{t-2} + ... + \psi_p Z_{t-p} + \epsilon_t \tag{4.1}$$

$$Z_t = \epsilon_t + \varphi_1 \epsilon_{t-1} + \varphi_2 \epsilon_{t-2} + ... + \varphi_q \epsilon_{t-q} \tag{4.2}$$

The AR(p) model takes into account lagged values of the variable up to order p, while the MA(q) model considers lagged values of the error term up to order q. In Equation 4.1 and Equation 4.2, the sequence $\{\epsilon_t\}$ is considered to be white noise, meaning it consists of uncorrelated random variables with zero mean and variance σ^2 ($\{\epsilon_t\} \sim N(0, \sigma^2)$) [107, 82, 60, 97, 43].

The combination of the AR(p) and MA(q) models yields the hybrid ARMA(p,q) model, expressed as follows [96, 95, 23, 107]:

$$Z_t = \sum_{i=1}^{p} \psi_i Z_{t-i} + \epsilon_t - \sum_{j=1}^{q} \varphi_j \epsilon_{t-j} \tag{4.3}$$

In [48], the ARMA(p,q) model additionally includes a constant term C:

$$Z_t = C + \sum_{i=1}^{p} \psi_i Z_{t-i} + \epsilon_t - \sum_{j=1}^{q} \varphi_j \epsilon_{t-j} \tag{4.4}$$

The prediction error ϵ_t represents the gap between the predicted local market price generated by the ARMA(p,q) model and the actual observed local market price Z_t. To clarify ϵ_t in Equation 4.4, this equation can be decomposed into Equation 4.5 and Equation 4.6 to explicitly define ϵ_t. As mentioned above, in Equation 4.6, ϵ_t is considered white noise [107, 82, 60, 97, 43].

$$\hat{Z}_t = C + \sum_{i=1}^{p} \psi_i Z_{t-i} - \sum_{j=1}^{q} \varphi_j \epsilon_{t-j} \tag{4.5}$$

$$Z_t = \hat{Z}_t + \epsilon_t \tag{4.6}$$

Equation 4.4 is often rewritten with the use of a backshift operator/lag operator B, which is represented as $B^k Z_t = Z_{t-k}$ [48, 82]. The new, equivalent formulation of the ARMA model is represented in Equation 4.7:

$$\left(1 - \sum_{i=1}^{p} \psi_i B^i\right) Z_t = \left(1 + \sum_{j=1}^{q} \varphi_j B^j\right) \epsilon_t + C \tag{4.7}$$

In Equation 4.7, there are p auto-regressive parameters $\psi_1, \psi_2, ..., \psi_p$, and q moving average parameters $\varphi_1, \varphi_2, ..., \varphi_q$. If q equals zero, the ARMA model operates akin to an AR(p) model, and conversely, when p is zero, it functions akin to an MA(q) model [96]. The methodology of the AR(I)MA model is described by [16]. In the ARMA(p,q) model, the parameters p and q dictate the order of the auto-regressive (AR) and moving average (MA) terms, respectively [95]. Besides determining the orders p and q, it is necessary to estimate the coefficients ψ and φ associated with the AR and MA terms, as well as the standard deviation σ of the error term [95]. The methodology for obtaining these coefficients and orders is outlined in the Box-Jenkins approach, elaborated in Box-Jenkins approach section.

An important premise of the ARMA model is that the time series of the stochastic variable, denoted as Z_t, should exhibit stationarity [23]. Stationarity in a time series implies that each forecasted point originates from a consistent distribution with constant mean and variance. In other words, the mean and variance should remain consistent over time [23]. If this condition is not met, there exist two methods to achieve stationarity in the time series [23]:

1. **Box-Cox transformations**: This technique involves applying either the logarithm or the square root to the original time series. While it is a straightforward approach, it does not always ensure a stable mean and variance [23, 24, 43].

2. **Differencing**: This method involves computing the differences between consecutive observations (change series), resulting in what is known as the Auto-Regressive Integrated Moving Average (ARIMA) model [107, 23]. This extension of the ARMA model is further elaborated in the ARIMA model section.

4.1.2 ARIMA model

The ARIMA(p,d,q) model is an extension of the ARMA(p,q) model, where the d stands for the order of differentiation, referring to the integrated part of the model [48, 107]. This differencing term d is applied to the time series until the series becomes stationary [48]. Applying d differences corresponds with Equation 4.8 [48]:

$$Z_t^{(d)} = Z_t^{(d-1)} - Z_{t-1}^{(d-1)} \tag{4.8}$$

According to [23], typically a first-order differencing (d = 1) is adequate to achieve a stable mean. Using the backshift operator B, this differencing process of Z_t can be described as [107, 23, 48]:

$$\begin{aligned} Z_t^{(1)} &= Z_t - Z_{t-1} \\ \nabla^1 Z_t &= Z_t - Z_{t-1} \\ \nabla^1 Z_t &= (1 - B) Z_t \end{aligned} \tag{4.9}$$

The formal formulation of the ARIMA(p,d,q) model is represented in Equation 4.10. In the ARIMA model, the additional order parameter d should be estimated on top of the p and q orders of the AR and MA terms.

$$Z_t^{(d)} = C + \sum_{i=1}^{p} \psi_i Z_{t-i}^{(d)} + \sum_{j=1}^{q} \varphi_j \epsilon_{t-j} + \epsilon_t \tag{4.10}$$

Using the backshift operator, Equation 4.10 can be rewritten in Equation 4.11:

$$\left(1 - \sum_{i=1}^{p} \psi_i B^i\right) (1 - B)^d Z_t = \left(1 + \sum_{j=1}^{q} \varphi_j B^j\right) \epsilon_t + C \tag{4.11}$$

The ARIMA model in Equation 4.11 does not encompass seasonal patterns, despite their presence in electricity prices [107, 60]. Local electricity market prices often exhibit daily, weekly, and annual seasonal variations [23, 107, 6, 48, 70, 75, 24, 93, 106]. Therefore, to account for this seasonality, the Seasonal ARIMA (SARIMA) model is employed.

4.1.3 SARIMA model

The Seasonal ARIMA (SARIMA) model extends the capabilities of the ARIMA model to account for seasonal patterns inherent in the stochastic process Z_t [23, 78]. The SARIMA model type has been successfully applied to forecast electricity prices [78]. The SARIMA model is denoted as $SARIMA(p,d,q)(P,D,Q)_S$, where S indicates the order of seasonality [23]. The parameters P, D, and Q must be estimated to captue the auto-regressive, differencing, and moving average effects at a specified seasonal level [48, 78]. The general expression of $SARIMA(p,d,q)(P,D,Q)_S$ is provided in Equation 4.12 [48, 23].

$$\begin{aligned} &\left(1 - \sum_{i=1}^{p} \psi_i B^i\right) \left(1 - \sum_{j=1}^{P} \zeta_j B^{Sj}\right) (1 - B)^d (1 - B^S)^D Z_t = \\ &\qquad C + \left(1 + \sum_{i=1}^{q} \varphi_i B^i\right) \left(1 + \sum_{j=1}^{Q} \theta_j B^{Sj}\right) \epsilon_t \end{aligned} \tag{4.12}$$

In Equation 4.12, the coefficients ψ_i represent the non-seasonal auto-regressive components, ζ_j denote the coefficients for the seasonal auto-Regressive component, φ_i represent the non-seasonal moving average component, and lastly θ_j represents the seasonal Moving Average component [23].

Considering the presence of seasonal patterns in electricity prices, this research focuses on the *daily seasonality* that is present in the local market price time series. When observing hourly electricity price data, capturing the daily seasonality includes a term in Equation 4.12 with S equal to 24. This represents the daily periodicity of the local price time series, resulting in Equation 4.14. Typically, a seasonal difference term (D=1) is adequate for captuing seasonal variations [48]. Concrete examples of applying seasonality and differencing terms in electricity price forecasting for the day-ahead market are discussed in detail in [24].

$$\left(1-\sum_{i=1}^{p}\psi_i B^i\right)\left(1-\sum_{j=1}^{P}\zeta_j B^{24j}\right)(1-B)^d(1-B^{24})^D Z_t = C+\left(1+\sum_{i=1}^{q}\varphi_i B^i\right)\left(1+\sum_{j=1}^{Q}\theta_j B^{24j}\right)\epsilon_t \tag{4.13}$$

In Equation 4.14, the term $(1-B^{24})Z_t$ represents a day seasonal difference, which can be described as $Z_t - Z_{t-24}$. [48]. As concrete example, the SARIMA$(1,0,1)(1,0,1)_{24}$ can be formulated as:

$$(1-\psi_1 B)\left(1-\zeta_{24}B^{24}\right)Z_t = C+(1+\varphi_1 B)\left(1+\theta_{24}B^{24}\right)\epsilon_t \tag{4.14}$$

4.1.4 ARIMAX model

The Auto-regressive integrated moving average with exogenous variables model (ARIMAX) is an extension of ARIMA model that incorporates exogenous variables in the forecasting process [48, 56, 82]. These exogenous variables are additional time series that are known to co-vary with the local market price time series [107]. In this research, the exogenous variable that can be included in the price forecast is the wholesale market price. The prediction of the wholesale market price at time t (X_t) is assumed to be accurate and is utilized as an exogenous variable in the ARIMAX model to predict the local electricity market price. Historical data on the wholesale market price are publicly available. As an extension to Equation 4.11, ARIMAX is formulated in Equation 4.15:

$$Z_t^{(d)} = C+\sum_{i=0}^{h}\mu_i X_{t-i}+\sum_{i=1}^{p}\psi_i Z_{t-i}^{(d)}+\sum_{j=1}^{q}\varphi_j\epsilon_{t-j} \tag{4.15}$$

In the ARIMAX model, μ represents the coefficients associated with the exogenous variable, which, like, ψ and φ, must be estimated. Additionally, h denotes the order of the exogenous variable, indicating the number of historical values of the exogenous time series considered when forecasting the next value in the time series.

4.1.5 SARIMAX model

Lastly, combining section ARIMAX model with the seasonality elements of SARIMA model, the most sophisticated forecasting model is obtained, namely the SARIMAX model [58].

With the daily seasonality of the price time series as described in SARIMA model, combined with wholesale electricity price data as an exogenous variable, the most sophisticated local market price forecast is obtained. The mathematical formulation of the SARIMAX model is described as Equation 4.16, similar to [58]. Here, similar to the previous section, X represents the exogenous variable, namely the wholesale electricity price time series. In the Econometrics Modeler of Matlab, one parameter μ can be estimated, limiting the order h that corresponds to the exogenous lagged values. As a result, the mathematical formulation becomes:

$$\left(1-\sum_{i=1}^{p}\psi_i B^i\right)\left(1-\sum_{j=1}^{P}\zeta_j B^{Sj}\right)(1-B)^d(1-B^S)^D Z_t = C+\mu_1 X_1+\left(1+\sum_{i=1}^{q}\varphi_i B^i\right)\left(1+\sum_{j=1}^{Q}\theta_j B^{Sj}\right)\epsilon_t \tag{4.16}$$

4.1.6 Box-Jenkins approach

To estimate and fit the (S)AR(I)MA(X)-type models to the available data, the methodology of Box-Jenkins is followed [16, 21]. According to [16], the estimation process of (S)AR(I)MA(X) models involves three iterative stages: 1) identifying the tentative model, 2) estimating the model, and 3) verifying the accuracy of the estimated model.

1) Model identification

In this stage, the configuration and order parameters of the SARIMA$(p,d,q)(P,D,Q)_S$ model are determined. This entails estimating the parameters p, d, q, P, D, Q. Initially, as discussed in the ARIMA model section, it is essential to ensure that the time series Z_t exhibits stationarity. This can be achieved by employing transformations, such as taking the logarithm function instead of the original Z_t time series. Furthermore, the order d is established by differencing the time series Z_t iteratively until a stationary time series is achieved [1]. The stationarity of the series can be confirmed through the examination of the Autocorrelation Function (ACF) and Partial Autocorrelation Function (PACF) plots. Following this, the orders p and q are determined using the ACF and PACF plots [95, 48, 82, 43, 81, 1]. These function plots aid in identifying interdependencies between a variable and its lagged values [48, 6]. This phase yields initial parameter estimates, which serve as a foundation for the subsequent iterative model estimation process [16].

2) Model estimation

During the model estimation stage, the parameter estimates from stage 1 are compared, and the coefficients are determined [81]. In addition to determining the order parameters, it is necessary to estimate the coefficients ψ and φ of the AR and MA terms, the constant term C, and the standard deviation σ of the error term [95]. Additionally, the seasonal coefficients ζ and θ are determined. These coefficient estimations can be conducted using methods such as the Least Square Method or Maximum Likelihood [52, 82, 43, 81, 16]. To identify which model best fits the data, statistical criteria such as the Akaike information criterion (AIC) and Schwarz Bayesian information criterion (BIC) can be employed. These criteria are expressed as follows:

$$\mathrm{AIC} = 2\mathrm{k} - 2ln(\mathrm{L}) \tag{4.17}$$

$$\mathrm{BIC} = \mathrm{n}ln(\sigma^2) + \mathrm{k}ln(n) \tag{4.18}$$

Here, k is the number of estimated parameters, L is the maximized value of the likelihood function, n is the sample size, σ^2 is the error variance [81, 107]. Different formulas of the AIC and BIC are used in literature, for example in [81, 48, 16]. In the above equations, the estimated model with the smallest AIC and BIC values is chosen to be the best fit [81]. Selecting the model with the smallest values of the AIC and BIC ensures a balance between the complexity of the model (number of inputs) and its goodness of fit [48].

Initially, it is beneficial to analyze the ARIMA model without exogenous variables to ascertain the orders of the parameters p, d, and q. Subsequently, the ARIMAX model, which incorporates the wholesale market price as an exogenous variable, can be fitted [48]. However, it should be noted that the final determination of the parameters p and q is made by evaluating at the AIC of the complete ARIMAX model [48].

3) Diagnostic checking
In the third stage, it is assessed whether the parameters and coefficients determined in stages 1 and 2 result in a satisfactory fit of the model while avoiding overfitting [81]. The goodness of fit of the model can be evaluated by examining the residuals of the model [16]. Specifically, ARIMA models assume that the error term (residual) behaves as white noise, e.g. zero mean and constant variance [107, 60, 43, 97, 82, 1]. In other words, the residuals should follow a normal distribution with a mean of zero and σ standard deviation. Therefore, the residuals are tested on the following aspects via ACF and PACF analysis [81, 6, 16]:

- Autocorrelation: Residuals should not exhibit correlation with lagged residual values.
- Homoskedasticity: The variance of the residuals should remain constant.
- Normality: Residuals should conform to a normal distribution with zero mean.

If the residuals do not conform to the characteristics of white noise, additional features/models are required to achieve an appropriate fit [81, 1]. In such cases, adjustments to the order parameters p, P, q, and Q may be necessary, and the iterative process of the three stages is restarted [1].

4.2 Residual analysis

In the final state of the Box-Jenkins approach, known as diagnostics checking, the residuals of the SARIMAX model are investigated to ensure their adherence to the white noise assumption: zero mean and constant variance, in line with the principles of ARIMA model methodologies [16, 1, 107, 60, 82, 97, 23].

In this stage, it is important to gain insight into the distribution of the SARIMAX model's residuals, which serve as essential inputs for generating price scenarios [63, 111]. Analyzing these residuals allows for the detection of any remaining auto-correlation in the prediction errors, which can indicate the need for refining or extending the SARIMAX model to better capture the underlying patterns [81, 1].

When the SARIMAX model is effectively fitted within the Box-Jenkins methodology, the residuals ideally conform to a Gaussian (Normal) distribution, characterized by a zero mean and standard deviation σ [23, 16]. The estimation of the standard deviation σ is typically accomplished using methods like the Least Square Method or Maximum Likelihood Function [52, 82, 43, 81, 16]. This white noise prediction errors serve as input in the scenario generation stage to generate scenarios.

4.3 Scenario generation

In the Residual analysis section, it is determined that the residuals of the SARIMAX model exhibit characteristics of white noise ($\{\epsilon\} \sim N(0, \sigma)$), with a constant σ determined through the Box-Jenkins approach. [107, 82, 60, 97, 43].

Utilizing the estimated white noise of the prediction error, along with the parameters of the (S)AR(I)MA(X)-type model, historical local market price values, and historical local market price residuals, a desired number of scenarios can be generated by sampling the error terms from the defined Gaussian distribution [23]. In other words, a random number following a normal distribution is generated for each scenario time step [95, 96].

Before initiating scenario generation, it is crucial to specify the number of scenarios (N_Ω), denoted as ω [23]. The algorithm described in [23] is employed to generate N_Ω scenarios for predicting the local market price, comprising seven sequential steps:

- **Step 1**: Initialize the scenario counter $\omega \leftarrow 0$.
- **Step 2**: Update the scenario counter $\omega \leftarrow \omega + 1$, and initialize the time period counter: $t \leftarrow 0$.
- **Step 3**: Update time period counter: $t \leftarrow t + 1$.
- **Step 4**: Randomly generate prediction error: $\epsilon_t \sim N(0, \sigma)$.
- **Step 5**: Using the SARIMAX model expression, obtain the price prediction $Z_{t\omega}$.
- **Step 6**: If $t < N_T$ return to step 3), else proceed to step 7).
- **Step 7**: If $\omega < N_\Omega$ return to step 2), otherwise, all scenarios have been generated and the algorithm concludes.

In this algorithm, each scenario is assigned an equal probability of $1/N_\Omega$. However, given the probability distribution nature of local market prices, a considerable number of scenarios are needed to adequately approximate the distribution. This amplifies the need to reduce the number of scenarios, to maintain tractability of the stochastic optimization problem [45, 96, 73]. The subsequent section elaborates a scenario reduction technique to reduce the number of scenarios.

4.4 Scenario reduction

As mentioned before, solving a stochastic program via scenario generation becomes increasingly complex as the number of scenarios increases [111, 96, 23]. Hence, to ensure tractability of the scenario-based optimization model, it is essential to reduce the number of scenarios while preserving the stochastic properties as closely as possible [96, 46, 95, 73, 23]. In essence, the reduced scenario set should still yield an optimal solution that closely approximates that of the original problem with the complete set of scenarios [73]. The general concept of scenario reduction involves eliminating improbable scenarios and grouping scenarios with similar characteristics.

The optimal solution obtained using the reduced scenario set resembles the optimal solution derived from the original scenario set when the two scenario sets are sufficiently close in terms of *probability distance* [73, 23, 46]. Probability distance serves as a metric to measure the similarity between two distinct scenario sets representing the same stochastic process [23]. The goal is to ensure that the final reduced scenario set possesses a probability measure that closely aligns with the original probability measure, indicating minimal probability distance between the two sets [95, 23, 49, 73, 45, 31]. The Kantorovich Distance, denoted as $D_K(\cdot)$, stands out as the most commonly employed probability distance measure in stochastic programming [73]. Further elaboration on this distance metric is provided next..

Kantorovich Distance

Kantorovich Distance $D_K(Q, Q')$ quantifies the probability distance between two distinct scenario sets (Ω and Ω') associated with the same stochastic process. These scenario sets possess probability functions Q and Q', respectively. Utilizing the Kantorovich Distance enables the assessment of the proximity between different scenario sets representing identical stochastic processes, and reduces and bundles scenarios using the KD matrix [96, 95]. In the case of discrete probability distributions, the Kantorovich Distance is used to obtain the optimal reduced scenario set Ω_S. The Kantorovich Distance matrix is comprised by the product of the cost function and the occurrence probability of all generated scenarios [96].

The overarching objective of the scenario reduction is to identify a subset of scenarios $\Omega_S \subset \Omega$, accompanied by adjusted probabilities. This adjustment aims to ensure that the reduced probability function Q' associated with scenario subset Ω_S closely approximates the original probability function Q corresponding to the initial scenario set Ω [23, 46, 49, 96].

The Kantorovich Distance $D_K(Q, Q')$ is determined by solving the problem called the 'Monge-Kantorovich mass transportation problem', represented in Equation 4.19 [45, 23, 49, 46, 73, 95]:

$$D_K(Q,Q') = \min_{\rho(\omega,\omega')} \Big\{ \sum_{\substack{\omega\in\Omega \\ \omega'\in\Omega_S}} c(\omega,\omega')\rho(\omega,\omega') : \\ \rho(\omega,\omega') \geq 0, \forall\omega\in\Omega, \forall\omega'\in\Omega_S, \\ \sum_{\omega'\in\Omega_S} \rho(\omega,\omega') = \pi_\omega, \forall\omega\in\Omega, \\ \sum_{\omega\in\Omega} \rho(\omega,\omega') = \pi_{\omega'}, \forall\omega'\in\Omega_S \Big\} \tag{4.19}$$

In Equation 4.19:

- ω is a realization of a scenario belonging to scenario set Ω ($\omega \in \Omega$). π_ω is a scenario probability of scenario ω, in the scenario set Ω, according to probability distribution Q.
- ω' is a realization of a scenario belonging to scenario set Ω_S ($\omega' \in \Omega_S$). $\pi_{\omega'}$ is a scenario probability of scenario ω', in the scenario set Ω_S, according to probability distribution Q'.
- $\rho(\omega,\omega')$ represents the joint probability defined over $Q \times Q'$ [45].
- $c(\omega,\omega')$ represents the cost function; a non-negative, continuous, symmetric function. The cost function is represented by the norm of the local electricity prices, representing the vector distance between ω and ω'.

An equivalent notation of Equation 4.19 is represented in Equation 4.20. This equivalency is maintained because the stochastic elements are typically integrated solely within the objective function and/or on the right-hand sides of the optimization problem. For elaboration on this equivalency, please consult [31].

$$D_K(Q,Q') = \sum_{\omega\in\Omega\setminus\Omega_S} \pi_\omega \min_{\omega'\in\Omega_S} c(\omega,\omega') \tag{4.20}$$

The Monge-Kantorovich mass transportation problem poses significant computational challenges, particularly when dealing with a large nubmer of scenarios ω [45, 23]. Efficiently solving Equation 4.19 or its equivalent Equation 4.20 using algorithms is generally difficult, with few available solutions in practice [46]. As a result, various heuristic algorithms have been developed, with two primary approached being backward reduction and forward selection, both derived from Equation 4.20 [23]. These heuristics, although efficient and effective, realy on simplifications to manage computational complexitiy [31, 73]. Using the forward selection algorithm tends to exhibit slightly better performance compared to backward reduction [31]. According to studies by [95, 49], forward selection is particularly advantageous when the reduced number of scenarios is less than one-fourth of the total of scenarios generated, which is the case in this research.

Forward selection algorithm

This algorithm initiates with an empty set of scenarios ($\Omega_S = \emptyset$), where each iteration involves the addition of one non-selected scenario ($\Omega\setminus\Omega_S$) to the scenario set Ω_S. The scenario selected for inclusion in Ω_S is chosen to minimize the KD between the reduced and original scenario sets (Ω_S and Ω respectively) [73, 23]. The algorithm finishes when one of the two stop conditions is met; either a pre-defined number of scenarios or a 'threshold' of Kantorovich Distance is reached [73]. As this algorithm is heuristic in nature, there is no guarantee of obtaining an optimal reduced scenario set after iterations. However, empirical testing conducted in [31, 49, 73] demonstrates that the resulting reduced scenario sets are a good approximation to the optimal value of the original problem.

The algorithm of the forward selection generates a sequence of reduced scenario sets (Ω_S) until it converges to the optimal reduced scenario set Ω_S^*. This progression can be denoted as:

$\Omega_S^{[0]}, \Omega_S^{[1]}, \Omega_S^{[i]}, ..., \Omega_S^*$, where the superscript [i] represents the i-th iteration of the algorithm. At each iteration, one scenario is incrementally added to Ω_S, resulting in a gradual increase in the cardinality of the reduced scenario set until the final reduced scenario set Ω_S^* is obtained. $N_{\Omega_S^*}$ denotes the number of scenarios included in reduced scenario set Ω_S^*. Additionally, $\Omega_J^{[i]}$ is used to denote the set of non-selected scenarios in the first i steps of the forward selection algorithm. The combination of non-selected scenarios and the reduced scenario set sums up to the original scenario set: $\Omega_J^{[i]} \cup \Omega_S^{[i]} = \Omega$ [23].

The forward selection algorithm is described in several steps, following the methodology described in [23, 45]:

- **Step 0: scenario pre-processing**
  - Initialize the reduced scenario set: $\Omega_S^{[0]} = \emptyset$.
  - Define the set of non-selected scenarios: $\Omega_J^{[0]} = \{1, ..., N_\Omega\}$
  - Calculate the cost function $c(\omega, \omega')$, which defines the Kantorovich Distance for each pair of scenarios in the original scenario set $\omega, \omega' \in \Omega$. Here, the stochastic local electricity price is $\mathbf{u}$, and with scenarios ω, the stochastic local price is represented as: $\mathbf{u} = \{\mathbf{u}(\omega), \omega = 1, 2, ..., N_\Omega\}$. Then, the cost function is formulated as the norm of the difference between two distinct scenario realizations ω and ω':

$$c(\omega, \omega') = ||\mathbf{u}(\omega) - \mathbf{u}(\omega')|| \tag{4.21}$$

- **Step 1: choice of starting scenario**
  The starting scenario is the first scenario that is added to the reduced scenario set Ω_S. The first scenario to be added to Ω_S is formulated as:

$$\omega_1 = \arg\{\min_{\omega' \in \Omega} \sum_{\omega \in \Omega} \pi_\omega c(\omega, \omega')\} \tag{4.22}$$

  Since the reduced scenario set is still empty, the Kantorovich distance of all scenario pairs in Ω is calculated. ω_1 is added to $\Omega_S^{[1]}$. The non-selected scenarios are formulated as: $\Omega_J^{[1]} = \{1, ..., N_\Omega\} \backslash \omega_1$.

- **Step i: selection of scenarios to be added to reduced set**
  When generalizing step 1 into iteration i, Equation 4.22 changes into Equation 4.23 and Equation 4.24, where each iteration scenario ω_i is added to the reduced scenario set Ω_S. This can be described as: $\Omega_S^{[i]} = \Omega_S^{[i-1]} \cup \{\omega_i\}$. Simultaneously, ω_i is removed from the non-selected scenario set defined as $\Omega_J^{[i]} = \Omega_J^{[i-1]} \backslash \{\omega_i\}$.

$$\omega_i \in \arg \min_{\omega \in \Omega_J^{[i-1]}} d_\omega^{[i]} \tag{4.23}$$

  where

$$d_\omega^{[i]} = \sum_{\omega' \in \Omega_J^{[i-1]} \backslash \{\omega\}} \pi_{\omega'} c^{[i]}(\omega', \omega), \qquad \forall \omega \in \Omega_J^{[i-1]} \tag{4.24}$$

  In Equation 4.23 and Equation 4.24, the cost function $c(\cdot)$ needs to be updated each iteration. The updated cost function is calculated by Equation 4.25:

$$c^{[i]}(\omega, \omega') = \min\Big\{c^{[i-1]}(\omega, \omega'), c^{[i-1]}(\omega, \omega_{i-1})\Big\}, \qquad \forall \omega, \omega' \in \Omega_J^{[i-1]} \tag{4.25}$$

  Step i is iterated $N_{\Omega_S^*} - 1$ times, where $N_{\Omega_S^*}$ represents the number of scenarios in the optimal reduced scenario set Ω_S^*.

- **Step $N_{\Omega_S^*} + 1$: redistribution of probabilities**
  In this final step, the probabilities are reallocated to the optimal reduced scenario set Ω_S^*. The probabilities associated with the non-selected scenarios ($\omega \in \Omega_J^*$) are added to the selected scenarios in the reduced scenario set ($\omega \in \Omega_S^*$). By construction, $\Omega_J^* \cup \Omega_S^* = \Omega$. It is assumed that all deleted scenarios have a probability of zero [96], and the probability associated with a deleted scenario is transferred to the nearest remaining scenario based on the distance metric c on Ω [96, 49, 95].

  Thus, the preserved scenario inherits a new probability equal to the sum of its original probability and the probabilities of the deleted scenarios with the closes distance c. The redistribution of probabilities from deleted scenarios to the nearest scenario that is not eliminated is determined via the *optimal redistribution rule*[46]:

$$\pi_\omega^* = \pi_\omega + \sum_{\omega' \in J(\omega)} \pi_{\omega'} \tag{4.26}$$

  In Equation 4.26, $J(\omega)$ is defined as the set of scenarios $\omega' \in \Omega_J^*$ such that:

$$\omega = \arg \min_{\omega'' \in \Omega_S^*} c(\omega'', \omega'). \tag{4.27}$$

  Note that in Equation 4.26, the cost function $c(\omega'', \omega')$ is the cost function that is calculated in step 0, not the updated cost function from step i.

5 Risk management in stochastic optimization

This chapter provides the theoretical background on incorporating risk management in stochastic programming. The Conditional Value at Risk (CVaR) risk measure is used in this research to cope with the profit volatility of the day-ahead market caused by LEM price uncertainty [20]. Both subsections elaborate on existing theories.

In the literature, it becomes apparent that risk management is a crucial element when coping with uncertainties in stochastic optimization problems [2]. For example, [59] considers risk management in stochastic optimization as further research to reduce day-ahead market infeasibility. Incorporating a risk measure in the formulation of the stochastic optimization allows the agent to cope with the uncertainties of the market resulting in profit volatility (i.e. probability of having low profit) [25, 20, 86, 23]. Hence, this research incorporates risk management of the agent participating in the LEM day-ahead market. The next two sections provide the framework for incorporating CVaR in a stochastic program to account for risk management.

5.1 CVaR derivation

In general, stochastic optimization problems are *risk-neutral* problem formulations. Namely, stochastic programs represent the *expected* profit in the objective function. Adding the CVaR risk measure to the optimization problem adds the possibility for the agent to reflect his risk attitude in the optimal bidding schedule.

CVaR is a popular, suitable risk measure to represent risk [74, 110]. CVaR is widely incorporated as a risk measure in stochastic optimization, for example in [25, 110, 77, 20]. The CVaR risk measure is applicable as a tool in optimization modeling due to its robustness regarding its input [77, 86, 3, 2]. Besides, CVaR can be integrated into the objective function of a linear program to put off unfavorable uncertainty realizations [20]. Additionally, CVaR satisfies the axioms of a *coherent* risk measure and is linear [77, 86, 3, 2, 55], resulting in a convex, tractable problem [8, 74, 86]. Hence, every local optimum qualifies as a global optimum, which is a significant advantage of CVaR [83]. Detailed information on the axioms of risk measures is provided in Uncertainty set construction via risk measures.

As firstly introduced by [87, 86], CVaR can be simultaneously determined by finding the solution of a convex, elementary optimization problem. The function to be minimized is described in [87, 86] as:

$$F_\alpha(x,\zeta) = \zeta + \frac{1}{1-\alpha}\mathbb{E}\{[f(x,y)-\zeta]^+\}, \quad \text{where} [t]^+ = \max\{0,t\} \tag{5.1}$$

In Equation 5.1, x represents the decision variable, and y represents the uncertainty that affects the loss [87]. In this research, the uncertainty corresponds to the stochastic local market clearing price. The decision variables x represent the behavior of the agent in the LEM. Finally, $f(x,y)$ represents the random loss function [90].

CVaR is defined as the expected value of the profit that is smaller than the (1 - α) $\times$100 % of the whole profit distribution [23, 2, 55, 33]. In case of a cost minimization problem, CVaR considers the $(1-\alpha)\times 100\%$ of the scenario expectations that incur the highest expected costs [89]. In the case of a maximization problem, CVaR represents the average profit obtained by the (1 - α) $\times$ 100% lowest profit scenarios [72]. Hence, α in Equation 5.1 represents the confidence interval of the CVaR term [108]. As mentioned in [20], the value of α commonly lies between 0.90 and 0.99. In other words, only the 10%-1% worst-case expected profits are considered in the CVaR term. When α is set to 0, the agent exhibits risk-neutral behavior.

Furthermore, the function in Equation 5.1 is a convex function and is piece-wise linear with respect to ζ [86, 87, 110]. As defined in [86, 90], in optimality, ζ represents the Value-at-Risk of the problem. More elaboration on the Value-at-Risk risk measure can be found in the Risk measures section.

Importantly, the function described in Equation 5.1 can be minimized by formulating it as elementary linear program [87, 83, 77, 86, 55]. The function presented in Equation 5.1 can namely be converted to a linear problem through the introduction of an additional decision variable [110]. This problem derivation is described in CVaR optimization problem.

Multiple characteristics of the function derived in Equation 5.1 can be derived [87, 86, 90]:

1. $F_\alpha(x, \zeta)$ is convex with respect to α.
2. $\text{VaR}_\alpha(x)$ is a minimum point of function $F_\alpha(x, \zeta)$ with respect to ζ.
3. Minimizing $F_\alpha(x, \zeta)$ with respect to ζ yields $\text{CVaR}_\alpha(x)$:

$$\text{CVaR}_\alpha(x) = \min_{\zeta} F_\alpha(x, \zeta) \tag{5.2}$$

Examining the convexity characteristics of the random loss vector $f(x, y)$ revails the significant advantages of CVaR [90]. If $f(x, y)$ is convex in the decision variable x, $\text{CVaR}_\alpha(x)$ is convex in x. Moreover, given the convexity of $f(x, y)$ in x, the minimization function $F_\alpha(x, \zeta)$ as described in Equation 5.1 is convex in both x and ζ [86]. Based on this characteristic, the following property holds [90, 86, 87]:

$$\min_{x \in X} \text{CVaR}_\alpha(x) = \min_{(x,\zeta) \in X \times \Re} F_\alpha(x, \zeta) \tag{5.3}$$

With optimizer (x^*, ζ^*) as solution for the minimization of $F_\alpha(x, \zeta)$ over X $\times$ $\Re$, x^* minimizes $\text{CVaR}_\alpha(x)$ over set X. In addition, ζ^* represents the $\text{VaR}_\alpha(x)$[87]. Regarding the values of the objective functions, the following property holds:

$$\text{CVaR}_\alpha(x^*) = F_\alpha(x^*, \zeta^*) \tag{5.4}$$

To conclude, rather than directly minimizing $\text{CVaR}_\alpha(x)$, the minimization function illustrated in Equation 5.1 is employed to preserve the convexity within the problem [86, 90]. Minimizing $F_\alpha(x, \zeta)$ (Equation 5.1) simultaneously in both x and ζ to integrate risk yields a more tractable problem compared to minimizing $\text{CVaR}_\alpha(x)$ in X [86]. In next section, Equation 5.1 is translated to fit into a stochastic optimization problem.

5.2 CVaR optimization problem

According to Equation 5.3, incorporating $\text{CVaR}_\alpha(x)$ is equivalent to minimizing the function $F_\alpha(x, \zeta)$ in both x and ζ [86, 90]. This section focuses on transforming the function $F_\alpha(x, \zeta)$ outlined in the previous section into a solvable minimization problem in the application of stochastic optimization.

The derivation of a tractable equivalent problem incorporating CVaR into the stochastic program closely follows the approach outlined in [86, 90]. In theory, CVaR can be integrated into both the constraints and/or to the objective function within stochastic optimization [86]. This section elaborates on the derivation process by incorporating CVaR into the *constraints* of the optimization problem.

First, let $\alpha_i \in (0, 1)$ denote the confidence interval specified by the decision maker, and ω_i represent the loss tolerance for constraints i = 1, ..., l [90]. For each constraint i, a confidence interval and loss tolerance are defined. The decision maker can select a value for α_i, where a higher value reflects a more risk-averse decision maker [100, 25, 23]. Note that the loss tolerance ω is absent when incorporating CVaR in the objective function. When formulating CVaR in the objective function, the goal is to minimize the function $F_\alpha(x, \zeta)$. When constructing CVaR for the constraints, the problem incorporating $\text{CVaR}_\alpha(x)$ is rewritten into the equivalent problem incorporating $F_\alpha(x, \zeta)$ [86, 90, 87]:

$$\begin{aligned} &\min_{x \in X} g(x) && \iff && \min_{x, \zeta_1, \ldots, \zeta_l \in X \times \Re \times \ldots \Re} g(x) \\ &\text{s.t } \text{CVaR}_{\alpha_i}(x) \leq \omega_i, \quad i = 1, \ldots, l && && \text{s.t. } F_{\alpha_i}(x, \zeta_i) \leq \omega_i, \quad i = 1, \ldots, l \end{aligned}$$

The expected value component within $F_{\alpha_i}(x, \zeta_i)$ in Equation 5.1 ($\mathbb{E}\{[f(x, y) - \zeta]^+\}$) can be reformulated for finite, discrete probability spaces, which aligns with the scenarios generated in this research [55, 29]. Then, function $F_\alpha(x, \zeta)$ is rewritten into:

$$F_{\alpha_i}(x, \zeta_i) = \zeta_i + \frac{1}{1 - \alpha_i} \sum_{k=1}^{N} p_k [f(x, y_k) - \zeta_i]^+ \tag{5.5}$$

In Equation 5.5, y_k denotes the random vector y of risk vectors within the discrete probability space Y. Every y_k has probability p_k, for k = 1, ..., N [90, 86]. Subsequently, the constraint $F_\alpha(x, \zeta) \leq \omega$ is restructured into a system of inequalities, as represented in Equation 5.6 [90, 86]. This transformation is achieved through the introduction of additional (auxiliary) variables, η_k [55].

$$\begin{aligned} & f(x, y_k) - \zeta - \eta_k \leq 0, && k = 1, ..., N \\ & \zeta + \frac{1}{1 - \alpha} \sum_{k=1}^{N} p_k \eta_k \leq \omega \\ & \eta_k \geq 0, && k = 1, ..., N \end{aligned} \tag{5.6}$$

Following the approach in [90], the minimization problem is formulated below. In the cases where the loss function f is linear in x, the constraints of the minimization problem also maintain linearity [90]. Below, Equation 5.9 represents the linearized expression of $F_{\alpha_i}(x, \zeta_i)$, wherein the auxiliary variable η_k captures the positive part of $[f(x, y_k) - \zeta_i]^+$ in Equation 5.8.

$$\min_{x, \zeta_1, ..., \zeta_i \in X \times \Re \times ... \Re} g(x) \tag{5.7}$$

$$\text{s.t. } f(x, y_k) - \zeta - \eta_k \leq 0, \quad k = 1, ..., N \tag{5.8}$$

$$\zeta + \frac{1}{1 - \alpha} \sum_{k=1}^{N} p_k \eta_k \leq \omega \tag{5.9}$$

$$\eta_k \geq 0, \quad k = 1, ..., N \tag{5.10}$$

The optimization problem described in Equation 5.7 until Equation 5.10 represent the linearized form of the function introduced in Equation 5.1.

6 Robust modeling of price uncertainty

In this chapter, the theoretical framework of having an *uncertainty set* in an optimization problem to integrate price uncertainty is provided. The goal of Uncertainty set modeling is to provide an outline on how to integrate price uncertainty to obtain a general robust problem. Additionally, the budget of uncertainty is introduced to adjust the size of the uncertainty set, adjusting the risk attitude of the agent. Afterward, Uncertainty set construction via risk measures derives a different uncertainty set using a coherent and comonotone risk measure. Both subsections elaborate on existing theories.

Robust optimization constitutes a modeling framework that can incorporate price uncertainty *without* explicitly modeling its complete underlying probability distribution. As opposed to stochastic optimization methods, robust optimization does not necessitate knowledge of the complete probability distribution of uncertainty electricity prices [26]. Instead, robust optimization functions with only the range of uncertainty, often defined by distribution bounds,uncertainty set, or robust sets, without requiring the full probability distribution as an input [111, 99, 88, 54]. Consequently, while Scenario-based modeling of price uncertainty may encounter computational complexity issues due to requiring a large number of scenarios, robust-based modeling of price uncertainty does not encounter this issue [111, 9].

Robust optimization makes use of interval ranges [13, 5], where the optimal solution is designed to withstand all potential scenarios within an uncertainty set [10, 94, 9, 54]. Robust optimization aims to optimize based on the worst-case realization within a specified uncertainty set [26, 13, 35, 74], resulting in a min-max type formulation [111, 41, 62, 9, 54]. For instance, an uncertainty set may be defined as $u \in 4, 7$, where no assumption is made regarding the probability of u within the uncertainty set [99]. Hence, robust optimization proves beneficial when dealing with stochastic process that are complex to capture.

The initial step in formulating a robust optimization problem is constructing the uncertainty set to encompass the uncertain LEM prices [10]. Instead of elaborating on the distribution of the uncertainty within the uncertainty set, the set represents the *support* of the uncertainty. The range interval of the local market price is predetermined, where the range (box) interval is represented as $[\bar{c}_j - d_j, \bar{c}_j + d_j]$ [13, 111, 18]. In general, this range forecast is symmetric around the point forecast [8, 47, 111]. Within the range interval, $\bar{c}_j$ represents the point forecast value of the LEM price (mean) and d_j represents the (standard) deviation from the mean forecast value. Both $\bar{c}_j$ and d_j are derived from the (S)AR(I)MA(X) point forecast model, as elaborated in stage 1 of Scenario-based modeling of price uncertainty. To construct the range interval, both a mean price and standard deviation forecast are required.

The decision-maker ensurer that the solution remains feasible for any realization of uncertainty within the predefined uncertainty set [9]. Consequently, solutions derived from robust optimization can be overly conservative [88, 12, 109], a phenomenon commonly referred to as the 'price of robustness' [12]. In extreme cases, robust optimization may lead to scenarios where no solution adequately safeguards against uncertainty [88]. To mitigate over-conservatism [13], restricting the uncertain LEM price to lie within *ellipsoidal uncertainty sets* is employed, which helps eliminate consideration of the least probable outcomes and enhances the traceability of the optimization problem [13]. However, modeling uncertainty using ellipsoidal sets is complex. As a result, [12] have introduced the concept of *polyhedral uncertainty sets* to represent the uncertainty parameters, which result in a tractable, linear problem [13, 5, 57].

The size of the uncertainty set significantly influences the conservativeness of the optimization model [47], as larger uncertainty set tend to yield more conservative optimal solutions [111]. Adjusting the size of the uncertainty set can be achieved by introducing the concept of a *budget of uncertainty* [111, 10], resulting in less conservative outcomes. Rather than directly considering the worst-case realization of the box interval $[\bar{c}_j - d_j, \bar{c}_j + d_j]$, the budget of uncertainty allows for the adjustment of the level of conservatives in robust optimization [26, 11, 98, 10]. Hence, even with a large uncertainty set, the conservativeness of the optimal solution can be reduced. The budget of

uncertainty (Γ) determines the maximum number of times the price is allowed to deviate from its mean forecast ($\bar{c}_j$) [26, 98]. Therefore, Γ should be pre-defined by the agent. Opting for a smaller budget of uncertainty results in a reduced polyhedral uncertainty set compared to the original range interval [57]. Introducing the budget of uncertainty reduces over-conservative solutions while maintaining high level of confidence [111, 10]. Thus, risk management in robust optimization can be effectively implemented through through the budget of uncertainty.

The primary advantage of polyhedral uncertainty sets is that the robust version of the linear programming problem remains linear, maintaining its traceability [13]. In other words, the sub-problem can be reformulated as a linear problem [9]. To obtain this robust linear problem, the original min-max problem is initially translated into its robust counterpart [98, 34]. Subsequently, the problem is transformed into a single-level problem using duality theory [111, 5, 57]. This robust problem, which integrates an uncertainty set to represent stochastic prices, is derived in Uncertainty set modeling.

6.1 Uncertainty set modeling

A standard optimization problem can be written in the form:

$$\begin{aligned} &\text{minimize } \mathbf{c}'\mathbf{x} \\ &\text{subject to } \mathbf{A}\mathbf{x} \leq \mathbf{b} \\ &\mathbf{x} \in \mathcal{X} \end{aligned} \tag{6.1}$$

In Equation 6.1, $\mathbf{A} \in \mathbb{R}^{m \times n}$, $\mathbf{b} \in \mathbb{R}^m$, and $c \in \mathbb{R}^n$. In total, there are m constraints in Equation 6.1. Lastly, $x \in \mathcal{X}$, where $\mathcal{X}$ is a polyhedron [13]. Next, the coefficients i and j are defined, representing the coefficients of the $\mathbf{A}$ matrix. Then, $N = \{1, 2, ..., n\}$, $j \in N$, $i = \{1, 2, ..., m\}$.

In this chapter, only uncertainty in the cost vector $\mathbf{c}$ in the objective function is present. Hence, each entry c_j, $j \in N$ takes values in the range $[\bar{c}_j - d_j, \bar{c}_j + d_j]$, where d_j is represented as the deviance from mean $\bar{c}_j$ [11, 18, 13, 12]. It is assumed in this research that each entry c_j in the objective function can be subject to deviation from its nominal value ($d_j > 0, \forall j \in N$). The mean forecast $\bar{c}_j$ and the deviance of the point forecast d_j (standard deviation) are determined via the output of the point forecast model SARIMAX.

Next, the budget of uncertainty parameter Γ_0 is introduced to facilitate control and adjustment of the risk-preference of the decision-maker [18]. Γ_0 is constrained within the range $[0, n]$, where 0 indicates deviation from the mean forecast value $\bar{c}_j$ is completely excluded in the problem, while n implies complete protection of the cost function against deviations in all cost coefficients $\bar{c}_j$ [13, 12]. Therefore, varying $\Gamma_0 \in [0, n]$ enables adjustment of the level of conservatism in the solution of the robust optimization problem [12]. Furthermore, Γ_0 is assumed to take only integer values [11]. The following equation is obtained from including the budget of uncertainty [13]:

$$\sum_{j=1}^{n} |z_{0j}| \leq \Gamma_0, \quad \Gamma_0 \in [0, n] \tag{6.2}$$

In Equation 6.2, z_{0j} represents the scaled deviation of $\bar{c}_j$ from its nominal value c_j [13]. This means that in general z_{0j} takes on values in the interval [-1,1] [13]. When the nominal value c_j exceeds $\bar{c}_j$, z_{oj} takes a positive value, meaning that the worst-case term incorporates the possibility of having higher costs than originally forecasted. The reverse also holds. In other words, z_{0j} can be represented as:

$$z_{0j} = \frac{c_j - \bar{c}_j}{d_j} \tag{6.3}$$

In order to construct the robust counterpart of Equation 6.1, a *polyhedral uncertainty set* $\mathcal{C}$ is formulated [13]. This research uses an uncertainty set that is also called the box interval [111]. The uncertainty set $\mathcal{C}$ is defined as:

$$\mathcal{C} = \{(c_j)|\ c_j = \bar{c}_j + d_j z_{0j},\ \forall j,\ \mathbf{z_0} \in \mathcal{Z}_0\} \tag{6.4}$$

with

$$\mathcal{Z}_0 = \left\{ \mathbf{z_0} \;\middle|\; |z_{0j}| \leq 1, \forall j, \sum_{j=1}^{n} |z_{0j}| \leq \Gamma_0 \right\} \tag{6.5}$$

Equation 6.1 is reformulated into its robust counterpart, incorporating the uncertainty set $\mathcal{C}$ as formulated in Equation 6.4:

$$\begin{aligned} \min_x \ \max_{c_j \in \mathcal{C}} \ & \mathbf{c}'\mathbf{x} \\ \text{s.t. } & \mathbf{a_i}'\mathbf{x} \leq b_i, \quad \forall i \\ & \mathbf{x} \in \mathcal{X} \end{aligned} \tag{6.6}$$

The robust counterpart described in Equation 6.6, which includes uncertainty in cost vector $\mathbf{c}$, can be reformulated to eliminate the uncertainty set $\mathcal{C}$, and to have z_0 as decision variable in the sub maximization problem [13, 11]. In other words, Equation 6.6 is equivalently expressed as:

$$\begin{aligned} \min_x \ & \left(\sum_{j=1}^{n} \bar{c}_j x_j + \max_{z_0 \in \mathcal{Z}_0} \sum_{j=1}^{n} d_j |x_j| z_{0j} \right) \\ \text{s.t.} & \sum_{j=1}^{n} a_{ij} x_j \leq b_i, \quad \forall i, \\ & x \in X \end{aligned} \tag{6.7}$$

where $\mathcal{Z}_0$ is represented by Equation 6.8:

$$\mathcal{Z}_0 = \left\{ \mathbf{z_0} \;\middle|\; |z_{0j}| \leq 1, \forall j, \sum_{j=1}^{n} |z_{0j}| \leq \Gamma_0 \right\} \tag{6.8}$$

Taking the maximum term out of Equation 6.7 and including the properties of $\mathcal{Z}_0$, $\max_{z_0 \in \mathcal{Z}_0} \sum_{j=1}^{n} d_j |x_j| z_{0j}$ can be rewritten in Equation 6.9 [11]. Note that the absolute sign around z_{0j} can be left out, because in the maximization problem the worst-case cost realization is sought. This means that the costs c_j is taken as maximum ($c_j > \bar{c}_j$), resulting in positive z_{0j} values. Here, a vector $\mathbf{x}^*$ is given, meaning that x_j is not a decision variable in this representation.

$$\begin{aligned} \beta_0(\mathbf{x}^*, \Gamma_0) = \max_{z_{0j}, \forall j \in N} \quad & \sum_{j=1}^{n} d_j |x_j^*| z_{0j} \\ \text{s.t.} \quad & \sum_{j=1}^{n} z_{0j} \leq \Gamma_0 \\ & 0 \leq z_{0j} \leq 1 \quad \forall j \in N \end{aligned} \tag{6.9}$$

Equation 6.9 can be rewritten in the simplistic form Equation 6.10, where there are two constraints, such that right-hand side vector represents the column vector: $[\Gamma_0 \ 1]^T$.

$$\begin{aligned} \max_{z_{0j}, \forall j \in N} \quad & \sum_{j=1}^{n} d_j |x_j^*| z_{0j} \\ \text{s.t.} \quad & \sum_{j=1}^{n} z_{0j} \leq \Gamma_0 \\ & z_{0j} \leq 1 && \forall j \in N \\ & z_{0j} \geq 0 && \forall j \in N \end{aligned} \tag{6.10}$$

Next, the dual problem of Equation 6.10 is considered in Equation 6.11, which is used to finally represent the final, linear proble [11, 13, 12, 34]. Here, two dual variables p_0 q_{0j} are introduced for the dual problem in Equation 6.11:

$$\begin{aligned} \min_{p_0; q_{0j} \forall j \in N} \quad & \Gamma_0 p_0 + \sum_{j=1}^{n} q_{0j} \\ \text{s.t.} \quad & p_0 + q_{0j} \geq d_j |x_j^*| && \forall j \in N, \\ & q_{0j} \geq 0 && \forall j \in N, \\ & p_0 \geq 0 \end{aligned} \tag{6.11}$$

To end up with the final dual representation of the sub problem, $|x_j^*|$ is substituted back to $|x_j|$:

$$\begin{aligned} \min_{p_0; q_{0j} \forall j \in N} \quad & \Gamma_0 p_0 + \sum_{j=1}^{n} q_{0j} \\ \text{s.t.} \quad & p_0 + q_{0j} \geq d_j |x_j| && \forall j \in N, \\ & q_{0j} \geq 0 && \forall j \in N, \\ & p_0 \geq 0 \end{aligned} \tag{6.12}$$

Including Equation 6.12 into the robust counterpart defined in Equation 6.7, the final, robust mixed integer program is formulated as [18] in Equation 6.13. Here, $|x_j^*|$ is replaced with y_j, meaning that at optimality, the following three characteristics hold [13]:

- y_j equals $|x_j|$ for any j.
- p_0 will equal the $\lceil \Gamma_0 \rceil$-th greatest $d_j |x_j|$.
- $q_{0j} = \max(0, d_j |x_j| - p_0)$

$$\begin{aligned} \min_{x_j, q_{0j}, y_j \forall j \in N; p_0} \quad & \sum_{j=1}^{n} c_j x_j + p_0 \Gamma_0 + \sum_{j=1}^{n} q_{0j} \\ & \sum_{j=1}^{n} a_{ij} x_j \leq b_i, && i = \{1, ..., m\} \\ & p_0 + q_{0j} \geq d_j y_j && \forall j \in N \\ & q_{0j} \geq 0 && \forall j \in N \\ & y_j \geq 0 && \forall j \\ & p_0 \geq 0 \\ & -y_j \leq x_j \leq y_j && \forall j \\ & x \in X \end{aligned} \tag{6.13}$$

Equation 6.13 is derived according to the methodology from [11, 13, 12, 18]. The decision-maker needs to assign the budget of uncertainty Γ_0 in the interval [0,n] as input to the optimization problem [13].

6.2 Uncertainty set construction via risk measures

In the Uncertainty set modeling section, a general robust optimization problem is derived in Equation 6.13, based on the introduction of the budget of uncertainty as a risk-attitude parameter. By adjusting this parameter, the conservativeness of the optimal solution can be adjusted [18]. In addition, the polyhedral uncertainty set $\mathcal{C}$ as defined in Equation 6.4 is provided as input to the robust optimization model, meaning that the parameters $\bar{c}_j$ and d_j are estimated before the robust optimization problem is executed. However, instead of defining the budget of uncertainty Γ_0 separately as a parameter in Equation 6.13, the uncertainty set itself can be constructed to incorporate the decision maker's risk-attitude as well as historical data [13]. This is different from the derivation in Uncertainty set modeling, where the size of the uncertainty set is constructed and adjusted afterward by the budget of uncertainty parameter.

This section establishes the connection of coherent risk measures with uncertainty sets in robust optimization [17, 8]. This connection leads to the possibility that uncertainty sets in itself can be constructed taking into account the risk attitude of the decision maker [17]. The derivation is based on a linear problem where the uncertainty is located in the constraints, thus removing uncertainty in the objective function. Without loss of generality, it is possible to rewrite the linear problem, remove the uncertainty from the objective function, and include it in the constraints as follows [13]:

$$\begin{aligned} &\min_x \ \mathbf{c}'\mathbf{x} \\ &\text{s.t. } \mathbf{A}\mathbf{x} \leq \mathbf{b} \\ &\quad \mathbf{x} \in \mathcal{X} \end{aligned} \quad \Longleftrightarrow \quad \begin{aligned} &\min_x \ t \\ &\text{s.t } \mathbf{c}'\mathbf{x} \leq t \\ &\quad \mathbf{A}\mathbf{x} \leq \mathbf{b} \\ &\quad \mathbf{x} \in \mathcal{X} \end{aligned} \quad \Longleftrightarrow \quad \begin{aligned} &\min_x \ t \\ &\text{s.t. } \mathbf{A}\mathbf{x} \leq \mathbf{b} \\ &\quad \mathbf{x} \in \mathcal{X} \end{aligned}$$

Note in the equivalence above that the uncertainty of $\mathbf{c}$ is incorporated as a row in matrix $\mathbf{A}$, and t as an entry in vector $\mathbf{b}$ [8]. As a result, the right representation only represents uncertainty in matrix $\mathbf{A}$. However, for clarity, the derivation is continued with the middle formulation above, since in this research the risk is concerned with uncertain local market price c. The uncertainty is represented as $\tilde{\mathbf{c}}$, where N historical observations make up potential realizations of $\tilde{\mathbf{c}}$: $\mathbf{c_1}, ..., \mathbf{c_N}$ [13].

In order to incorporate the risk-attitude of the decision maker, a numerical value $\mu(\tilde{\mathbf{c}}'\mathbf{x})$ is assigned to the random variable $\tilde{\mathbf{c}}'\mathbf{x}$ [23]. Here, the function μ serves as the *risk measure*, symbolizing the risk attitude of the decision-maker [13]. Equation 6.14 represents the incorporated risk measure in the optimization problem:

$$\begin{aligned} &\min_x \ t \\ &\text{s.t. } \mu(\tilde{\mathbf{c}}'\mathbf{x}) \leq t, \\ &\quad \mathbf{A}\mathbf{x} \leq \mathbf{b} \\ &\quad \mathbf{x} \in \mathcal{X} \end{aligned} \tag{6.14}$$

6.2.1 Risk measures

Let $\mathcal{S}$ be an almost surely bounded random variable, and $\mathcal{R}$ denote the space of real numbers. In addition, let X and Y represent realizations of uncertainty, where these random variables can signify either loss or gain. Then, any function μ: $\mathcal{S} \rightarrow \mathcal{R}$ can theoretically be regarded as a risk measure [17]. The practical interpretation of a risk measure can be defined as the minimal capital necessary to adjust a position X to a level where it becomes "acceptable" in terms of risk tolerance [8, 9, 3]. Nevertheless, some risk measures make more sense than others. Generally, a risk measure is subject to two axioms, namely *monotonicity* and *translation invariance* [8, 13, 9].

- **Monotonicity**: if $X \leq Y$ almost surely, then $\mu(X) \leq \mu(Y),\ \forall X, Y \in \mathcal{S}$. This axiom represents the case where the random variable X is consistently smaller than random variable Y, meaning that the risk measure of random variable X is also lower than that of Y [17]. In this context, the realization of uncertainty represents loss, where lower loss results in less risk.
- **Translation invariance**: $\mu(X + a) = \mu(X) - a,\ \forall X \in \mathcal{S},\ a \in \mathcal{R}$. This axiom represents the case where a deterministic amount a is added to the uncertain random variable X. Consequently, the capital requirement is reduced by the exact amount a, since a is a real, deterministic number.

Value-at-Risk
A widely used risk measure is **Value-at-risk (VaR)**[86, 74, 8]. VaR is defined as a value z, such that the probability of obtaining less profit than z is less than 1 - α [23]. The formula of VaR is commonly defined as follows, similar to [90, 83, 87, 22, 77, 20, 23]. Let random variable X represent losses, with cumulative distribution function $F_X(z) = \mathbb{P}\{X \leq z\}$. Then, with confidence level $\alpha \in (0, 1]$, VaR is defined as:

$$\text{VaR}_\alpha(X) = \min\{z | F_X(z) \geq \alpha\} \tag{6.15}$$

In the case of a confidence level of 0.95, 95% of the uncertain realizations yield fewer losses than the VaR, while 5% of the uncertain realizations result in greater losses than the VaR [51]. It is important to note here that loss is defined in relation to the *expected* value of the uncertainty. VaR indicates potential losses due to local market price fluctuations [51]. However, VaR encounters difficulties that restrict the functional use of VaR as a risk measure:

- VaR can properly be used when the uncertainty conforms to a (log)normal distribution. However, frequently, uncertainty does not adhere to a normal distribution, as loss distributions may exhibit "fat tails" [86]. When uncertainty follows an different distribution, optimization of VaR appears to be difficult due to instability and numerical difficulties [8, 86, 74].
- VaR does not incorporate the expected loss magnitude beyond the threshold amount (VaR) [86].
- The risk counterpart of the problem including the VaR risk measure can yield a non-convex problem, rendering it intractable [74].

Given the constraints of VaR and other risk measures that only adhere to the two mentioned axioms, the application of *coherent risk measures* proves to be more fitting for integrating risk management in the problem [3, 13].

6.2.2 Coherent risk measures

According to [74, 3, 17], coherent risk measures satisfy two additional axioms in addition to the axioms described above, namely *subadditivity* and *positive homogeneity*:

- **Subadditivity**: $\mu(X + Y) \leq \mu(X) + \mu(Y),\ \forall X, Y \in \mathcal{S}$. This axiom acknowledges that diversification of stochastic realizations results in an overall reduction in risk compared to considering individual uncertainty realizations separately [8].
- **Positive homogeneity**: $\mu(\lambda X) = \lambda\mu(X),\ \forall X \in \mathcal{S}, \lambda \geq 0$. This axiom stands for the fact that risk scales linearly with the size of random variable X [17]. Additionally, due to this axiom, the subadditivity axiom is equivalent to a convexity axiom [8].

The aforementioned four axioms applicable to coherent risk measures ensure the preservation of convexity of the problem. This is advantageous as convexity of the problem leads to computational tractability [8, 74]. Coherent risk measures are valuable for attaining conservative solutions, without compromising the convexity of the problem [8].

Intuitively, coherent risk measures represent the worst-case expected value over a family of distributions [13]. Mathematically, μ is a coherent risk measure function if and only if there exists a family of probability measures $\mathcal{Q}$ such that the following equation holds [17, 3, 13]:

$$\mu(X) = \sup_{q \in \mathcal{Q}} \mathbb{E}_q[X], \quad \forall X \in \mathcal{S} \tag{6.16}$$

In Equation 6.16, X represents a random variable, $\mathbb{E}_q[X]$ denotes the expected value of X given probability measure q [17]. The probability measure q in Equation 6.16 is part of the family of probability measures $\mathcal{Q}$. Then, Equation 6.16 illustrates that a coherent risk measure $\mu(X)$ can alternatively expressed in a dual form. This dual representation involves taking the worst-case expected value over a family $\mathcal{Q}$ of "generating measures" or "generalized scenarios" [17, 8]. According to [3], the family $\mathcal{Q}$ of "generating measures" in Equation 6.16 can be expressed as a set of "generalized scenarios" each representing a distinct probability measure q. Most importantly, a risk measure is coherent if and only if it can be expressed (via its dual form) into the worst-case expected value over a family of distributions $\mathcal{Q}$ [8].

For simplicity, let the historical observations of the uncertainty $\tilde{\mathbf{c}}$, $\mathbf{c_1}, ..., \mathbf{c_N}$ all have a probability of 1/N. In other words, all historical observations have equal probability [13]. Then, the coherent risk measure $\mu(\tilde{\mathbf{c}}'\mathbf{x})$ as generally formulated in Equation 6.16 can be rewritten into Equation 6.17, similar to [13, 17, 9, 8]. q represents a probability measure in the family of probability measures $\mathcal{Q}$.

$$\mu(\tilde{\mathbf{c}}'\mathbf{x}) = \sup_{q \in \mathcal{Q}} \mathbb{E}_q[\tilde{\mathbf{c}}'\mathbf{x}] = \sup_{q \in \mathcal{Q}} \sum_{i=1}^{N} (\mathbf{c}_i'\mathbf{x}) q_i = \sup_{q \in \mathcal{Q}} \left(\sum_{i=1}^{N} q_i \mathbf{c}_i \right)' \mathbf{x} = \sup_{c \in \mathcal{C}} \mathbf{c}'\mathbf{x}, \tag{6.17}$$

where

$$\mathcal{C} = conv \left(\left\{ \sum_{i=1}^{N} q_i \mathbf{c}_i \;\middle|\; \mathbf{q} \in \mathcal{Q} \right\} \right) \tag{6.18}$$

Note here that uncertainty set $\mathcal{C}$ in Equation 6.18 is either a subset of or equal to the convex hull of the historical observations $\mathbf{c}_1, ..., \mathbf{c}_N$. By incorporating Equation 6.17 into the minimization problem, an equivalent formulation is obtained from Equation 6.14:

$$\begin{aligned} \min_{x} \; & t \\ \text{s.t. } & \mathbf{c}'\mathbf{x} \leq t, \quad \forall c \in \mathcal{C} \\ & \mathbf{A}\mathbf{x} \leq \mathbf{b}, \\ & \mathbf{x} \in \mathcal{X} \end{aligned} \tag{6.19}$$

where $\mathcal{C}$ is represented by Equation 6.18.

Starting from a coherent risk measure μ as represented in Equation 6.14, Equation 6.19 now represents the equivalent robust optimization problem, including a unique convex (not necessarily polyhedral) uncertainty set $\mathcal{C}$ that incorporates deviating realizations of c [13, 17, 8]. The structure of the convex uncertainty set depends on the chosen coherent risk measure of the decision maker [17]. However, as discussed in Uncertainty set modeling, it is advantageous for a robust optimization problem to be formulated with a *polyhedral uncertainty set* [13]. In the upcoming section, a more specific subclass of coherent risk measures is introduced that allows the equivalence between risk measure formulation and a specific type of polyhedral uncertainty sets.

6.2.3 Comonotonic risk measures

In general, computation of the family of probability measures $\mathcal{Q}$ is complex [17]. In this subsection, a subclass of coherent risk measures is introduced, namely *comonotone risk measures*. When the risk measure μ is constructed as a comonotone risk measure, the family of probability measures

$\mathcal{Q}$ can be constructed in such a manner that the corresponding uncertainty set is a polyhedron [17, 13].

Next, the derivation of a comonotone risk measure is provided. Remember that a risk measure is a function μ: $\mathcal{S} \rightarrow \mathcal{R}$. A random variable X is comonotonic if its support $\mathcal{S}$ follows complete order structure: for any $\mathbf{x}, \mathbf{y} \in \mathcal{S}$, either $\mathbf{x} \leq \mathbf{y}$ or $\mathbf{y} \leq \mathbf{x}$ [13, 17]. Then, for any comonotonic random variables X and Y, if Equation 6.20 holds, the risk measure is said to be comonotonic:

$$\mu(X + Y) = \mu(X) + \mu(Y) \tag{6.20}$$

Unlike the axiom of subadditivity for coherent risk measures, where diversification typically results in overall reduced risk, for comonotonic risk measures, diversification does not imply risk reduction [17, 3].

Coherent and comonotonic risk measures formulate a class of polyhedral uncertainty sets in robust optimization [17]. The mathematical proof of reformulating the comonotonic and coherent risk measure into a class of polyhedral uncertainty sets for certain types of distributions is further elaborated in [17, 8, 13, 111]. Nevertheless, this result serves to bridge stochastic optimization and robust optimization together [111].

6.2.4 Conditional Value at Risk

Conditional Value at Risk (CvaR) is an important example of a coherent, comonotone risk measure utilized in the stochastic optimization models within this research. Hence, the formulation of CVaR in stochastic optimization is provided in Risk management in stochastic optimization. Overall, CVaR represents the conditional expectation of the profit, given that the profit is less than or equal to the VaR value. In other words, CVaR is the expected value of the worst (1 - α)×100 % cases of profit [8], where α denotes the confidence interval and lies between 0 and 1 [100]. The parameter α is used to reflect the risk attitude of the decision-maker, influencing the conservatism of the optimal solution. $\alpha = 1$ reflects solely the worst-case scenario of the profit realization. Conversely, setting $\alpha = 0$ yields CVaR as the mean value of all potential profit realizations [100]. Thus, a higher α implies a more risk-averse attitude of the decision-maker [100].

The risk measure CVaR offers several advantages over the regular VaR [90, 86]. Importantly, CVaR being a coherent risk measure ensures a convex, tractable problem formulation [90, 74, 86, 103, 79]. As mentioned in the Risk measures section, VaR does not quantify the expected loss beyond the threshold value, whereas CVaR effectively predicts the expected loss in the tail of the distribution [86, 103, 79]. The risk measure CVaR is defined in Equation 6.21, similar to [8, 9, 83]:

$$\mathrm{CVaR}_\alpha(X) = \mu(X) \triangleq \inf_{v \in \mathbb{R}} \left\{ v + \frac{1}{1-\alpha} \mathbb{E}\left[(X - v)^+\right] \right\} \tag{6.21}$$

for any $\alpha \in (0, 1]$. Here, X represents the random variable, and $[t]^+ = \max\{0, t\}$. To show the connection with VaR (Equation 6.15), CVaR can be similarly be described as [69, 83, 22]:

$$\mathrm{CVaR}_\alpha(X) = \mathbb{E}\left[X | X \geq \mathrm{VaR}_\alpha(X)\right] \tag{6.22}$$

On top of being coherent, CVaR is also comonotonic. As a result, the risk measure CVaR can equivalently be rewritten into a polyhedral uncertainty set in robust optimization [8]. As mentioned before, the uncertainty is represented in vector $\tilde{\mathbf{c}}$, with N data points $\{\mathbf{c}_1, ..., \mathbf{c}_N\}$ [100]. Each entry of $\mathbf{c}_i$ has corresponding probability $\mathbf{p}_i$ [9]. For the risk measure CVaR, the family of probability measures $\mathcal{Q}$ can be represented as [8, 9]:

$$\mathcal{Q} = \{\mathbf{q} \in \Delta^N \ : \ q_i \leq p_i/\alpha\} \tag{6.23}$$

In Equation 6.23, $\mathbf{q}$ denotes a probability distribution within the family of probability measures $\mathcal{Q}$. The term Δ^N refers to the probability simplex in an N-dimensional space, implying that each component of $\mathbf{q}$ is non-negative and the sum of all N components of element $\mathbf{q}$ is one. Then, $\mathcal{Q}$ is used to formulate the uncertainty set that corresponds to CVaR in robust optimization, as can be seen in Equation 6.24 [100, 13, 9, 8]. Note again that c represents the uncertainty vector, and c_i and c_j represent data points in that uncertainty vector. Also, α corresponds to the confidence level set by the decision-maker, where a higher value indicates a more conservative solution [100].

$$\mathcal{C} = conv\left(\frac{1}{1-\alpha}\sum_{i\in I} p_i c_i + \left(1 - \frac{1}{1-\alpha}\sum_{i\in I} p_i\right) c_j \;\; : \right.$$
$$\left. I \subseteq \{1,...,N\}, j \in \{1,...,N\}\backslash I \;,\; \sum_{i\in I} p_i \leq 1-\alpha \right\}\Bigg) \tag{6.24}$$

The set described in Equation 6.24 forms a *polytope*, meaning that the robust optimization problem as formulated in Equation 6.25 can be rewritten into a linear program [9, 8]. Moreover, when setting the probability of each historical observation c_i to have equal probability ($p_i = 1/N$), and $\alpha = j/N$ for some $j \in \mathbb{Z}_+$, the uncertainty set $\mathcal{C}$ outlined in Equation 6.24 can be interpreted as the convex hull of all j-point averages of the historical observations of the uncertainty $\mathbf{c}_1, ..., \mathbf{c}_N$ [9, 8]. Lastly, Equation 6.24 can be inserted as uncertainty set in a robust optimization problem as follows:

$$\begin{aligned} &\min_x \; t \\ &\text{s.t. } \mathbf{c}'\mathbf{x} \leq t, \quad \forall c \in \mathcal{C} \\ &\quad \mathbf{A}\mathbf{x} \leq \mathbf{b}, \\ &\quad \mathbf{x} \in \mathcal{X} \end{aligned} \tag{6.25}$$

To sum up, uncertainty sets to represent price uncertainty in robust optimization can be constructed by using coherent and comonotonic risk measures. Risk management in stochastic optimization derives how the CVaR risk measure can be incorporated in stochastic programming. On the other hand, as elaborated in this chapter, CVaR is a coherent and comonotone risk measure that can be equivalently written into a polyhedral uncertainty set in the robust optimization problem in Equation 6.25 [8]. The polyhedral uncertainty set representing CVaR in robust optimization is formulated in Equation 6.24. Consequently, the uncertainty set derived in Conditional Value at Risk is different from the (box interval) uncertainty set derived in Uncertainty set modeling. In Uncertainty set modeling, the size of the uncertainty set is constructed and afterward the budget of uncertainty parameter is adjusted to adjust the risk attitude of the agent. In Conditional Value at Risk, the uncertainty set is constructed incorporating the decision maker's risk attitude.

7 Stochastic optimization applied to battery asset modeling

This chapter introduces the two stochastic optimization models developed in this research. Both stochastic optimization models are *risk-neutral* by nature, because a stochastic program represents the *expected profit* in the objective function [99]. After introducing the risk-neutral SO models, this chapter extends both models to incorporate risk management, applying the theoretical framework provided in Risk management in stochastic optimization.

Based on the scenario generation and reduction technique as described in Scenario-based modeling of price uncertainty, the final product of the scenario-based modeling method is a set of reduced scenarios Ω_S^*, each scenario with obtained optimal probability π_ω^*. This set of scenarios represents possible realizations of the local market price, for the day-ahead window (24 hours). Then, the objectives of the battery models are to maximize the revenue from discharging the battery, while minimizing the costs of charging the battery [110, 105, 102]. Hence, the models can be formulated as maximization or minimization problems. The uncertainty of the LEM price is only present in the objective function of the stochastic programs.

Two bid types are considered in this research, however, only one of them is used for the bidding strategies for the agent owning the BESS participating in the day-ahead LEM. For *price-quantity point bids*, clearance of the bid depends on the local market clearing price [59]. Namely, when the local market clearing price is higher (lower) than the submitted price of the charging (discharging), the bids are not cleared in the LEM [59]. This is also called economic bidding [59]. On the other hand, *self-scheduled bids* are cleared regardless of the realization of the local market clearing price [59, 50, 72]. When an agent submits a self-schedule bid, the agent is willing to supply/buy energy regardless of the energy price [72]. According to [59, 50], submitting a single price-quantity point per time step results in higher profit compared to submitting one self-scheduled bid per time step. Hence, the models developed in this research submit price-quantity point bids (economic bids), rather than self-scheduled bids.

7.1 Model 1: single bid (base model)

The risk-neutral SO model 1 is based on [50, 110], and serves as a benchmark in this research. In SO model 1, the charging and discharging decision variables of the BESS (x_t^d and x_t^c) have only time in their index, meaning that for every time t, one (dis)charging bid can be submitted to the market operator. All scenarios ω belonging to the reduced scenario set Ω_S^* represent a local market price realization for every time step t. In the objective function (Equation 7.1), $c_{t,\omega}$ represents the forecasted local market price for scenario ω. A realization of scenario $\omega = 1$, obtaining the local market price forecast for day-ahead hours T = 1 until T = 24 is represented as $c_{t,1} = [c_{1,1}\ c_{2,1}\ c_{3,1}\ ...\ c_{24,1}]$. The (dis)charging quantities of the battery (x_t^d and x_t^c) are submitted to the day-ahead market as price-quantity points, meaning the bids have both a price and a quantity. In SO model 1, the bid price that corresponds to a (dis)charging quantity at time t is the *expected price* at time t ($\hat{c}_t = \sum_{\omega \in \Omega_S} \pi_\omega^* c_{t,\omega}$). Finally, the objective function of the SO model 1 (the base model) is formulated as a minimization problem in Equation 7.1, multiplying the bid prices with the bid quantities:

$$\min_{x^d, x^c, u} \sum_{\omega \in \Omega_S^*} \pi_\omega^* \sum_{t=1}^{T} c_{t,\omega} \left(x_t^c - x_t^d \right) \tag{7.1}$$

Next, the constraints of SO model 1 are derived from [110, 72, 44, 105, 59, 102, 19, 50]. SO model 1 incorporates the inability of the battery to submit opposing bids at time t [72, 110]. Hence, at time t the agent owning the battery asset can either submit a charging/buying bid (x_t^c) or a discharging/selling bid (x_t^d). This is ensured via the binary variable (u_t) [110, 105], where in this research $u_t = 0$ represents the charging mode of the battery, and $u_t = 1$ represents the discharging mode of the battery. The binary variable u_t forces the bidding quantity of the opposing state of

the battery at time t to zero. This is ensured via the following constraints:

$$x_t^c - x_{max}^c\,(1-u_t) \leq 0 \qquad \forall t$$
$$x_t^d - x_{max}^d\,u_t \leq 0 \qquad \forall t$$
$$u_t \in \{0,1\} \qquad \forall t$$
$$x_t^c, x_t^d \geq 0 \qquad \forall t$$

In these constraints, x_{max}^c and x_{max}^d represent the maximum charge and discharge rate of the battery, respectively [72, 105, 102]. Hence, when the agent submits a price-quantity point to the market operator, x_t^c and x_t^d cannot exceed these maximum (dis)charge rates.

Furthermore, the state of charge (SOC) variable (e_t) should remain within the capacity bounds of the battery (e_{min} and e_{max}) for the entire time horizon [72]. Lastly, η_d and η_c represent the discharging and charging efficiency of the battery and Δt represents the time step length [110, 105, 102, 50]. Mathematically, these constraints are represented as:

$$e_t = e_{t-1} + \eta_c\,\Delta t\,x_t^c - \frac{1}{\eta_d}\,\Delta t\,x_t^d \qquad \forall t$$
$$e_{min} \leq e_t \leq e_{max} \qquad \forall t$$

7.2 Model 1 with risk management

This chapter extends the risk-neutral SO model 1 as elaborated in Model 1: single bid (base model) to account for the risk-attitude of the agent owning the battery asset. Following the theoretical outline provided in Risk management in stochastic optimization, this chapter applies the provided risk theory to SO model 1. Firstly, SO model 1 is extended by incorporating the charging risk of the agent bidding in the day-ahead market via CVaR. Afterward, SO model 1 with discharging risk management via CVaR is considered. Lastly, simultaneous charging and discharging risk in SO model 1 is considered. While risk management for SO model 1 is similarly present in existing literature, this chapter provides a more extensive elaboration on the complete problem derivation.

In literature, CVaR has been widely implemented as a risk measure in linear programs in the context of price uncertainty in energy systems [108], for example in [110, 90, 103, 77, 20, 72, 89, 2, 55]. Scoping down and applying risk management on a battery asset operating in the energy market, literature is explored. For example, [110] incorporates the charging risk of a battery asset in stochastic optimization, but leaves the discharging risk for future work. The optimization model described in [110] has the ability to submit a single bid per time step, similar to SO model 1. [72] briefly describes adding risk management as a future direction, and briefly introduces CVaR as a risk measure. [55] also incorporates charging and discharging risk in a battery energy storage system, but with a different purpose. In this paper, not the trade-off between risk and profit is considered, but the focus lies on minimizing system operating costs. However, similar to SO model 1, one bid per time step can be submitted to the market. Then, [89] introduces CVaR for multiple BESS, and allows multiple values for ζ, one for each BESS. Similar to SO model 1 constructed in this research, the optimization model proposed in this paper enables one bid per time step for every battery energy storage system.

Adding the CVaR term to the objective function of SO model 1 ensures that the agent also cares about minimizing the average costs in scenarios that incur high loss [72, 55]. To add the CVaR risk measure to SO model 1, the minimization function $F_\alpha(x,\zeta)$ is derived for the single bid battery model application. Adapting the discrete minimization function in Equation 5.5 for the battery model with scenario-based modeling, the minimization function representing the CVaR is adapted to:

$$\min_{x^c,x^d,\zeta} F_\alpha(x^c,x^d,\zeta) = \zeta + \frac{1}{1-\alpha}\sum_{\omega\in\Omega_S^*}\pi_\omega\left[f(x^c,x^d,c_\omega)-\zeta\right]^+ \tag{7.2}$$

In Equation 7.2, $f(x^c, x^d, c_\omega)$ represents the loss function. c_ω represents the price uncertainty realization for scenario ω with corresponding probability π_ω, for the whole time horizon. The decision variables x_c and x_d are incorporated in the loss function because the loss function is a function of the bid quantities.

It is important to note that the loss function f(x,y) as first introduced in Equation 5.1 represents the loss function for the *whole* time horizon of a scenario realization (the aggregate). This is clearly illustrated in for example [39, 33]. In [33], the random variable y is represented as a factor in the "total wealth at the end of the examined period". In other words, the loss function is concerned with the totality of the examined period. In this research, x^c, x^d represent the decision variables of the charging and discharging quantities over the whole time horizon. In this research, y_k represents the LEM price scenario vector c_ω. k equals ω, namely a price scenario realization. A price scenario realization is a vector with length T. Hence, the loss function f(x,y) is the *aggregate* loss over the complete time horizon (1:T) of SO model 1.

Next, the minimization formula Equation 7.2 is represented as a system of inequalities, via the introduction of z_ω. Adding decision variable z_ω in the objective function and adding the two constraints in Equation 7.3, the problem remains a linear program. Linearity of the problem is desired for the tractability of the problem [110]. There are ω auxiliary variables z_ω, each of them representing $\max(0,\ f(x^c, x^d, z_\omega) - \zeta)$ of respective scenario ω. In the objective function of Equation 7.3, each value of z_ω is multiplied with its scenario probability to obtain the expected profit of the worst (1-α) $\times$ 100% of the uncertainty realizations. The battery model formulation in Equation 7.3 is used to extend the risk-neutral SO model 1 with a risk attitude:

$$\begin{aligned} \min_{x^c, x^d, \zeta} \quad & \left(\zeta + \frac{1}{1-\alpha} \sum_{\omega \in \Omega_S^*} \pi_\omega z_\omega \right) && \\ \text{s.t} \quad & f(x^c, x^d, c_\omega) - \zeta \leq z_\omega && \forall \omega \\ & z_\omega \geq 0 && \forall \omega \end{aligned} \tag{7.3}$$

In the next sections, the loss functions $f(x^c, x^d, z_\omega)$ in Equation 7.3 need further specification. In this research, the loss function can be two-fold. Namely, the loss is caused by high potential charging costs of the battery, as well as negative revenue in case of discharging the battery. The next sections describe the separate risks of charging and discharging, as well as the simultaneous risk. Namely, the loss function for charging risk, discharging risk, or simultaneous (dis)charging risk is different. Hence, in the application of the CVaR extensions for SO model 1 from Equation 7.3, the loss function construction, $f(x^c, x^d, c_\omega)$, needs adaptation.

7.2.1 SO Model 1 with battery charging risk

To add the CVaR risk measure to SO model 1, the additional minimization term from Equation 7.3 is added to the objective function. In Equation 7.1, the stochastic optimization is formulated as a minimization problem. Hence, the CVaR term appearing in the new objective function also represents a minimization problem, formulated as [110, 55, 89, 77]:

$$\min_{x^d, x^c, \zeta} \ \beta \left(\zeta + \frac{1}{1-\alpha} \sum_{\omega \in \Omega_S^*} \pi_\omega z_\omega \right) \tag{7.4}$$

In Equation 7.4, β is the risk parameter, representing the trade-off of the agent between minimizing risk and minimizing the expected value. In other words, β represents the trade-off between the expected profit of the agent and its profit variability [23]. The larger β, the more risk-averse the agent becomes, and more emphasis is put on the CVaR term. $\beta = 0$ represents a risk-neutral

attitude of the agent [72]. As a consequence of the construction of β in the final objective function (Equation 7.8), β lies within the range 0 and 1.

In addition, z_ω represent the auxiliary variables, represented for each scenario ω [110, 72]. The loss function $f(x^c, c_\omega)$ for charging risk is represented in Equation 7.5. Here, x^d is not present in the loss function, because the loss function is only concerned with charging bids. The risk of the set of decision variables x_t^c is represented for the scenario dependent LEM price forecast $c_{t,\omega}$.

$$f(x^c, c_\omega) = \sum_{t=1}^{T} c_{t,\omega} x_t^c \qquad \forall \omega \tag{7.5}$$

Hence, in the case of four scenarios $\omega = 1, 2, 3, 4$, the loss function is constructed for:

$$f(x^c, c_1) = \sum_{t=1}^{T} c_{t,1} x_t^c$$
$$f(x^c, c_2) = \sum_{t=1}^{T} c_{t,2} x_t^c$$
$$f(x^c, c_3) = \sum_{t=1}^{T} c_{t,3} x_t^c$$
$$f(x^c, c_4) = \sum_{t=1}^{T} c_{t,4} x_t^c$$

Equation 7.6 is the CVaR constraint that is needed to maintain the linearity of the model. The risk represents the chance of high charging costs in case of a high local market price $c_{t,\omega}$. Note here that ζ can be positive or negative.

$$z^\omega \geq \sum_{t=1}^{T} c_{t,\omega} x_t^c - \zeta \qquad \forall \omega \tag{7.6}$$

$$z^\omega \geq 0 \qquad \forall \omega \tag{7.7}$$

In optimality, z_ω is constructed as [23, 55]:

$$z_\omega = [f(x^c, c_\omega) - \zeta]^+ = \left[\sum_{t=1}^{T} c_{t,\omega} x_t^c - \zeta \right]^+$$

These values of z_ω for all scenarios ω are normalized in the objective function by multiplying them with their scenario probability. This is because each of the auxiliary variables z_ω is concerned with the loss function of *one* scenario, and the CVaR term in the objective function determines the *expected* profit in the worst $(1-\alpha) \times 100\%$ of the cases.

Together with the battery constraints as described in Model 1: single bid (base model), SO model 1 with the charging CVaR extension is formulated below. The formulation of SO model 1 with charging risk is similar to the risk formulation in [110].

$$\min_{x_t^c, x_t^d, u, \zeta} \; (1-\beta) \left(\sum_{\omega \in \Omega_S^*} \pi_\omega \sum_{t=1}^{T} c_{t,\omega} \left(x_t^c - x_t^d \right) \right) + \beta \left(\zeta + \frac{1}{1-\alpha} \sum_{\omega \in \Omega_S^*} \pi_\omega z_\omega \right) \tag{7.8}$$

$$\sum_{t=1}^{T} c_{t,\omega} x_t^c - \zeta \leq z_\omega \qquad \forall\omega \tag{7.9}$$

$$x_t^c - x_{max}^c (1 - u_t) \leq 0 \qquad \forall t \tag{7.10}$$

$$x_t^d - x_{max}^d u_t \leq 0 \qquad \forall t \tag{7.11}$$

$$e_t = e_{t-1} + \eta_c \Delta t x_t^c - \frac{1}{\eta_d} \Delta t x_t^d \qquad \forall t \tag{7.12}$$

$$e_{min} \leq e_t \leq e_{max} \qquad \forall t \tag{7.13}$$

$$u_t \in \{0, 1\} \qquad \forall t \tag{7.14}$$

$$x_t^c, x_t^d \geq 0 \qquad \forall t \tag{7.15}$$

$$z^\omega \geq 0 \qquad \forall\omega \tag{7.16}$$

$$\beta \in [0, 1] \tag{7.17}$$

$$\alpha \in (0, 1) \tag{7.18}$$

7.2.2 SO model 1 with battery discharging risk

This chapter represents the discharging risk of SO model 1 via the CVaR risk measure. The construction of SO model 1 with the discharging risk is very similar to the charging risk, the difference lies in the representation of the loss function $f(x^d, c_\omega)$ in the CVaR constraint. Note here that the loss function is only a function of x^d and c_ω, and x^c is not included. This is due to the fact that this section only incorporates the discharging risk of the model.

To follow the structure of SO model 1 as described in Model 1: single bid (base model), the objective function is formulated as a minimization problem, similar to [23, 20, 2]:

$$\min_{x_t^c, x_t^d, u, \zeta} (1 - \beta) \left(\sum_{\omega \in \Omega_S^*} \pi_\omega \sum_{t=1}^{T} c_{t,\omega} \left(x_t^c - x_t^d \right) \right) + \beta \left(\zeta + \frac{1}{1 - \alpha} \sum_{\omega \in \Omega_S^*} \pi_\omega z_\omega \right) \tag{7.19}$$

The loss function of discharging risk is represented as:

$$f(x^d, c_\omega) = -\sum_{t=1}^{T} c_{t,\omega} x_t^d \qquad \forall\omega \tag{7.20}$$

Similar to the loss function of charging risk (Equation 7.5), Equation 7.20 has one scenario dependent stochastic variable (uncertainty), the LEM price $c_{t,\omega}$. The risk of discharging is concerned with obtaining a lower revenue than expected, since the LEM price $c_{t,\omega}$ realization is lower than expected. Due to the minimization formulation, more loss results in a less negative loss function (larger value). Accordingly, the CVaR constraints are formulated as:

$$z_\omega \geq -\sum_{t=1}^{T} c_{t,\omega} x_t^d - \zeta \qquad \forall\omega \tag{7.21}$$

$$z_\omega \geq 0 \qquad \forall\omega \tag{7.22}$$

The formulation of ζ can be both positive or negative in the CVaR constraint, dependent on whether the sign of ζ in the objective function is negative or positive. Changing them both accordingly results in the same optimization problem results, but the sign of ζ reverses. This is allowed since VaR is defined relative to zero [87]. For coherence, the construction of ζ is kept the same throughout the research.

By construction of the stochastic program in case of discharging risk only, in optimality the auxiliary variable z_ω is equal to $\max(0, -\sum_{t=1}^{T} c_{t,\omega} x_t^d - \zeta)$:

$$z_\omega = [f(x^d, c_\omega) - \zeta]^+ = \left[-\sum_{t=1}^{T} c_{t,\omega} x_t^d - \zeta \right]^+ \tag{7.23}$$

7.2.3 SO model 1 with battery discharging and charging risk

The final extension of SO model 1 is to add simultaneous the discharging and charging risk CVaR to the optimization model. The formulation is again similar to the previous two sections, only the loss function in the CVaR constraint changes into Equation 7.24. The loss function of both discharging and charging risk consists of the addition of the two individual loss functions of previous two sections. Again, there are ω realizations of the expected LEM price $c_{t,\omega}$, constructing ω loss functions $f(x^c, x^d, c_\omega)$.

$$f(x^c, x^d, c_\omega) = \sum_{t=1}^{T} c_{t,\omega} \left(x_t^c - x_t^d \right) \qquad \forall \omega \tag{7.24}$$

Implementing the system of inequalities as generally represented in Equation 7.3, the CVaR constraints become:

$$z_\omega \geq \sum_{t=1}^{T} c_{t,\omega} \left(x_t^c - x_t^d \right) - \zeta \qquad \forall \omega \tag{7.25}$$

$$z_\omega \geq 0 \qquad \forall \omega \tag{7.26}$$

By the construction of z_ω, as the system of inequalities represented in Equation 7.3, in optimality, the auxiliary variables has ω realizations equal to $\max(0, \sum_{t=1}^{T} c_{t,\omega}(x_t^c - x_t^d) - \zeta)$:

$$z_\omega = [f(x^c, x^d, c_\omega) - \zeta]^+ = \left[\sum_{t=1}^{T} c_{t,\omega}(x_t^c - x_t^d) - \zeta \right]^+ \tag{7.27}$$

The final stochastic optimization problem including CVaR for both discharging and charging risk is represented as:

$$\min_{x_t^c, x_t^d, u, \zeta} (1-\beta) \left(\sum_{\omega \in \Omega_S^*} \pi_\omega \sum_{t=1}^{T} c_{t,\omega} \left(x_t^c - x_t^d \right) \right) + \beta \left(\zeta + \frac{1}{1-\alpha} \sum_{\omega \in \Omega_S^*} \pi_\omega z_\omega \right) \tag{7.28}$$

$$\sum_{t=1}^{T} c_{t,\omega} \left(x_t^c - x_t^d \right) - \zeta \leq z_\omega \qquad \forall \omega \tag{7.29}$$

$$x_t^c - x_{max}^c \left(1 - u_t\right) \leq 0 \qquad \forall t \tag{7.30}$$

$$x_t^d - x_{max}^d u_t \leq 0 \qquad \forall t \tag{7.31}$$

$$e_t = e_{t-1} + \eta_c \Delta t x_t^c - \frac{1}{\eta_d} \Delta t x_t^d \qquad \forall t \tag{7.32}$$

$$e_{min} \leq e_t \leq e_{max} \qquad \forall t \tag{7.33}$$

$$u_t \in \{0, 1\} \qquad \forall t \tag{7.34}$$

$$x_t^c, x_t^d \geq 0 \qquad \forall t \tag{7.35}$$

$$z^\omega \geq 0 \qquad \forall \omega \tag{7.36}$$

$$\beta \in [0, 1] \tag{7.37}$$

$$\alpha \in (0, 1) \tag{7.38}$$

7.3 Model 2: multiple bids

This chapter outlines the risk-neutral SO model 2, relaxing the constraint of being able to submit one price-quantity point per time step to the market operator. Risk-neutral SO model 2 is mainly based on [50], with some novel additions.

Model 1: single bid (base model) allows the agent to submit one (dis)charging price-quantity point to the market operator per time step, similar to [59]. According to [37], having more price-quantity points at the same time step results in equal or higher expected profit in the stochastic optimization model [50]. Hence, similar to [50], SO model 2 relaxes the constraint of only being able to bid one (dis)charging quantity-price point per time step to the market operator. For SO model 2, the agent wants to know the bidding quantity of power to be charged or discharged for *every* scenario in the reduced scenario set [23].

In SO model 2, the agent can submit a bid for every reduced scenario $\omega \in \Omega_S^*$, for every time step t. The bid price of a price-quantity point in SO model 2 is equal to the corresponding scenario price. The agent can submit multiple bids at the same time step, upper bounded by the number of reduced scenarios Ω_{S^*}. As a result, the discharging decision variable $x^d_{t,\omega}$ and the charging decision variable $x^c_{t,\omega}$ are matrices of size $T \times |\Omega_{S^*}|$. Note here that similar to SO model 1, the battery cannot submit both charging and discharging bids for the same time step. In the objective function (Equation 7.39), the total expected profit of the agent with the battery asset is determined, over the day-ahead time horizon. To align with the formulation of SO model 1, the problem is formulated as a minimization problem.

$$\max_{x^d,x^c} \sum_{\omega\in\Omega_S^*} \pi^*_\omega \left[\sum_{t=1}^{T} c_{t,\omega}\left(x^d_{t,\omega} - x^c_{t,\omega}\right)\right] \quad \Longleftrightarrow \quad \min_{x^d,x^c} \sum_{\omega\in\Omega_S^*} \pi^*_\omega \left[\sum_{t=1}^{T} c_{t,\omega}\left(x^c_{t,\omega} - x^d_{t,\omega}\right)\right] \tag{7.39}$$

7.3.1 Battery constraints

Similar to SO model 1, the battery constraints are derived from [110, 72, 44, 105, 59, 102, 19, 50]. For every time t and scenario ω, the binary variable u_t ensures the battery is either in a discharging or charging state [110, 72, 105]. Hence, SO model 2 can submit multiple charging or discharging price-quantity bids at time t. However, it is not allowed to submit price-quantity points at time t that are in opposing battery state. Hence, the binary variable only has subscript t. Similar to SO model 1, the binary variable u_t is a decision variable in the final stochastic optimization problem. The inability to submit opposing bids in SO model 2 is ensured via:

$$x^c_{t,\omega} - x^c_{max}(1-u_t) \leq 0, \qquad \forall t,\omega \tag{7.40}$$
$$x^d_{t,\omega} - x^d_{max}u_t \leq 0, \qquad \forall t,\omega \tag{7.41}$$
$$x^d_{t,\omega}, x^c_{t,\omega} \geq 0, \qquad \forall t,\omega \tag{7.42}$$
$$x^d_{max}, x^c_{max} \geq 0 \tag{7.43}$$
$$u_t \in \{0,1\} \qquad \forall t,\omega \tag{7.44}$$

In the constraints above, $x^c_{t,\omega}$ and $x^d_{t,\omega}$ are upper bounded by the maximum charging and discharging power of the battery x^c_{max} and x^d_{max}, respectively [110, 72, 105, 102]. The decision variables $x^c_{t,\omega}$ and $x^d_{t,\omega}$ are lower-bounded by zero.

Furthermore, $e_{t,\omega}$ represents the state of charge (SOC) for every *individual* scenario ω at every time step, meaning that within the time horizon of a scenario, the state of charge of the battery remains within the capacity bounds (e_{min} and e_{max}) [105, 50, 108]. For every scenario ω, a separate bidding schedule is created that remains within the state of charge boundaries of the battery. Similar to

SO Model 1, η_d and η_c represent the discharging and charging efficiency of the battery, and Δt represents the time step length [110, 105, 102, 50].

$$e_{t,\omega} = e_{t-1,\omega} + \eta_c x^c_{t,\omega} \Delta t - \frac{1}{\eta_d} x^d_{t,\omega} \Delta t, \quad \forall t, \omega \tag{7.45}$$

$$e_{min} \leq e_{t,\omega} \leq e_{max}, \quad \forall t, \omega \tag{7.46}$$

7.3.2 Monotonicity constraints of bidding curves

With the allowance of submitting multiple price-quantity points to the market operator, SO model 2 should create piece-wise constant, monotonic bidding curves for the selling and buying bids resulting from the model [36]. Hence, different day-ahead price realizations can result in different (dis)charging quantities submitted to the market at time t [23]. In the case of a selling/discharge curve, the bidding curve of the agent should be monotonically increasing (non-decreasing) [28]. In the case of a buying/charging curve, the bidding curve of the agent should be monotonically decreasing (non-increasing) [50, 23, 36]. A monotonically decreasing buying curve is represented as:

When having n price-quantity charge points $(P_0, x_0), (P_1, x_1), ..., (P_n, x_n)$*, monotonically decreasing means that* $P_0 \leq P_1 \leq ... \leq P_n$*, while* $x_0 \geq x_1 \geq ... \geq x_n$ [37].

Similar to [50], SO model 2 adds two decision variables, $\Delta x^c_{t,\omega}$ and $\Delta x^d_{t,\omega}$, that represent the incremental quantity increase of the bidding curve at time t for buying and selling price-quantity points in the day-ahead local electricity market. The monotonicity constraints for the bidding curve are elaborated for the buying curve to clarify the construction of the bidding curves for the agent. The monotonicity constraints for the selling (discharging) curve work in the exact opposite direction.

Constructing a monotonically decreasing bidding curve in the case of a charging state of the battery at time t is performed as follows:

- Sort the scenario price realizations $c_{t,\omega}$ at time t from low to high. Here, $O_{t,\omega}$ is used to represent the ranking of the scenario price realization, meaning that the lowest scenario price realization is ranked as $O_{t,\omega} = 1$ and the highest scenario price realization is ranked as $O_{t,\omega} = O^{max}_t$ [50].
- Two distinct scenarios (ω and ω') with the same price realization obtain the same ranking $O_{t,\omega} = O_{t,\omega}$. When having two equal price realizations, the scenario with the lowest index number is added to the distinct scenario subset Ω^{dist}_t. For example, when $\omega = 1$ and $\omega = 4$ have the same price realization for time t = 4, $\omega = 1$ is added to the distinct scenario set Ω^{dist}_4.
- Lastly, starting from O^{max}_t, the quantity $x^c_{t,\omega}$ is determined via the optimization model. Next, the scenario with the second highest price realization is considered, and again $x^c_{t,\omega}$ is constructed. For this scenario, the bid quantity equals the bid quantity of the O^{max}_t scenario plus its incremental quantity increase $\Delta x^c_{t,\omega}$. In other words, the bidding quantity of scenario ω at time step t is equal or larger than the buying bidding quantity of scenario ω', which is the scenario closest to ω with higher scenario price realization [50]. This iteration continues for all other scenarios, in descending price order.

Mathematically, the monotonicity constraints for the buying curve are ensured via [50]:

$$x^c_{t,\omega} = \Delta x^c_{t,\omega} \qquad \forall \omega \in \Omega^{dist}_t, t \ : \ O_{t,\omega} = O^{max}_t \tag{7.47}$$

$$x^c_{t,\omega} = x^c_{t,\omega'} + \Delta x^c_{t,\omega} \qquad \forall (\omega, \omega') \in \Omega^{dist}_t, t \ : \ O_{t,\omega'} = O_{t,\omega} + 1 \ \wedge \ 1 < O_{t,\omega'} \leq O^{max}_t \tag{7.48}$$

$$\Delta x^c_{t,\omega} \geq 0 \qquad \forall \omega \in \Omega^{dist}_t \tag{7.49}$$

The constraints above are illustrated in Figure 3. Here, the black price-quantity point is considered first, since this is the scenario with the highest price. Then the blue price-quantity point, and

lastly the red price-quantity point is considered. Note here that the blue price-quantity point has zero incremental quantity increase ($\Delta x^c_{t,\omega} = 0$ compared to the black price-quantity point. The red price-quantity point has a non-zero incremental quantity increase compared to the blue price-quantity point. Elaboration on the meaning of having (non-)zero incremental quantity increase $\Delta x^c_{t,\omega}$ and $\Delta x^d_{t,\omega}$ is stated in the Active price-quantity point constraints.

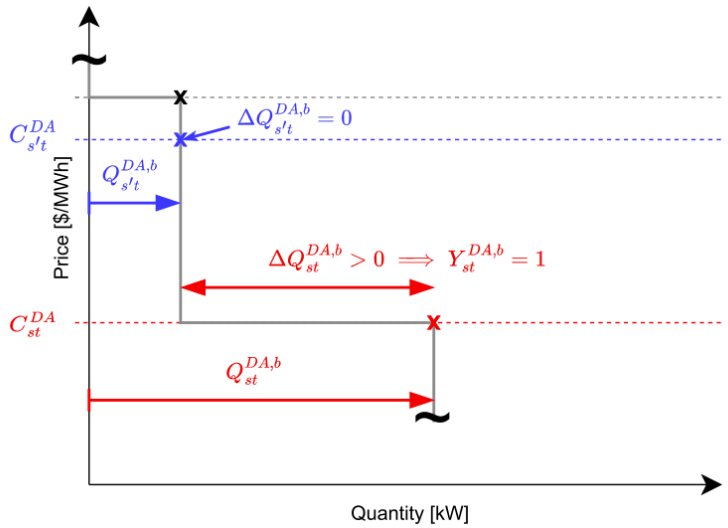

Figure 3: *Mathematical construction for buying price-quantity points of a buying curve [50]*

Similar constraints are constructed for the selling (discharge) monotonic bidding curve. Instead of iterating through the scenario realizations from the highest to the lowest scenario price, the selling bidding curve iterates through the scenarios from the lowest to the highest scenario prices. Hence, $O_{t,\omega}$ can be used reversely for the selling bidding curve. The mathematical construction of the constraints is represented as [50]:

$$x^d_{t,\omega} = \Delta x^d_{t,\omega} \qquad \forall \omega \in \Omega^{dist}_t, t \ : \ O_{t,\omega} = 1 \tag{7.50}$$

$$x^d_{t,\omega} = x^d_{t,\omega'} + \Delta x^d_{t,\omega} \qquad \forall (\omega, \omega') \in \Omega^{dist}_t, t \ : \ O_{t,\omega} = O_{t,\omega'} + 1 \ \wedge \ 1 < O_{t,\omega} \leq O^{max}_t \tag{7.51}$$

$$\Delta x^d_{t,\omega} \geq 0 \qquad \forall \omega \in \Omega^{dist}_t \tag{7.52}$$

7.3.3 Non-anticipativity constraints

The reduced scenario set Ω^*_S may have different scenarios with an *identical* local market price forecast at time t, denoted as $c_{t,\omega}$. The non-anticipativity constraints ensure that having an equal local market price prediction for two different scenarios at time t ($c_{t,\omega} = c_{t,\omega'}$) results in equal bidding quantity at time t ($x^c_{t,\omega} = x^c_{t,\omega'}$ and $x^d_{t,\omega} = x^d_{t,\omega'}$) for both price-quantity points for buying and selling power [23, 50, 28]. With this construction, ω is in the distinct scenario set, while ω' represents the scenarios not part of the distinct scenario set. As elaborated in Monotonicity constraints of bidding curves, the distinct scenario set (Ω^{dist}_t) is constructed with the notion that in case of similar price realizations for different scenarios, the scenario with the lowest index is added to the distinct scenario set Ω^{dist}_t. Hence, in the construction of the non-anticipativity constraints, having $c_{t,\omega} = c_{t,\omega'}$ automatically ensures that $\omega \in \Omega^{dist}_t$ and $\omega' \notin \Omega^{dist}_t$, as well as $\omega' > \omega$. Mathematically, the non-anticipativity constraints are constructed as [50]:

$$x^c_{t,\omega} = x^c_{t,\omega'} \qquad \forall \omega \in \Omega^{dis}_t, \ \omega' > \omega, \ t, \quad c_{t,\omega} = c_{t,\omega'} \tag{7.53}$$

$$x^d_{t,\omega} = x^d_{t,\omega'} \qquad \forall \omega \in \Omega^{dis}_t, \ \omega' > \omega, \ t, \quad c_{t,\omega} = c_{t,\omega'} \tag{7.54}$$

7.3.4 Active price-quantity point constraints

In Monotonicity constraints of bidding curves, the meaning of $\Delta x^c_{t,\omega}$ and $\Delta x^d_{t,\omega}$ is provided. In the constraints described in this section, the distinction between an *active* price-quantity point and an *inactive* price-quantity point is made.

When $\Delta x^c_{t,\omega}$ ($\Delta x^d_{t,\omega}$) exceeds the minimum threshold quantity (Δx_{min}), the price-quantity point of the corresponding bid is a *corner point* on the constructed buying (selling) curve. When a charging bid $\Delta x^c_{t,\omega}$ or a discharging bid $\Delta x^d_{t,\omega}$ exceeds the minimum threshold quantity, the price-quantity point of the corresponding bid is called an 'active' bid. When a charging bid $\Delta x^c_{t,\omega}$ or a discharging bid $\Delta x^d_{t,\omega}$ is lower than the minimum threshold quantity, the price-quantity point of the corresponding bid is called an 'inactive' bid [50]. Inactive price-quantity points do not creative new corner points on the bidding curves. For example, in Figure 3 the blue price-quantity point represents an inactive price-quantity point. As stated in [50], inactive price-quantity points do not add information to the bidding curves.

Two binary variables are introduced to represent whether the price-quantity point is active or inactive. $Y^c_{t,\omega}$ and $Y^d_{t,\omega}$ are equal to 1 in case of an active price-quantity point (meaning $\Delta x^c_{t,\omega} \geq \Delta x_{min}$ or $x^d_{t,\omega} \geq \Delta x_{min}$), and 0 in case of an inactive price-quantity point [50]. In Figure 3, the red price-quantity point has an incremental bidding quantity of non-zero. In addition, Δx_{min} is considered very small in this example. As a result, the red price-quantity point is an active price-quantity point. In the constraints below, the upper bound of the incremental bidding quantity $\Delta x^c_{t,\omega}$ and $\Delta x^d_{t,\omega}$ is represented by large numbers M^c_x and M^d_x, respectively [50].

Due to the Non-anticipativity constraints, different scenarios ω with the same local price prediction at time t are enforced to have the same bidding quantities ($x^c_{t,\omega}$ and $x^d_{t,\omega}$) [23, 50, 28]. The active price-quantity point constraints are constructed in a way that only scenarios in the distinct scenario set Ω^{dist}_t can have non-zero incremental bidding quantities ($\Delta x^c_{t,\omega}$ and $\Delta x^d_{t,\omega}$) and hence be active price quantity points. To illustrate, having two scenarios ω and ω' with equal price prediction for time t, where $\omega' > \omega$, the scenario with the lowest index number (ω) can be an active price-quantity point, while the scenario with the higher index number (ω') is never an active price-quantity point.

Mathematically, the active price-quantity point constraints are represented as [50]:

$$\Delta x_{min}\ Y^c_{t,\omega} \leq \Delta x^c_{t,\omega} \leq M^c_x\ Y^c_{t,\omega} \qquad \forall \omega \in \Omega^{dist}_t,\ t \tag{7.55}$$

$$\Delta x_{min}\ Y^d_{t,\omega} \leq \Delta x^d_{t,\omega} \leq M^d_x\ Y^d_{t,\omega} \qquad \forall \omega \in \Omega^{dist}_t,\ t \tag{7.56}$$

7.3.5 State of charge constraint of active price-quantity points

The SO models considered in this research only consider a BESS asset for a single agent. Hence, after constructing the bidding curves for the agent owning the battery, the battery should remain within its capacity bounds (e_{min} and e_{max}) during the whole time horizon. After all, the battery cannot discharge more than the capacity that empties the battery at time t.

As previously described in the state of charge constraint Equation 7.45, every scenario in itself should remain within the capacity bounds of the battery during the whole time horizon. If this is not the case, the limitation arises that there is an asymmetrical incentive for charging and discharging the battery. If not every individual scenario should remain within the capacity bounds of the battery, there is an incentive to have multiple discharging bids at time t because this directly adds revenue to the agent. However, in the charging state of the battery, the agent would never submit multiple price-quantity points at time t since this only adds costs to the objective function. Hence, it is important to have a state of charge constraint for every scenario separately ($e_{t,\omega}$. However, since the BESS asset is the only asset considered in this research, there should also be a constraint that targets the capacity of the battery from an aggregate perspective. Hence, this SoC (e_t) targets the overall state of charge constraint for the time horizon. This is different from the bidding model constructed in [50], where multiple assets are considered.

When actually submitting the price-quantity points to the market operator, care should be given to the active price-quantity points that represent the corner points on the bidding curves. *It is*

important to note that the actual price-quantity points that are submitted to the market operator are the incremental quantity increases ($\Delta x^c_{t,\omega}$ and $\Delta x^d_{t,\omega}$) together with their corresponding scenario prices. Hence, the state of charge over time e_t, dropping the scenario index, is influenced by the incremental quantities of the price-quantity points ($\Delta x^c_{t,\omega}$ and $\Delta x^d_{t,\omega}$).

$$e_t = e_{t-1} + \eta_c \Delta t \sum_{\omega \in \Omega_t^{dis}} \Delta x^c_{t,\omega} - \frac{1}{\eta_d} \Delta t \sum_{\omega \in \Omega_t^{dis}} \Delta x^d_{t,\omega} \qquad \forall t \tag{7.57}$$

$$e_{min} \leq e_t \leq e_{max} \qquad \forall t \tag{7.58}$$

7.3.6 SO model 2 mathematical overview

$$\min_{x^d, x^c} \sum_{\omega \in \Omega_S^*} \pi^*_\omega \left[\sum_{t=1}^{T} c_{t,\omega} \left(x^c_{t,\omega} - x^d_{t,\omega} \right) \right] \tag{7.59}$$

Battery constraints

$$\begin{cases} x^c_{t,\omega} - x^c_{max}(1 - u_t) \leq 0, & \forall t, \omega \\ x^d_{t,\omega} - x^d_{max} u_t \leq 0, & \forall t, \omega \\ x^d_{t,\omega}, x^c_{t,\omega} \geq 0, & \forall t, \omega \\ x^d_{max}, x^c_{max} \geq 0 & \\ u_t \in \{0, 1\} & \forall t, \omega \\ e_{t,\omega} = e_{t-1,\omega} + \eta_c x^c_{t,\omega} \Delta t - \dfrac{1}{\eta_d} x^d_{t,\omega} \Delta t, & \forall t, \omega \\ e_{min} \leq e_{t,\omega} \leq e_{max}, & \forall t, \omega \end{cases}$$

Monotonicity constraints

$$\begin{cases} x^c_{t,\omega} = \Delta x^c_{t,\omega} & \forall \omega \in \Omega_t^{dist}, t \ : \ O_{t,\omega} = O_t^{max} \\ x^c_{t,\omega} = x^c_{t,\omega'} + \Delta x^c_{t,\omega} & \forall (\omega, \omega') \in \Omega_t^{dist}, t \ : \ O_{t,\omega'} = O_{t,\omega} + 1 \ \wedge \ 1 < O_{t,\omega'} \leq O_t^{max} \\ \Delta x^c_{t,\omega} \geq 0 & \forall \omega \in \Omega_t^{dist} \\ x^d_{t,\omega} = \Delta x^d_{t,\omega} & \forall \omega \in \Omega_t^{dist}, t \ : \ O_{t,\omega} = 1 \\ x^d_{t,\omega} = x^d_{t,\omega'} + \Delta x^d_{t,\omega} & \forall (\omega, \omega') \in \Omega_t^{dist}, t \ : \ O_{t,\omega} = O_{t,\omega'} + 1 \ \wedge \ 1 < O_{t,\omega} \leq O_t^{max} \\ \Delta x^d_{t,\omega} \geq 0 & \forall \omega \in \Omega_t^{dist} \end{cases}$$

Non-anticipativity constraints

$$\begin{cases} x^c_{t,\omega} = x^c_{t,\omega'} & \forall \omega \in \Omega_t^{dis}, \ \omega' > \omega, \ t, \quad c_{t,\omega} = c_{t,\omega'} \\ x^d_{t,\omega} = x^d_{t,\omega'} & \forall \omega \in \Omega_t^{dis}, \ \omega' > \omega, \ t, \quad c_{t,\omega} = c_{t,\omega'} \end{cases}$$

Active price-quantity point constraints

$$\begin{cases} \Delta x_{min} \ Y^c_{t,\omega} \leq \Delta x^c_{t,\omega} \leq M^c_x \ Y^c_{t,\omega} & \forall \omega \in \Omega_t^{dis}, \ t \\ \Delta x_{min} \ Y^d_{t,\omega} \leq \Delta x^d_{t,\omega} \leq M^d_x \ Y^d_{t,\omega} & \forall \omega \in \Omega_t^{dis}, \ t \end{cases}$$

State of charge constraints of active price-quantity points

$$\begin{cases} e_t = e_{t-1} + \eta_c \Delta t \sum_{\omega \in \Omega_t^{dis}} \Delta x^c_{t,\omega} - \dfrac{1}{\eta_d} \Delta t \sum_{\omega \in \Omega_t^{dis}} \Delta x^d_{t,\omega} & \forall t \\ e_{min} \leq e_t \leq e_{max} & \forall t \end{cases}$$

7.4 Model 2 with risk management

This chapter extends the risk-neutral SO model 2 as elaborated in Model 2: multiple bids to account for the risk-attitude of the agent owning the battery asset. SO model 2 allows submitting multiple bids at the same time step, one for every reduced scenario $\omega \in \Omega_S^*$. The objective function and constraints for the risk-neutral SO model 2 are represented in SO model 2 mathematical overview. Similar to Model 1 with risk management, this chapter starts with formulating the stochastic problem with charging risk, then discharging risk, and lastly with simultaneous charging and discharging risk. Adding risk to SO model 2 is newly derived in this research.

Examining existing literature on risk management for a stochastic bidding model that allows for multiple price-quantity point submissions per time step, literature is limited. [2] serves as a base for the risk management extension of SO model 2 since this paper has the ability to submit multiple bids per time step. In [2], a wind power producer with a battery energy storage system (BESS) participates in the day-ahead and real-time energy market. Risk management is added to deal with uncertain wind power generation and electricity prices. Lastly, [108] formulates CVaR for an integrated energy system, including amongst others a battery storage system, where the problem is formulated as a two-stage optimization problem. Similar to [2], SO model 2 can submit multiple bids per time step.

The methodology of adding the risk attitude of the agent to SO model 2 is very similar to Model 1 with risk management. The difference between these models is that SO model 1 considers the decision variables x_t^c and x_t^d, while SO model 2 considers $x_{t,\omega}^c$ and $x_{t,\omega}^d$. Consequently, the loss functions $f(x^c, x^d, z_\omega)$ are different for SO models 1 and 2, since the expected costs are constructed differently (Equation 7.1 and Equation 7.39). The meaning of a bid quantity $x_{t,\omega}^c$ or $x_{t,\omega}^d$ is interpreted in a different way than for SO model 1 (x_t^c, x_t^d). Namely, SO model 2 allows multiple price-quantity points per time step, where the increments of the price-quantity points are the actual bid quantities submitted to the market operator. As a result, the CVaR constraint that is added to maintain the linearity of the problem is formulated differently from SO model 1 with risk management, because of the difference in the loss function construction f(x,y).

Similar to Model 1 with risk management, the loss functions are different for charging risk, discharging risk, and simultaneous charging and discharging risk. Despite the different loss functions, the CVaR term that is added to the objective function of SO model 2 is similar to Model 1 with risk management. The general form of incorporating CVaR into a stochastic program is introduced in Model 1 with risk management, and is also applicable for SO model 2 with risk management. The general formulation is represented in Equation 7.3, containing an additional objective term and two constraints. In the following sections, the loss functions require more specification.

As mentioned in Model 1 with risk management, the loss function $f(x^c, x^d, c_\omega)$ constructs the loss over the *aggregate* time horizon (t = 1:T). This also applies to the CVaR formulation in SO model 2. As a result, z_ω remains with only the scenario index in SO model 2, and ζ remains to be one value, which equals the VaR in optimality [86, 90]. The following sections derive the loss functions specifically for the incorporated type of risk; charging risk, discharging risk, and simultaneous charging and discharging risk, and formulate the stochastic programs accordingly.

7.4.1 SO model 2 with battery charging risk

To illustrate the construction of the loss function for SO model 2 with charging risk (f(x^c, c_ω)), an example is constructed. Suppose scenarios $\omega = 1, 2, 3$ are present and only one time step is considered. Hence, the aggregate of the loss function consists of time step 1 only. Only charging risk is considered here, potentially having bid quantities $x_{1,1}^c$, $x_{1,2}^c$, and $x_{1,3}^c$. The expected costs are calculated as:

$$\begin{aligned} \text{exp. costs} &= \sum_{\omega \in 1,2,3} \pi_\omega c_{t,\omega} x_{t,\omega}^c \\ &= \pi_1 c_{1,1} x_{1,1}^c + \pi_2 c_{1,2} x_{1,2}^c + \pi_3 c_{1,3} x_{1,3}^c \end{aligned} \tag{7.60}$$

In Equation 7.60, the three scenario price realizations $c_{1,1}, c_{1,2}$, and $c_{1,3}$ are used to construct the expected costs. However, for the construction of the loss function *all* the bids of time step 1 will acquire only *one* scenario price realization (either $c_{1,1}, c_{1,2}$, or $c_{1,3}$), against which all the bids of time step 1 will be submitted.

Hence, the construction of the loss function $f(x^c, c_1)$ for scenario 1 is constructed in Equation 7.61. Here, the three terms all have the same uncertainty realization, namely $c_{1,1}$. Here, for the loss function in Equation 7.61, the sum of π_ω is equal to 1, meaning that *all* charging bid quantities $(x^c_{1,\omega})$ are taken into account. However, it is important to note that not all price scenario realizations are taken into account into Equation 7.61. The scenario price is the uncertainty in the loss function, and hence there are ω different loss functions to be constructed, one for each scenario price.

$$f(x^c, c_1) = \pi_1 c_{1,1} x^c_{1,1} + \pi_2 c_{1,1} x^c_{1,2} + \pi_3 c_{1,1} x^c_{1,3} \tag{7.61}$$

For completeness, the loss functions of scenarios 2 and 3 are presented below:

$$f(x^c, c_2) = \pi_1 c_{1,2} x^c_{1,1} + \pi_2 c_{1,2} x^c_{1,2} + \pi_3 c_{1,2} x^c_{1,3} \tag{7.62}$$

$$f(x^c, c_3) = \pi_1 c_{1,3} x^c_{1,1} + \pi_2 c_{1,3} x^c_{1,2} + \pi_3 c_{1,3} x^c_{1,3} \tag{7.63}$$

To generalize above example, the loss function for charging risk in SO model 2 is expressed as:

$$f(x^c, c_\omega) = \sum_{t=1}^{T} c_{t,\omega} \left[\sum_{\omega \in \Omega_S^*} \pi_\omega x^c_{t,\omega} \right] \qquad \forall \omega \tag{7.64}$$

In Equation 7.65, the uncertainty c_ω is outside of the scenario aggregation $\sum_{\omega \in \Omega_S^*} \pi_\omega x^c_{t,\omega}$, since a loss function realization $f(x^c, c_\omega)$ of uncertainty c_ω represents *one* scenario realization. Still, within one loss function realization, it is important to take into account *all* scenario charging bids $x^c_{t,\omega}$, normalizing them with corresponding scenario probability. To clarify, instead of using ω, ω' is used to represent the scenario probabilities in Equation 7.65. This is done to illustrate that the probabilities used in the $\sum_{\omega \in \Omega_S^*}$ term are different from the probability used in $c_{t,\omega}$. However, it should be noted that it holds that $\omega, \omega' \in \Omega_S^*$. Adding the prime to the ω symbol is purely illustrative, but does not change the scenario set and corresponding probabilities.

$$f(x^c, c_\omega) = \sum_{t=1}^{T} c_{t,\omega} \left[\sum_{\omega' \in \Omega_S^*} \pi_{\omega'} x^c_{t,\omega'} \right] \qquad \forall \omega \tag{7.65}$$

Then, similar to SO model 1, the construction of z_ω in optimality is equal to:

$$z_\omega = [f(x^c, c_\omega) - \zeta]^+ = \left[\sum_{t=1}^{T} c_{t,\omega} \left(\sum_{\omega' \in \Omega_S^*} \pi_{\omega'} x^c_{t,\omega'} \right) - \zeta \right]^+ \qquad \forall \omega \tag{7.66}$$

z_ω is constructed with the loss function $f(x^c, c_\omega)$ of only the price uncertainty of particular scenario ω: $c_{t,\omega}$. Since price uncertainty $c_{t,\omega}$ corresponds to specific scenario probability π_ω, the values of z_ω are scenario dependent, and need to be normalized in the objective function to incorporate the scenario probability of a certain scenario price $c_{t,\omega}$. This explains the 'double' presence of π_ω, both present in the objective function (Equation 7.67) and the CvaR constraint (Equation 7.68). In the CvaR constraint Equation 7.68, all scenarios ω' are considered in the term $\sum_{\omega' \in \Omega_S^*} \pi_{\omega'} x^c_{t,\omega'}$, due to incorporating *all* charging bids at time t. In Equation 7.68, $c_{t,\omega}$ is outside of this inner term, and hence the scenario price $c_{t,\omega}$ is for a specific ω, with scenario probability π_ω. This is normalized in the objective function to construct the expected costs in the worst $(1-\alpha) \times 100\%$ cases. Similar

to Model 1 with risk management, the construction of β in the objective function adjusts the risk attitude of the agent.

Besides these additions, the constraints represented in SO model 2 mathematical overview remain.

$$\min_{x_t^c, x_t^d, u, \zeta} \; (1-\beta)\left(\sum_{\omega\in\Omega_S^*} \pi_\omega \sum_{t=1}^{T} c_{t,\omega}\left(x_{t,\omega}^c - x_{t,\omega}^d\right)\right) + \beta\left(\zeta + \frac{1}{1-\alpha}\sum_{\omega\in\Omega_S^*} \boldsymbol{\pi_\omega} z_\omega\right) \tag{7.67}$$

$$z_\omega \geq \left[\sum_{t=1}^{T} c_{t,\omega}\left(\sum_{\omega'\in\Omega_S^*} \boldsymbol{\pi_{\omega'}} x_{t,\omega'}^c\right)\right] - \zeta \qquad \forall\omega \tag{7.68}$$

$$z_\omega \geq 0 \qquad \forall\omega \tag{7.69}$$

7.4.2 SO model 2 with battery discharging risk

SO model 2 with battery discharging risk is equal to SO model 2 with battery charging risk, apart from the loss function representing a different function. The objective function and two CVaR constraints as represented in Equation 7.3 also apply to SO model 2 with discharging risk. To construct the loss function for the discharging risk, it is important to recognize that the example from the charging risk section of SO model 2 also applies to the discharging risk. Hence, full elaboration on the construction of the loss function of SO model 2 can be found in SO model 2 with battery charging risk. However, the distinction between the loss function of charging risk and discharging risk is that only discharging bids are taken into account in the loss function $f(x^d, c_\omega)$, and not charging bids. Hence, the loss function of the battery discharging risk is represented as:

$$f(x^d, c_\omega) = -\sum_{t=1}^{T} c_{t,\omega}\left(\sum_{\omega'\in\Omega_S^*} \pi_{\omega'} x_{t,\omega'}^d\right) \qquad \forall\omega \tag{7.70}$$

Similar to the charging risk, ω' is used to illustrate the difference between the scenarios within the aggregate term $\sum_{\omega'\in\Omega_S^*}$ and the single scenario meant for the LEM price uncertainty $(c_{t,\omega})$. By construction, z_ω represents $\max(0, -\sum_{t=1}^{T} c_{t,\omega} \sum_{\omega'\in\Omega_S^*} \pi_{\omega'} x_{t,\omega'}^d - \zeta)$. Alternatively written, z_ω is represented as:

$$z_\omega = [f(x^d, c_\omega) - \zeta]^+ = \left[-\sum_{t=1}^{T} c_{t,\omega}\left(\sum_{\omega'\in\Omega_S^*} \pi_{\omega'} x_{t,\omega'}^d\right) - \zeta\right]^+ \qquad \forall\omega \tag{7.71}$$

To conclude, the objective function and the two CVaR constraints are represented next, incorporating the loss function from Equation 7.70:

$$\min_{x_t^c, x_t^d, u, \zeta} \; (1-\beta)\left(\sum_{\omega\in\Omega_S^*} \pi_\omega \sum_{t=1}^{T} c_{t,\omega}\left(x_{t,\omega}^c - x_{t,\omega}^d\right)\right) + \beta\left(\zeta + \frac{1}{1-\alpha}\sum_{\omega\in\Omega_S^*} \pi_\omega z_\omega\right) \tag{7.72}$$

$$z^\omega \geq \left[-\sum_{t=1}^{T} c_{t,\omega}\left(\sum_{\omega'\in\Omega_S^*} \pi_{\omega'} x_{t,\omega'}^d\right)\right] - \zeta \qquad \forall\omega$$

$$z^\omega \geq 0 \qquad \forall\omega$$

The rest of the original constraints in SO model 2 mathematical overview remain.

7.4.3 SO model 2 with battery discharging and charging risk

The final extension of SO model 2 is to incorporate simultaneous charging and discharging risk of the battery. The loss function is different compared to the previous two sections. However, the objective function and two CVaR constraints from Equation 7.3 also apply for this extension. Elaboration on the construction of the loss function for SO model 2 is stated in SO model 2 with battery charging risk. The loss function is the summation of the two previous loss functions, for charging and discharging separately. Again, ω' is used to denote the difference between the one particular scenario meant in $c_{t,\omega}$ and the aggregate scenario term $\sum_{\omega' \in \Omega_S^*} \pi_{\omega'}(x^c_{t,\omega'} - x^d_{t,\omega'})$. Hence, the loss function for simultaneous charging and discharging risk is represented as:

$$f(x^c, x^d, c_\omega) = \sum_{t=1}^{T} c_{t,\omega} \left(\sum_{\omega' \in \Omega_S^*} \pi_{\omega'} \left(x^c_{t,\omega'} - x^d_{t,\omega'} \right) \right) \qquad \forall \omega \tag{7.73}$$

By construction, z_ω is introduced to linearize the problem, and can be formulated as $\max(0, \sum_{t=1}^{T} c_{t,\omega} \sum_{\omega' \in \Omega_S^*} \pi_{\omega'} \left(x^c_{t,\omega'} - x^d_{t,\omega'} \right) - \zeta)$. Alternatively written, z_ω is represented as:

$$z_\omega = [f(x^c, x^d, c_\omega) - \zeta]^+ = \left[\sum_{t=1}^{T} c_{t,\omega} \left(\sum_{\omega' \in \Omega_S^*} \pi_{\omega'} \left(x^c_{t,\omega'} - x^d_{t,\omega'} \right) \right) - \zeta \right]^+ \qquad \forall \omega \tag{7.74}$$

The rest of the original constraints in SO model 2 mathematical overview remain. The final objective function including the simultaneous charging and discharging risk term and the two CVaR constraints is represented as:

$$\min_{x^c_t, x^d_t, u, \zeta} \; (1-\beta) \left(\sum_{\omega \in \Omega_S^*} \pi_\omega \sum_{t=1}^{T} c_{t,\omega} \left(x^c_{t,\omega} - x^d_{t,\omega} \right) \right) + \beta \left(\zeta + \frac{1}{1-\alpha} \sum_{\omega \in \Omega_S^*} \pi_\omega z_\omega \right) \tag{7.75}$$

$$z^\omega \geq \left[\sum_{t=1}^{T} c_{t,\omega} \left(\sum_{\omega' \in \Omega_S^*} \pi_{\omega'} \left(x^c_{t,\omega'} - x^d_{t,\omega'} \right) \right) \right] - \zeta \qquad \forall \omega$$

$$z^\omega \geq 0 \qquad \forall \omega$$

8 Robust optimization applied to battery asset modeling

In this chapter, the general robust optimization model as derived in Uncertainty set modeling (Equation 6.13) is applied to model the robust problem of the agent owning the BESS asset, participating in the LEM day-ahead market. This application of the general robust optimization model is newly derived in this research.

In this section, two decision variables x_j^c and x_j^d are introduced, representing the non-negative charge and discharge quantities respectively. This is different from the formulation in Uncertainty set modeling, where x_j could take negative values. Similar to before, $\bar{c}_j$ represents the non-negative mean local electricity price, where d_j represents the non-negative deviation from the mean point forecast $\bar{c}_j$.

The goal of the optimization problem is to minimize the cost of charging the BESS, while maximizing the revenue obtained when discharging the battery [72]. Incorporating the price uncertainty in the robust optimization problem, similar to Uncertainty set modeling, the objective function of the robust optimization problem in the application of a BESS asset is formulated as:

$$\min_{x^d,x^c} \left(\sum_{j=1}^{n} \bar{c}_j \left(x_j^c - x_j^d\right) + \max_{z_0 \in \mathcal{Z}_0} \sum_{j=1}^{n} d_j x_j^c z_{0j} + \max_{z_0 \in \mathcal{Z}_0} \sum_{j=1}^{n} d_j x_j^d z_{0j} \right) \tag{8.1}$$

where $\mathcal{Z}_0$ is formulated as:

$$\mathcal{Z}_0 = \left\{ \mathbf{z_0} \;\middle|\; |z_{0j}| \leq 1, \forall j, \sum_{j=1}^{n} |z_{0j}| \leq \Gamma_0 \right\} \tag{8.2}$$

The interpretation of each term in Equation 8.1 is formulated as:

- $\bar{c}_j \left(x_j^c - x_j^d\right)$: this term represents the mean cost of charging and the mean revenue of discharging the BESS.
- $\max_{z_0 \in \mathcal{Z}_0} \sum_{j=1}^{n} d_j x_j^c z_{0j}$: this term represents the worst-case scenario of the charging cost x_j^c, where maximum cost is considered. In the case of the battery, worst-case charging cost is the result of a high local market price.
- $\max_{z_0 \in \mathcal{Z}_0} \sum_{j=1}^{n} d_j x_j^d z_{0j}$: this term represents the worst-case scenario of the discharging revenue, maximizing the loss from discharging the battery compared to the mean forecasted local price. This term works in the opposite of revenue, making it a positive term in Equation 8.1.

The next two subsections elaborate on the derivation of the objective function described in Equation 8.1. From now on, the robust optimization problem is adapted to incorporate time evolution. In addition, the local market price forecast $\bar{c}$ consists of one value for each time step. Hence, for the time span of 24 hours with hourly local market price updates, $\bar{c}$ becomes a horizontal vector of 24x1 values. Hence, Equation 8.1 and Equation 8.2 are reformulated into Equation 8.3 and Equation 8.4 to clearly indicate the inclusion of time. When incorporating time, the budget of uncertainty Γ_0 becomes an integer defined on the interval [0,T] instead of [0,n].

$$\min_{x^d,x^c} \left(\sum_{t=1}^{T} \bar{c}_t \left(x_t^c - x_t^d\right) + \max_{z_0 \in \mathcal{Z}_0} \sum_{t=1}^{T} d_t x_t^c z_{0t} + \max_{z_0 \in \mathcal{Z}_0} \sum_{t=1}^{T} d_t x_t^d z_{0t} \right) \tag{8.3}$$

where $\mathcal{Z}_0$ is formulated as:

$$\mathcal{Z}_0 = \left\{ \mathbf{z_0} \;\middle|\; |z_{0t}| \leq 1, \forall j, \sum_{t=1}^{T} |z_{0t}| \leq \Gamma_0 \right\} \tag{8.4}$$

8.1 Charging state of BESS

For the charging state of the battery, the optimization problem is similar to the general formulation from Uncertainty set modeling. The only difference is the feasibility of x_t^c, because in Equation 8.5 x_t^c is non-negative. This eliminates the need for the absolute value around x_t^c. In Equation 8.5, the goal is to minimize the cost of charging the battery, and the 'worst-case' situation represents high charging costs for the agent. This optimization problem is formulated as:

$$\begin{aligned} \min_{x^c} \quad & \left(\sum_{t=1}^{T} \bar{c}_t x_t^c + \max_{z_0 \in \mathcal{Z}_0} \sum_{t=1}^{T} d_t x_t^c z_{0t} \right) \\ \text{s.t.} \quad & \sum_{t=1}^{T} a_{it} x_t^c \leq b_i \quad \forall i, \\ & x_t^c \geq 0, \quad \forall t \end{aligned} \tag{8.5}$$

The procedure from Robust modeling of price uncertainty is followed, where the sub maximization problem is transformed in a tractable, linear sub-problem [13, 11, 12, 18, 34].

$$\begin{aligned} \max_{z_0 \in \mathcal{Z}_0} \sum_{t=1}^{T} d_t x_t^c z_{0t} \quad \Longleftrightarrow \quad & \max_{z_0} \sum_{t=1}^{T} d_t x_t^{c*} z_{0t} \quad \Longleftrightarrow \quad \min_{p_0, q_0} \Gamma_0 p_0 + \sum_{t=1}^{T} q_{0t} \\ \text{s.t.} \quad & \sum_{t=1}^{T} z_{0t} \leq \Gamma_0 \qquad \text{s.t.} \quad p_0 + q_{0t} \geq d_t x_t^{c*} \\ & 0 \leq z_{0t} \leq 1 \qquad q_{0t}, p_0, x_t^{c*} \geq 0 \end{aligned}$$

The final robust linear problem is formulated similarly to Equation 6.13. In Equation 8.6, p and q are the dual variables introduced in the dual subproblem.

$$\begin{aligned} \min_{x^c, q_0, p_0} \quad & \sum_{t=1}^{T} c_t x_t^c + p_0 \Gamma_0 + \sum_{t=1}^{T} q_{0t} \\ \text{s.t.} \quad & \sum_{t=1}^{T} a_{it} x_t^c \leq b_i, && i = \{1, ..., m\} \\ & p_0 + q_{0t} \geq d_t x_t^c && \forall t \in T \\ & q_{0t}, x_t^c \geq 0 && \forall t \in T \\ & p_0 \geq 0 \end{aligned} \tag{8.6}$$

8.2 Discharging state of BESS

The goal of the discharging state of the battery is to maximize the revenue obtained by selling energy at the local market price c_t. Hence, if the discharging state is represented as a maximization problem, the sub-problem worst-case scenario represents negative revenue, because the possible downward deviation from the nominal value of the local price at time t ($\bar{c}_t$), is added to the cost of the agent (revenue loss).

The objective function of the discharging state of the battery is:

$$\max_{x^d} \left(\sum_{t=1}^{T} \bar{c}_t x_t^d - \max_{z_0 \in \mathcal{Z}_0} \sum_{t=1}^{T} d_t x_t^d z_{0t} \right) \quad \Longleftrightarrow \quad \max_{x^d} \left(\sum_{t=1}^{T} \bar{c}_t x_t^d + \min_{z_0 \in \mathcal{Z}_0} \sum_{t=1}^{T} d_t x_t^d z_{0t} \right) \tag{8.7}$$

Similarly, when transforming the maximization objective functions in Equation 8.7 into a minimization objective function, the similarity with the charging state of the battery is achieved:

$$\begin{aligned} \min_{x^d} \left(-\sum_{t=1}^{T} \bar{c}_t x_t^d + \max_{z_0 \in \mathcal{Z}_0} \sum_{t=1}^{T} d_t x_t^d z_{0t} \right) \\ \text{s.t.} \sum_{t=1}^{T} a_{it} x_t^d \leq b_i, \quad \forall i, \\ x_t^d \geq 0, \quad \forall t \end{aligned} \tag{8.8}$$

In Equation 8.8, the minimization sub-problem has decision variable z_0, where the values of z_{0t} can be both positive and negative, for all t. Finding the maximum over the term $d_t x_t^d z_{0t}$ then results in a positive term, where x_t^d and d_t are always non-negative and the decision variable z_{0t} becomes positive. As a result, the total sub-problem maximization term is positive in Equation 8.8, which satisfies the goal of finding the 'worst-case scenario' in terms of revenue loss.

The procedure from Robust modeling of price uncertainty is followed, where the sub maximization problem is transformed in a tractable, linear sub-problem [13, 11, 12, 18, 34]. Similar to the charging state problem, the absolute value surrounding x_t^d is dropped due to the restriction of x_t^d being non-negative. k and l are the dual variables from the sub-problem.

$$\begin{aligned} \max_{z_0 \in \mathcal{Z}_0} \sum_{t=1}^{T} d_t x_t^d z_{0t} \quad \Longleftrightarrow \quad & \max_{z_0} \sum_{t=1}^{T} d_t x_t^{d*} z_{0t} \quad \Longleftrightarrow \quad \min_{k_0, l_0} \Gamma_0 k_0 + \sum_{t=1}^{T} l_{0t} \\ & \text{s.t.} \sum_{t=1}^{T} z_{0t} \leq \Gamma_0 \qquad \text{s.t. } k_0 + l_{0t} \geq d_t x_t^{d*} \\ & 0 \leq z_{0t} \leq 1 \qquad\qquad l_{0t}, k_0, x_t^{d*} \geq 0 \end{aligned}$$

The final robust linear problem is formulated similarly to Equation 6.13. Looking at the objective function of Equation 8.9, it makes sense that the two terms with the dual variables are positive, meaning that these two terms work in the opposite direction of the mean revenue term $(-\sum_{t=1}^{T} c_t x_t^d)$. $(k_0 \Gamma_0)$ and $(\sum_{t=1}^{T} l_{0t})$ add costs to the objective function in the form of revenue loss.

$$\begin{aligned} \min_{x^d, l_0, k_0} \quad & -\sum_{t=1}^{T} c_t x_t^d + k_0 \Gamma_0 + \sum_{t=1}^{T} l_{0t} && \\ \text{s.t.} \quad & \sum_{t=1}^{T} a_{it} x_t^d \leq b_i, && i = \{1, ..., m\} \\ & k_0 + l_{0t} \geq d_t x_t^d && \forall t \in T \\ & l_{0t}, x_t^d \geq 0 && \forall t \in T \\ & k_0 \geq 0 && \end{aligned} \tag{8.9}$$

8.3 Simultaneous charging and discharging state of battery

As can be seen in Equation 8.3, the combination of charging and discharging the battery in the objective function results in one overall minimization problem, containing two sub-maximization problems:

$$\min_{x^d, x^c} \left(\sum_{t=1}^{T} \bar{c}_t \left(x_t^c - x_t^d \right) + \max_{z_0 \in \mathcal{Z}_0} \sum_{t=1}^{T} d_t x_t^c z_{0t} + \max_{z_0 \in \mathcal{Z}_0} \sum_{t=1}^{T} d_t x_t^d z_{0t} \right) \tag{8.10}$$

In this section, the distinction is made between the budget of uncertainty for the discharging and charging state of the battery (Γ_{0d} and Γ_{0c}). As a result of having two risk parameters, the

risk attitude of the decision-maker in the charging state of the battery can be different from the discharging state of the battery. Based on Equation 8.6 and Equation 8.9, the objective function containing both the worst-case discharging and charging state of the BESS is transformed into a robust, linear problem in Equation 8.11.

$$\min_{x^d,x^c,u,q_0,p_0,k_0,l_0} \left(\sum_{t=1}^{T} \bar{c}_t \left(x_t^c - x_t^d \right) + \left(p_0 \Gamma_{0c} + \sum_{t=1}^{T} q_{0t} \right) + \left(k_0 \Gamma_{0d} + \sum_{t=1}^{T} l_{0t} \right) \right) \tag{8.11}$$

The dual constraints from Equation 8.6 and Equation 8.9 are combined into the following set of constraints:

$$p_0 + q_{0t} \geq d_t x_t^c, \quad \forall t \qquad k_0 + l_{0t} \geq d_t x_t^d, \quad \forall t \tag{8.12}$$

$$q_{0t}, x_t^c \geq 0, \quad \forall t \qquad l_{0t}, x_t^d \geq 0, \quad \forall t \tag{8.13}$$

$$p_0 \geq 0 \qquad k_0 \geq 0 \tag{8.14}$$

In the dual constraints, x_t^c (x_t^d) is equal to zero when the battery is discharging (charging). Hence, in the charging state, the constraint $k_0 + l_{0t} \geq d_t x_t^d$ is always satisfied, while in the discharging state, the constraint $p_0 + q_{0t} \geq d_t x_t^c$ is always satisfied. This is true since the dual variables are non-negative.

Additionally, battery constraints are added to the optimization problem, where the binary variable u_j is inserted to denote the state of the battery [110, 105]. $u_t = 0$ represents the charging state of the battery at time t, and $u_t = 1$ represents the discharging state of the battery at time t. Here, when the battery is discharging, x_t^c is forced to zero. The reverse also holds, because when the battery is charging, x_t^d is forced to zero by the construction of the constraints:

$$x_t^c - x_{max}^c (1 - u_t) \leq 0, \quad \forall t \qquad x_t^d - x_{max}^d u_t \leq 0, \quad \forall t \tag{8.15}$$

$$u_t \in \{0, 1\} \quad \forall t \tag{8.16}$$

To incorporate the state of charge (SoC) of the BESS, the energy efficiency of charging and discharging is denoted as η_c and η_d respectively [110, 105]. Then, the variable e_t is used to represent the state of charge (SoC) of the BESS at time t. The stored energy in the battery always lies within the lower and upper bound e_{min} and e_{max} [110, 59, 7, 54, 79]:

$$e_t = e_{t-1} + \eta_c x_t^c \Delta t - \frac{1}{\eta_d} x_t^d \Delta t, \quad \forall t \tag{8.17}$$

$$e_{min} \leq e_t \leq e_{max}, \quad \forall t \tag{8.18}$$

$$u_t \in \{0, 1\}, \quad \forall t \tag{8.19}$$

$$e_t \geq 0, \quad \forall t \tag{8.20}$$

The following parameters are predefined and serve as input to the optimization problem: $\bar{c}_t$ (mean local price forecast), d_t ((standard) deviation from mean local price forecast), Γ_{0d} (budget of uncertainty for discharging state), Γ_{0c} (budget of uncertainty for charging state), x_{max}^c (maximum charge power), x_{max}^d (maximum discharge power), e_0 (initial state of charge), e_{min} (minimum stored energy in the battery), e_{max} (maximum stored energy in the battery), η_c (efficiency of charging battery), η_d (efficiency of discharging battery).

8.3.1 Case: identical budget of uncertainties

When investigating combined charge and discharge budgets of uncertainty, this case represents them to be equal. This case is used throughout the rest of this research, to obtain the numerical results. In this case, $\Gamma_{0c} = \Gamma_{0d} = \Gamma_0$. Then, only *one* budget of uncertainty (Γ_0) is selected by the agent owning the BESS, covering both the charging and discharging state of the battery.

Consequently, the agent has the same risk attitude for both charging and discharging the BESS. Next, the robust optimization problem from previous chapter, formulated in Equation 8.11 until Equation 8.20, can be *simplified* into the problem derived in this chapter. Due to the equality of the budgets of uncertainties, two dual variables are present instead of four. Also, the formulation of Equation 8.10 containing the two maximization sub-problems is converted into one maximization sub-problem in Equation 8.21.

$$\min_{x_t^c, x_t^d} \left(\sum_{t=1}^{T} \bar{c}_t \left(x_t^c - x_t^d \right) + \max_{z_0 \in \mathcal{Z}_0} \sum_{t=1}^{T} d_t z_{0t} \left(x_t^c + x_t^d \right) \right) \tag{8.21}$$

In Equation 8.21, only one budget of uncertainty can be appointed, instead of the two separate budgets of uncertainty for the discharging and charging state of the battery in Equation 8.11. Similar to before, the maximization term is rewritten into its robust counterpart, and using duality theory it is converted into a tractable sub-problem.

$$\begin{aligned}
\max_{z_0 \in \mathcal{Z}_0} \sum_{t=1}^{T} d_t z_{0t} \left(x_t^d + x_t^c \right) \quad \Longleftrightarrow \quad & \max_{z_0} \sum_{t=1}^{T} d_t z_{0t} \left(x_t^{d*} + x_t^{c*} \right) \quad \Longleftrightarrow \quad \min_{p_0, q_0} \Gamma_0 p_0 + \sum_{t=1}^{T} q_{0t} \\
& \text{s.t.} \sum_{t=1}^{T} z_{0t} \leq \Gamma_0 \qquad\qquad \text{s.t. } p_0 + q_{0t} \geq d_t \left(x_t^{d*} + x_t^{c*} \right) \\
& \quad 0 \leq z_{0t} \leq 1 \qquad\qquad q_{0t}, p_0, x_t^{d*}, x_t^{c*} \geq 0
\end{aligned}$$

Finally, the combined robust optimization problem with one budget of uncertainty Γ_0 becomes:

$$\min_{x^d, x^c, u, q_0, p_0} \left(\sum_{t=1}^{T} \bar{c}_t \left(x_t^c - x_t^d \right) + \left(p_0 \Gamma_0 + \sum_{t=1}^{T} q_{0t} \right) \right) \tag{8.22}$$

$$\begin{aligned}
& p_0 + q_{0t} \geq d_t \left(x_t^c + x_t^d \right), && \forall t \qquad && e_t = e_{t-1} + \eta_c x_t^c \Delta t - \frac{1}{\eta_d} x_t^d \Delta t, && \forall t \\
& x_t^c - x_{max}^c (1 - u_t) \leq 0, && \forall t, \qquad && e_{min} \leq e_t \leq e_{max}, && \forall t \\
& x_t^d - x_{max}^d u_t \leq 0, && \forall t \qquad && e_t \geq 0, && \forall t \\
& q_{0t}, x_t^c, x_t^d \geq 0, && \forall t, \qquad && p_0 \geq 0 \\
& u_t \in \{0, 1\}, && \forall t
\end{aligned}$$

As opposed to the final robust optimization problem formulated in Simultaneous charging and discharging state of battery, this special case deals with only two dual variables (p, q) instead of four (p, q, k, l), and one budget of uncertainty Γ_0. The optimization model represented in Equation 8.22 is used later in this research to develop the optimal bidding schedule of the agent owning the BESS, by varying the risk attitude Γ_0. Furthermore, it should be noted that the RO model submits price-quantity points to the market operator, indicating that a bid both contains a quantity and a price [59]. The argumentation for submitting price-quantity points instead of self-schedule bids is already provided in Stochastic optimization applied to battery asset modeling. Furthermore, the Numerical investigations of the models elaborates on the bid prices the RO model submits to the market operator.

As elaborated in Uncertainty set modeling, the meaning of dual variables p and q are represented below, similar to [13]:

- p_0 will equal the $\lceil \Gamma_0 \rceil$-th greatest $d_t(x_t^c + x_t^d)$.
- $q_{0t} = \max(0, d_t(x_t^c + x_t^d) - p_0)$

9 Numerical investigations of the models

This chapter investigates the model specifications before obtaining the numerical results. In this chapter, the price scenario specifications for the SO models are outlined, followed by the uncertainty set specification for the RO model. Based on constructed examples and simulations, multiple case studies are outlined and assessed by the outlined pre-clearance and post-clearance performance metrics introduced in this chapter.

9.1 Price scenarios for stochastic optimization

As elaborated in Scenario-based modeling of price uncertainty, obtaining a representable set of price scenarios consists of four subsequent stages, as depicted in Figure 2: point forecast, residual analysis, scenario generation, and scenario reduction.

9.1.1 Point forecast

As elaborated in Point forecast model, the (S)AR(I)MA(X)-type model is used to forecast the day-ahead LEM clearing price [82]. Due to a lack of accurate LEM historical data, public historical WSM data is set equal to the LEM historical data in this research [32]. The forecast interval is hourly, hence 24 hourly prices ahead are forecasted.

Due to the lacked availability of historical LEM data, the SAR(I)MAX model as described in Point forecast model cannot be used as forecasting model in this research. Instead, the SAR(I)MA model is used to forecast the day-ahead market prices, to capture the seasonality in the electricity price time series [107, 60]. The forecast in this research incorporates the *daily* seasonality of the LEM day-ahead market prices, as mentioned in for example [75].

First, three training sets and corresponding testing sets are selected. These Examples vary in length of the training set, where Example 1 has a training set duration of two months, Example 2 one month, and Example 3 one week. These sets are represented in Table 1:

Table 1: *Training and testing data sets*

Example	Training set	Testing set (prediction)
1	March 1st 00.00 - April 30th 23.00 (2015)	May 1st 00.00 - 23.00 (2015)
2	February 18th 00.00 - March 17th 23.00 (2015)	March 18th 00.00 - 23.00 (2015)
3	March 5th 2015 00.00 - March 11th 23.00 (2015)	March 12th 00.00 - 23.00 (2015)

The optimal SARIMA parameters (p,d,q)(P,D,Q) and S, as elaborated in SARIMA model, are found for Example 1. The Econometrics Modeler App from Matlab is used to obtain the LEM price forecast in this research. For coherence of the scenario generation algorithm, these optimal order parameters are also used for the scenario generation corresponding to Examples 2 and 3. Since this forecast incorporates daily seasonality, S automatically equals 24. To validate the goodness of fit of the forecasting model on the training set of Example 1, multiple methods are used:

- Investigate the AIC and BIC values of the tried combinations of p, d, q, P, D, Q. The lowest value is the best fit [81].
- Validate that the residuals (prediction errors) behave as white noise (e.g. normally distributed with zero mean and constant standard deviation σ) [107].
- Explore the Autocorrelation Function (ACF) plot that represents the autocorrelation of the residuals, to validate that the residuals do not have significant autocorrelation left in the residuals [81, 6].

Examples 1, 2, and 3 obtain their model coefficients $(\psi, \zeta, \varphi, \theta)$, constant term C, and their variance σ^2. In addition, generating scenarios requires knowledge of historical residuals (prediction errors) ϵ and historical LEM price values. The historical residuals are obtained via the Econometrics Modeler App and the historical LEM price values originate from the historical training set.

9.1.2 Scenario generation

In this stage, $N_\Omega = 100$ scenarios for the day-ahead time frame are generated for Examples 1, 2, and 3, in Matlab 2022b. Every scenario has equal probability $\frac{1}{N_\Omega}$. This is done via the algorithm elaborated in Scenario generation. The inputs required for generating the scenarios for the day-ahead are specified in the previous section. Besides these inputs, the algorithm generates a set of random errors with characteristics $\{\epsilon\} \sim N(0, \sigma)$ [16].

9.1.3 Scenario reduction

In this final stage, the scenario reduction algorithm as described in Scenario reduction is implemented in Matlab 2022b. For this research, the 100 scenarios created in the Scenario generation section, are reduced to an optimal reduced scenario set Ω_S^*, containing four and ten scenarios. The output of this algorithm is the scenario realization of the day-ahead time frame for Examples 1, 2, and 3, as well as their corresponding reduced scenario probabilities.

9.2 Simulations LEM price forecast

After the development of the scenario realizations for Examples 1, 2, and 3, following the theoretical framework of Scenario-based modeling of price uncertainty, simulations are performed on a larger scale for the Example training set duration with the *best* price prediction. Hence, ten simulations are executed with the same training set duration, for ten random days in 2015. The prediction days are represented in Table 2.

To determine the optimal training set duration, the performance metric Mean Absolute Percentage Error (MAPE) is determined for Examples 1, 2, and 3 [107]. MAPE enables the measurement of the accuracy of a fitted SARIMA model on the training data [107, 4]. The MAPE measures the average gap between the forecasted price and the actual price, as a percentage [107]. A lower MAPE represents a higher accuracy of the forecast. The MAPEs of Examples 1, 2, and 3 are determined with four price scenarios. The final MAPE value of an Example is the aggregate of the MAPE of the four scenarios, normalized with their scenario probabilities. Hence, one MAPE value per Example is obtained.

Table 2: *Training and testing data sets*

Simulation	Testing set (prediction)
1	March 12th 00.00 - 23.00 (2015)
2	April 10th 00.00 - 23.00 (2015)
3	May 8th 00.00 - 23.00 (2015)
4	June 10th 00.00 - 23.00 (2015)
5	June 24th 00.00 - 23.00 (2015)
6	July 11th 00.00 - 23.00 (2015)
7	October 18th 00.00 - 23.00 (2015)
8	November 3rd 00.00 - 23.00 (2015)
9	November 30th 00.00 - 23.00 (2015)
10	December 24th 00.00 - 23.00 (2015)

9.3 Uncertainty set for robust optimization

To obtain numerical results for the RO model outlined in Robust optimization applied to battery asset modeling, the box interval has to be constructed. For coherence, the same SAR(I)MA model used for scenario-based modeling in stochastic optimization is used to construct the box interval in robust optimization. Hence, similar to stage 1 of scenario-based modeling in stochastic optimization, the SARIMA$(1,0,1)(1,0,1)_{24}$ model is used to obtain the mean price forecast and its standard deviation to construct the box interval uncertainty set. These are the only two required price inputs in the constructed RO model in Case: identical budget of uncertainties. Then, the numerical results are obtained for all examples and simulations, similar to the stochastic

optimization models.

9.4 Model overview

Multiple optimization models are developed in this research. An overview of the optimization models is presented in Table 3, connecting the models used in the case studies to the correct chapter of the research. All of the optimization models are developed in Matlab 2022b GUROBI.

Table 3: *Optimization models developed in this research*

Model	Optimization methods	Risk management	Chapter
Model 1: single bid	Stochastic Optimization	No	Chapter 7.1
Model 1: single bid	Stochastic Optimization	Yes	Chapter 7.2
Model 2: multiple bids	Stochastic Optimization	No	Chapter 7.3
Model 2: multiple bids	Stochastic Optimization	Yes	Chapter 7.4
RO model	Robust Optimization	Yes	Chapter 8.3.1

Charging risk and discharging risk are incorporated separately as well as simultaneously in the SO models 1 and 2. However, the Numerical results section only incorporates the results of the risk management for *simultaneous* charging and discharging risk of the agent owning the battery, since this is the most contributing and valuable result. For the RO model, the numerical results are obtained for the case with identical budget of uncertainties: $\Gamma_{0c} = \Gamma_{0d} = \Gamma_0$.

9.5 Case studies

In this research, multiple case studies are conducted with the scenario sets from Examples 1, 2, and 3, and separately with the ten simulations with a one-week training set duration. All case studies are carried out with both four and ten scenarios. In all case studies below, the risk-neutral SO model 1 serves as a benchmark result, similar to [112, 50].

- Case study 1: comparison SO model 1 varying the risk-attitude of the agent (Chapter 7.1 and Chapter 7.2). Here, the risk parameter is β, ranging between 0-1 by construction of Model 1 with risk management. The study is conducted with β values: 0, 0.5, 0.999, meaning risk-neutral, medium risk-averse, and completely risk-averse. Then, pre-clearance and post-clearance performance is assessed.
- Case study 2: comparison SO model 2 varying the risk-attitude of the agent (Chapter 7.3 and Chapter 7.4). Again, the risk parameter is β. The study is conducted with β values: 0, 0.5, 0.999, meaning risk-neutral, medium risk-averse, and completely risk-averse. Then, pre-clearance and post-clearance performance is assessed.
- Case study 3: comparison of SO model 1 and SO model 2, for both risk-neutral and varying risk-attitude of the agent (Chapter 7.1, Chapter 7.2, Chapter 7.3, and Chapter 7.4). Case study 3 compares case studies 1 and 2 in terms of pre-clearance and post-clearance performance.
- Case study 4: comparison of SO model 1 with RO model (Chapter 7.1, Chapter 7.2, and Chapter 8.3.1). Both these models submit single price-quantity points per time step. In case study 4, SO model 1 has a ranging risk parameter β (0, 0.5, 0.999), while the RO model has a ranging Γ_0 (0, 3, 4, 6, 8). For case study 4, performance is assessed in terms of pre-clearance and post-clearance performance.

9.5.1 Data specifications

In Table 4, an overview of the used battery parameters is provided. In addition, the following risk parameters are used for stochastic optimization (Table 5) and robust optimization (Table 6).

Table 4: *Battery parameters used in case studies*

Specification	Symbol	Value	Unit
Charging efficiency	η_c	1	[-]
Discharging efficiency	η_d	1	[-]
Initial state of charge (SOC)	e_0	400	[kWh]
Minimum battery storage	e_{min}	0	[kWh]
Maximum battery storage	e_{max}	450	[kWh]
Maximum charge rate	x^c_{max}	450	[kW]
Maximum discharge rate	x^d_{max}	450	[kW]
Time step length	Δt	1	[h]

Table 5: *Risk parameters used in case studies 1, 2, 3, 4*

Specification	Symbol	Value
Confidence interval	α	0.95
Risk-coefficient	β	0-1

Table 6: *Risk parameters used in robust optimization model*

Specification	Symbol	Value
Budget of Uncertainty	Γ	0-8

9.5.2 Performance metrics

All case studies are evaluated by the following performance metrics. It is important here to make the distinction between pre-clearance performance and post-clearance performance.

- Pre-clearance performance concerns the performance directly obtainable from the optimization model. Within stochastic optimization, pre-clearance performance concerns the *expected costs/revenue and profit* [eur] and the *CVaR value* [eur] of the resulting bidding schedule. Note here that the expected profit is the expected revenue minus the expected costs. As elaborated in Stochastic optimization applied to battery asset modeling, the bid price of SO model 1 is the mean expected scenario price, and for SO model 2 the bid price is equal to a scenario price corresponding to the bid quantity. Furthermore, the confidence interval (α) for SO models 1 and 2 is set to 0.95, similar to [108, 72] and recommended in [86]. In other words, CVaR illustrates the expected profit of the worst 5% of the model realizations [89].

  For the RO model, *expected profit, envisioned profit, envisioned costs, envisioned revenue, and the dual variable p* are represented. To calculate the expected profit, the bid price is taken as the mean expected LEM price ($\bar{c}_t$). As a result, the expected profit is calculated as $\sum_{t=1}^{T} \bar{c}_t(x^d_t - x^c_t)$. The expected profit is directly obtainable from the RO model results. For the second method (the envisioned profit/costs/revenue), the bid prices are adjusted to include the chosen risk attitude of the agent; Γ_0 (the *robust* bid price). Then, the total envisioned profit is calculated as $\sum_{t=1}^{T}(\bar{c}_t \pm \frac{\Gamma_0}{24} \times d_t)(x^d_t - x^c_t)$. Hence, a chosen fraction of the standard deviation from the mean is included in the bid price of the agent. The $\pm$ is dependent on whether the bid is a charging or discharging bid. Hence, the envisioned profit calculation is calculated manually *after* the results of the RO model are obtained. For the RO model, Γ_0 between 0-8 is considered, since according to [13], Γ is always of the order $\sqrt{n}$. In this research, n represents the day-ahead time window, meaning $n = 24$ and $\sqrt{n} = 4.47$.

  The pre-clearance performance of all case studies is obtained for Examples 1, 2, and 3, and simulations 1 - 10. To assess the influence of the number of scenarios, performance is assessed for both four and ten scenarios.

- Post-clearance performance is the performance of the optimization model after the LEM has cleared. Acquiring the post-clearance performance results of the optimization models requires an additional step. Namely, the bid prices of the bidding schedule resulting from the model are compared with the market clearing price realization. Here, instead of the forecasted LEM prices, the *actual* LEM price realizations are used to check whether the submitted price-quantity points are cleared in the LEM. For the SO models, a selling bid (discharging) is cleared in the LEM when the bid price is lower or equal to the actual LEM price. A buying bid (charging) is cleared in the LEM when the bid price is higher or equal to the actual LEM price. For the RO model, the bid price that determines whether a bid is cleared in the LEM is the *robust* bid price, calculated as $\bar{c}_t \pm \frac{\Gamma_0}{24} \times d_t$.

  The post-clearance performance is obtained in monetary values, representing the *actual costs of the submitted charging bids* and the *actual revenue of the submitted discharging bids*. The actual costs and revenue of the bidding schedule are calculated by multiplying the *actual* market clearing price of the day-ahead time frame with only the *cleared* bids. There is no value in investigating the actual profit of the models since these results can be skewed to high profits in the case of high discharging bid clearance or negative profit in the case of high charging bid clearance. In addition, two percentages are represented to indicate the clearance performance of the models, namely the *% of bids cleared* and *% of bid quantity cleared*.

  The post-clearance performance of all case studies is obtained for Examples 1, 2, and 3, and simulations 1 - 10. To assess the influence of the number of scenarios, performance is assessed for both four and ten scenarios.

10 Numerical results

This chapter starts by obtaining the price scenarios of Examples 1 - 3 and simulations 1 - 10, used as input for the stochastic models. The mean and standard deviation of the used SARIMA point forecast model are also used to construct the uncertainty sets for the robust model. Afterward, this chapter elaborates on the pre- and post-clearance performance of the case studies described in Numerical investigations of the models.

10.1 Price scenarios

Following the four subsequent stages of scenario-based modeling, as described in Figure 2, the optimal set of reduced day-ahead scenarios is obtained, for Examples 1, 2, and 3. As elaborated in Numerical investigations of the models, the SARIMA model is used to forecast the LEM day-ahead prices. The SARIMA order parameters p, d, q, P, D, and Q are obtained by fitting the training set data of Example 1. The Matlab code of the price scenario algorithm can be found on Github [104].

10.1.1 SARIMA model Example 1

As elaborated in the Box-Jenkins approach, the Akaike Information Criterion (AIC) and the Schwarz Bayesian information criterion (BIC) are used to identify which model order parameters fit the training set of Example 1 best. An overview of different combinations of the order parameters and their corresponding AIC and BIC values are visualized in Table 7 and Table 8. The model with the lowest sum of AIC and BIC values is the SARIMA$(1,0,1)(1,0,1)_{24}$, providing the SARIMA$(1,0,1)(1,0,1)_{24}$ model as the best fit to the training set of Example 1.

Table 7: *AIC values of SARIMA(p,d,q)(P,D,Q)$_S$ model*

ARIMA / **Seasonality**	(1,0,0)	(1,0,1)	(0,0,1)	(1,1,1)
(1,0,0)	9217.3	9110.3	9697.7	9158.8
(1,0,1)	8852.1	**8836.1**	9571.0	8870.5
(0,0,1)	9217.3	8854,6	9819.7	9395.6
(1,1,1)	8855.9	8856.2	9610.6	8883.9

Table 8: *BIC values of SARIMA(p,d,q)(P,D,Q)$_S$ model*

ARIMA / **Seasonality**	(1,0,0)	(1,0,1)	(0,0,1)	(1,1,1)
(1,0,0)	9233.1	9136.6	9718.8	9186.1
(1,0,1)	8873.2	**8877.7**	9597.4	8902.1
(0,0,1)	9233.1	8881.0	9840.9	9422.0
(1,1,1)	8882.2	8887.7	9636.8	8915.4

Despite the AIC and BIC values, the residuals of the training set of Example 1 are investigated. First, it can be observed that the distribution of the residuals follows a normal distribution (Figure 4a). Besides, when investigating the Auto-correlation Function plot (ACF) (Figure 4b), it can be seen that there is a small auto-correlation left at lag 3, 23, and 25. However, this auto-correlation remains uncaptured in the other parameter model combinations as illustrated in Table 7 and Table 8. In other words, choosing another model parameter combination as investigated in this research does not reduce the residual auto-correlation of Example 1. Based on the residual distribution (Figure 4a), the ACF plot (Figure 4b), and the AIC (Table 7) and BIC values (Table 8), the SARIMA$(1,0,1)(1,0,1)_{24}$ model is the best fit to the training set of Example 1.

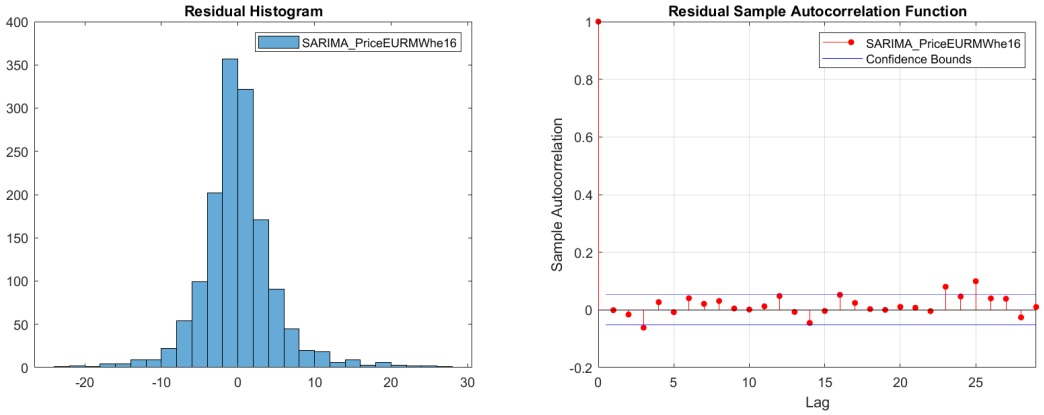

(a) Residual histogram *(b) ACF plot*

Figure 4: *SARIMA(1,0,1)(1,0,1)$_{24}$ model of Example 1*

10.1.2 SARIMA(1,0,1)(1,0,1)$_{24}$ model

The SARIMA(1,0,1)(1,0,1)$_{24}$ model is used as point forecast model in this research, for Examples 1, 2, and 3 and simulations 1 - 10. This is done for coherence of the scenario generation procedure. The mathematical formulation of the SARIMA(1,0,1)(1,0,1)$_{24}$ model is represented as:

$$\left(1-\psi_1 B\right)\left(1-\zeta_{24}B^{24}\right)Z_t = C + \left(1+\varphi_1 B\right)\left(1+\theta_{24}B^{24}\right)\epsilon_t \tag{10.1}$$

In Equation 10.1, Z_t represents the LEM price, and ϵ_t represents the prediction error. In Equation 10.1, the backshift operator B is represented as $B^k Z_t = Z_{t-k}$ [48, 82]. Hence, when rewriting Equation 10.1, the alternative mathematical formulation is represented as:

$$Z_t = \psi_1 Z_{t-1} + \zeta_{24} Z_{t-24} - \psi_1\zeta_{24} Z_{t-25} + C + \epsilon_t + \varphi_1\epsilon_{t-1} + \theta_{24}\epsilon_{t-24} + \varphi_1\theta_{24}\epsilon_{t-25} \tag{10.2}$$

Next, the model coefficients of the SARIMA(1,0,1)(1,0,1)$_{24}$ model (Equation 10.2) for Examples 1, 2, and 3 are found. These fitted model coefficients are represented in Table 9, whose values are used as input in the scenario generation algorithm. Note here that the variance is a constant value over the complete time horizon, since the SARIMA model assumes that the error term behaves as white noise, e.g. zero mean and constant variance [107, 60, 43, 97, 82, 1]. Despite the values displayed in Table 9, the LEM prices of the last day of the training set and the last day residuals (prediction errors) are used as input in the scenario generation algorithm.

Table 9: *SARIMA model coefficients of Examples 1, 2, and 3*

		Ex. 1	Ex. 2	Ex. 3
SARIMA model coefficient	Symbol	Value	Value	Value
Auto-regressive 1	ψ_1	0.8169	0.8361	0.8987
Seasonal Auto-regressive 24	ζ_{24}	0.9757	0.9961	0.9214
Moving average 1	φ_1	0.0499	−0.0083	−0.1695
Seasonal Moving average 24	θ_{24}	0.0152	−0.7980	−0.6167
Constant	C	0.2034	0	0.3034
Variance	σ^2	24.3772	14.6219	14.0110

As a third stage, the model coefficients in Table 9 are used to generate 100 scenarios for Examples 1, 2, and 3. Then, using the fast forward selection algorithm [95, 23], these scenarios are reduced to both four and ten scenarios. Figure 5 represents the day-ahead LEM price forecast of Example 1

with four scenarios. In Appendix B.1: Example 1 scenarios, the day-ahead LEM price forecast of Example 1 with 100 scenarios and 10 scenarios are visualized. The four scenarios generated for Example 2 are visualized in Figure 6. The other two sets of scenarios with 100 and 10 scenarios are represented in Appendix B.2: Example 2 scenarios. Lastly, Figure 7 represents the four scenarios of Example 3 while Appendix B.3: Example 3 scenarios represents the scenario realizations with 100 and 10 scenarios.

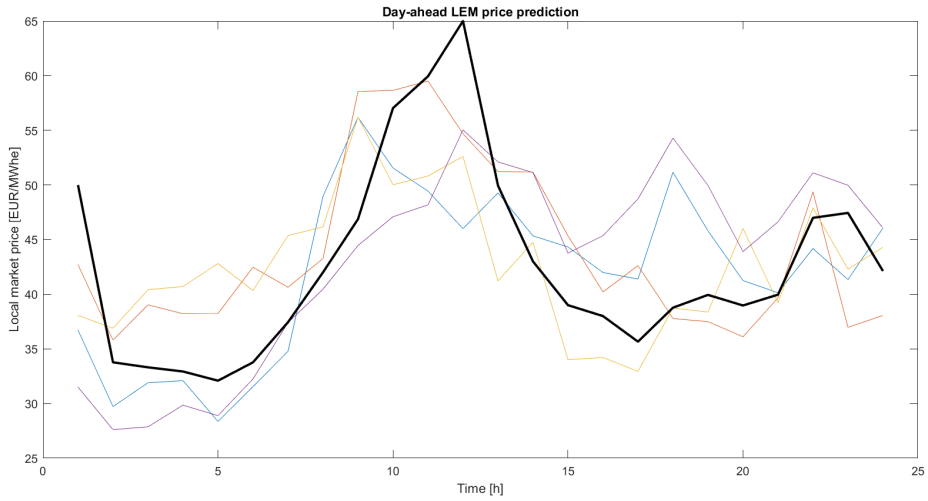

Figure 5: *Example 1 day-ahead price scenarios 1st of May 2015. Black: actual price 1st of May 2015. Colors: 4 scenario realizations*

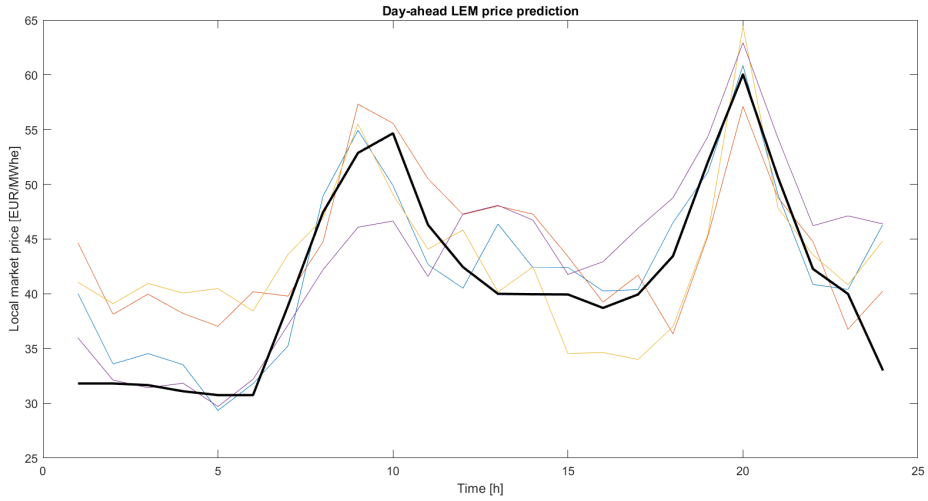

Figure 6: *Example 2 day-ahead price scenarios 18th of March 2015. Black: actual price 18th of March 2015. Colors: 4 scenario realizations*

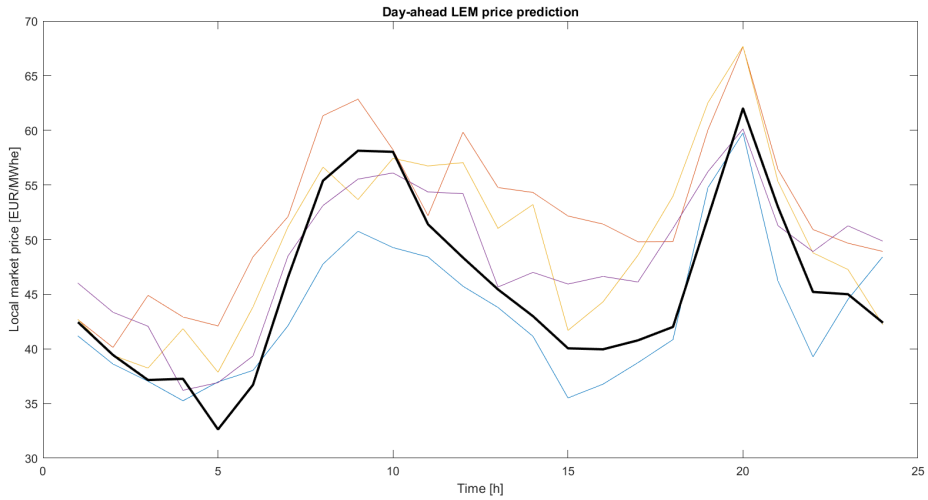

Figure 7: *Example 3 day-ahead price scenarios 12th of March 2015. Black: actual price 12th of March 2015. Colors: 4 scenario realizations*

10.2 Simulations LEM price forecast

As represented in the previous section, three Example forecasts of the day-ahead prices are developed. These forecasts have different training set durations, and the training set duration that fits the data best (by investigating the MAPE values) is used to develop *ten* simulations of the LEM price forecast for the day-ahead market.

Following the Numerical investigations of the models section, the MAPE values of Examples 1, 2, and 3 are obtained and represented in Table 10.

Table 10: *Mean Absolute Percentage Error of Examples 1, 2, and 3*

Example	MAPE
1	13.36 %
2	11.54 %
3	8.58 %

Example 3 has the lowest MAPE value, meaning that the accuracy of the forecast of Example 3 is the highest. The SARIMA$(1,0,1)(1,0,1)_{24}$ model takes into account daily seasonality but excludes other seasonalities, for example weekly seasonality or the different electricity patterns during weekdays and weekends [23, 107, 6, 48, 70, 75, 24, 93]. Hence, a shorter training set potentially excludes the seasonalities that cannot be captured by the SARIMA$(1,0,1)(1,0,1)_{24}$ model. As a result, a shorter training set duration is sufficient. According to [107], a MAPE of less than 10% is considered very good. The goodness of fit of Example 3 is strengthened by investigating the ACF plot of Example 3, where no auto-correlation is left in the residuals outside of the confidence bounds (see Appendix C).

Consequently, simulations 1-10 are performed with a training set duration of one week, similar to Example 3. The prediction days are represented in Table 2 and the training sets consist of one week before the prediction day. Similar to Examples 1, 2, and 3, the ten simulations consist of both four and ten scenarios.

10.3 Case study 1: SO model 1

Case study 1 is concerned with the pre-clearance and post-clearance performance of SO model 1 (single bid model). The risk-neutral SO model 1 acts as a benchmark model throughout all the case studies. Hence, for case study 1 the risk-neutral benchmark model (Model 1: single bid (base model)) enables the assessment of the performance of SO model 1 with risk management (Model 1 with risk management. In this case study, $\beta = 0.0001$ is considered risk-neutral, and $\beta = 0.999$ is considered fully risk-averse. The Matlab code for the SO model 1 bidding model can be found on Github [104].

In Appendix D.1, the pre- and post-clearance performance of SO model 1 is represented for Examples 1, 2, and 3, for both four and ten scenarios. In Appendix D.2 and Appendix D.3, the average pre- and post-clearance performance of simulations 1 - 10 are represented, for both four and ten scenarios, respectively. The average results of simulations 1 - 10 are also visualized in Figure 8 and Figure 9. Lastly, the expected costs and revenue of simulations 1 - 10 are compared with their actual costs and revenue. The actual costs represent the costs of the *cleared* charging bids multiplied by the *actual* LEM price. The actual revenue represents the revenue of the *cleared* discharging bids multiplied by the *actual* LEM price. This comparison is represented in Figure 10a and Figure 10b, for four and ten scenarios, respectively.

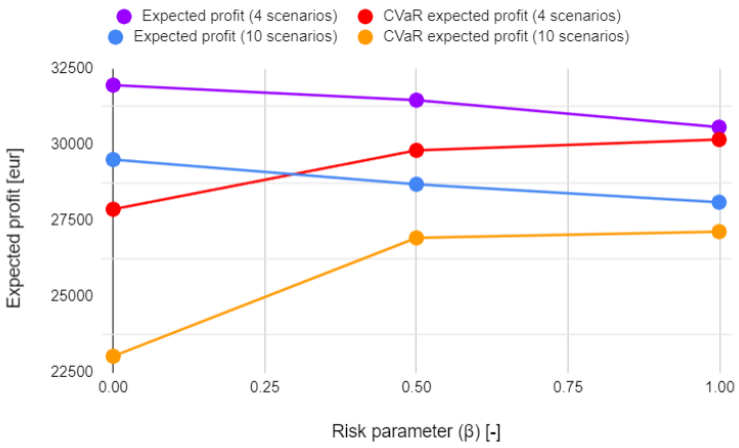

Figure 8: *Average pre-clearance performance simulations 1-10, 4 and 10 scenarios*

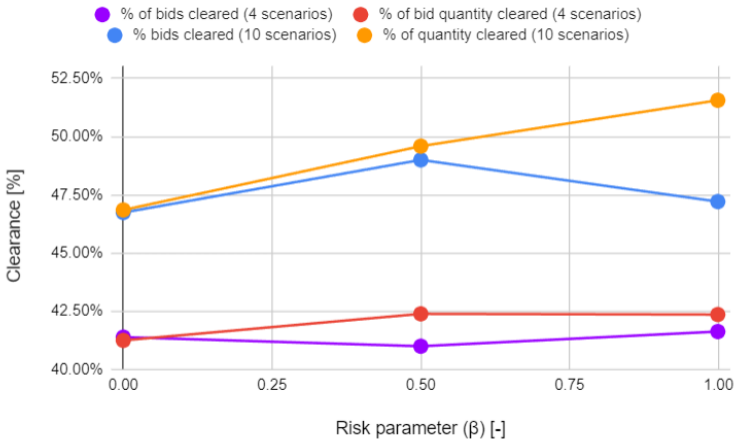

Figure 9: *Average post-clearance performance simulations 1-10, 4 and 10 scenarios*

(a) 4 scenarios

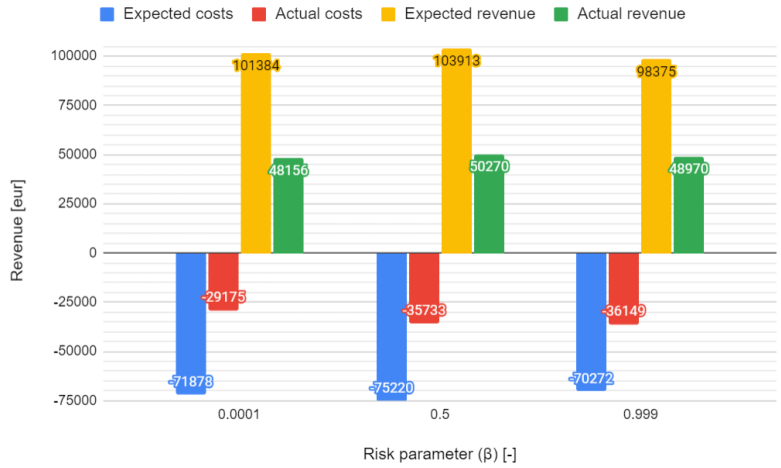

(b) 10 scenarios

Figure 10: *Comparison of expected costs/revenue (pre-clearance) and actual costs/revenue (post-clearance), case study 1*

To illustrate the model results of SO model 1, the model specifications of risk-neutral and risk-averse Example 1 (four scenarios) are elaborated, for the interval t = 18 until t = 24. The decision variables of the risk-neutral SO model 1 ($\beta = 0.0001$) of Example 1 are represented in Table 11a. To compare, the decision variables of the BESS with the bidding schedule of risk-averse SO model 1 of Example 1 ($\beta = 0.999$) is represented in Table 11b. Here, the bid quantities are represented, together with the state of charge of the battery (SoC). The state of charge of the battery must lie between 0 [kWh] and 450 [kWh], according to the battery specifications of Numerical investigations of the models. The bid price of SO model 1 is equal to the expected LEM price at time t, namely $\hat{c}_t = \sum_{\omega \in \Omega_S^*} \pi_\omega^* c_{t,\omega}$.

For Example 1, the mean expected LEM price (red) in comparison with the actual LEM price (black) is visualized in Figure 11. Hence, in Table 11 the price-quantity points for the day-ahead time frame $(\hat{c}, x_t^c)$ and $(\hat{c}, x_t^d)$ represent the bids of the agent, for the day-ahead LEM. Furthermore, the state of charge (e_t) over the day-ahead horizon for both the risk-neutral and risk-averse SO model 1 is represented in Figure 12.

Table 11: *(Decision) Variables and expected LEM price Example 1*

(a) $\beta = 0.0001$

time [h]	$\hat{c}_t$ [€/kWh]	x_t^c [kW]	x_t^d [kW]	SoC [kWh]
18	46.19	0	450	0
19	43.53	0	0	0
20	42.31	0	0	0
21	42.00	450	0	450
22	48.59	0	450	0
23	43.60	450	0	450
24	43.93	0	450	0

(b) $\beta = 0.999$

time [h]	$\hat{c}_t$ [€/kWh]	x_t^c [kW]	x_t^d [kW]	SoC [kWh]
18	46.19	0	450	0
19	43.53	0	0	0
20	42.31	307.61	0	307.61
21	42.00	142.39	0	450
22	48.59	0	450	0
23	43.60	138.58		138.58
24	43.93	0	138.58	0

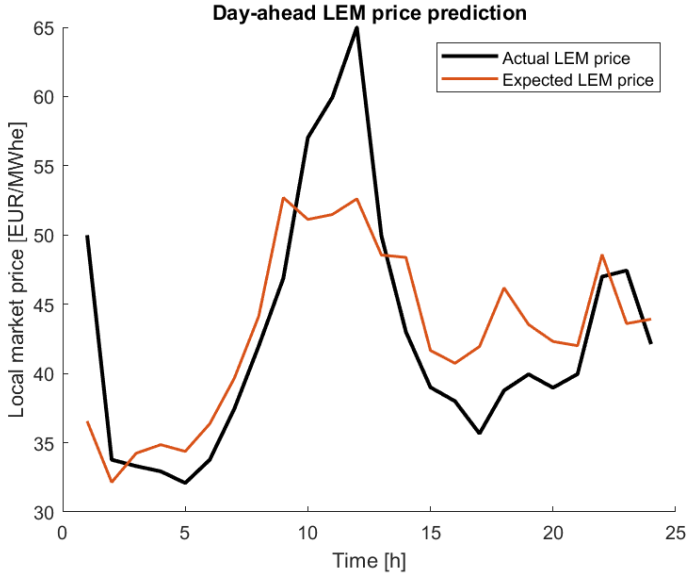

Figure 11: *Expected and actual LEM price Example 1, 4 scenarios*

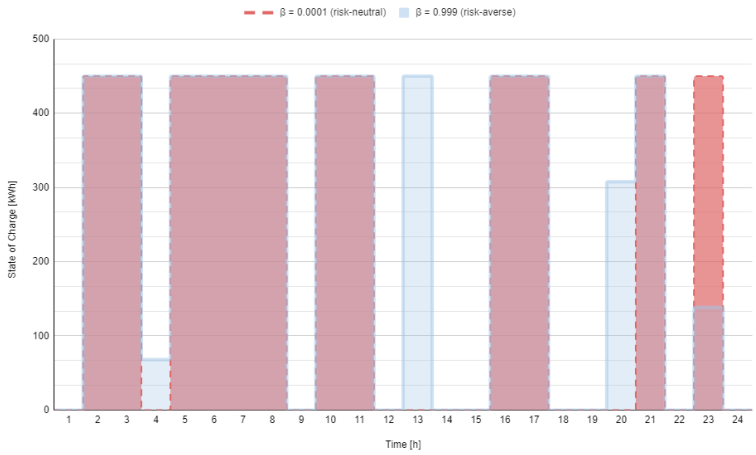

Figure 12: *BESS State of Charge Example 1*

10.3.1 Analysis case study 1

Pre-clearance performance

First, the analysis of SO model 1 with four scenarios is carried out. As represented in Appendix D.1, Appendix D.2 and Figure 8, the expected profit of the bidding schedule obtained for Simulations 1 - 10 and Examples 1 - 3 decreases as the agent owning the BESS becomes more risk-averse. On the other hand, the CVaR (the expected profit of the worst 5% of the profit realizations) increases when the agent becomes more risk-averse, meaning that the gap between the expected profit of the tail (worst 5 %) and the expected profit decreases. As observed in Figure 8, for the risk-averse attitude of the agent, the gap between the expected profit and the CVaR expected profit is the smallest. Hence, for $\beta = 0.999$, there is the smallest risk of obtaining a significantly smaller profit than anticipated. For the average simulation results of risk-neutral SO model 1, the gap between CVaR and the expected profit equals circa 4000 € (for $\beta = 0.0001$) and reduces to around 400€ (for $\beta = 0.999$) (Appendix D.2).

Looking at the pre-clearance performance of SO model 1 with ten scenarios instead of four, the same patterns appear, for both the simulations and examples. Hence, more risk-averse behavior increases the worst 5% of the expected profit, while the expected profit decreases. Observing Figure 8, the magnitude of the expected profit and the CVaR expected profit of simulations 1 - 10 is smaller when having ten scenarios compared to four scenarios (comparing the purple with the blue line and the red with the orange line).

Also, for the average performance of simulations 1 - 10 as represented in Figure 8, the magnitude of the decrease in expected profit is low when changing β, with a total profit deduction between the risk-neutral and risk-averse model of around 1500 € for both four and ten scenarios.

Post-clearance performance

Similar to the pre-clearance performance, first the post-clearance performance with four scenarios is analyzed. As represented in Appendix D.1, Appendix D.2 and Figure 9, the % of cleared bids and % of cleared quantity of simulations 1 - 10 and Examples 1, 2, and 3, remain stable when varying the risk attitude of the agent. The % clearance is observed around 41%.

The price-quantity points submitted by the agent change when varying the risk parameter, however, this does not significantly alter the % of bids cleared and the % of bid quantity cleared. This can be explained by investigating Figure 11. In Figure 11, both the expected and actual LEM prices are visualized, for Example 1 with four scenarios. It is observed that for every time t, the expected LEM price is either above or below the actual LEM price. Since the bid price of SO model 1 equals the expected LEM price at time t, for every time step, one of the two bid types (charging/buying or discharging/selling) is automatically declined by the market operator. When the agent becomes more risk-averse, the time steps that the model wants to submit a price-quantity point can change, as well as the quantity connected to some price-quantity points. To illustrate, for the risk-neutral SO model 1 of Example 1 the bid quantities are $x^c_{23} = 450$ and $x^d_{24} = 450$. For the Example 1 risk-averse model, these bid quantities are changed to $x^c_{23} = 138.58$ and $x^c_{24} = 138.58$ (Table 11). Changing the quantity of a price-quantity point does not change the % of bids cleared, because still the same expected LEM price $\hat{c}_t$ is submitted to the market operator. However, altering bid quantities can potentially change the % of bid quantity cleared.

As can be seen in Figure 11, during intervals of hours 3-9, 14-22, and 24, the expected LEM price is above the actual LEM price, meaning that in this interval, no *discharging/selling* bid will be cleared in the LEM. Adapting the discharging bid schedule of the agent *within* this interval does not increase the post-clearance performance of the agent. During intervals 1-2, 10-13, and 23, the situation is reversed, and *charging/buying* bids will not be cleared, also when adapting the charging schedule of the agent *within* these intervals.

Investigating the % clearance performance of simulations 1 - 10 with ten scenarios in Figure 9 and Appendix D.3, again no significant pattern of a changing % clearance is observed when varying the risk parameter. The % of bid quantity cleared increases from 46.85 % to 51.56 % when increasing β from 0.0001 to 0.999. However, for the % of bids cleared this pattern is not observed, since here the

metric changes from 46.74 % to 47.21 %. Investigating the % clearance for Examples 1, 2, and 3 in the case of ten scenarios, no consistent pattern is observed. Example 1 has stable clearance % when becoming more risk-averse, while Examples 2 and 3 indicate small improvement in % clearance. However, due to the larger sample size of the simulations, the post-clearance performance of the simulations is taken as the most valuable and reliable observation.

Comparing the magnitude of the % clearance performance of four and ten scenarios, an increase is observed in the case of ten scenarios. While the % clearance with four scenarios results in clearance around 41% for simulations 1 - 10, the % clearance with ten scenarios results in clearance around 48% for simulations 1 - 10 (for both % of bids cleared and % of bid quantity cleared). This can be observed in Figure 9.

Lastly, the expected costs/revenue are compared with the actual costs/revenue, for both four and ten scenarios. The results are represented in Figure 10, and provide similar patterns for four and ten scenarios. In the case of four scenarios, the expected costs and expected revenue do not change significantly when becoming more risk-averse. This is also represented in the expected profit, representing the expected revenue minus the expected costs (purple line in Figure 8). When investigating the actual costs and revenue, these values represent a relatively constant fraction of the expected costs/revenue. This constant behavior is correlated to the stable clearance performance metrics observed (% of bids cleared and % of bid quantity cleared). Namely, for the actual costs and revenue calculation, only the *cleared* bids are taken into account. In addition, the actual costs/revenue can deviate from the expected costs/revenue pattern because the *actual* LEM price is used instead of the mean bid price. Overall, the actual costs increase from around 35182 € to 40117 € when increasing β from 0.0001 to 0.999. On the other hand, the actual revenue decreases slightly from 51102 € to 49680 €.

In the case of ten scenarios, similar patterns are observed. As also observed in Figure 8, the expected profit is lower in the case of ten scenarios. This difference in magnitude can also be observed when comparing Figure 10a with Figure 10b, where both expected costs and revenue are lower in the case of ten scenarios. However, the actual revenue has a similar magnitude for four and ten scenarios. This can be mostly attributed to the higher % clearance in the case of ten scenarios (moving from around 41% for four scenarios to 48% for ten scenarios). Besides, the actual clearing price influences this magnitude, potentially deviating from the % clearance patterns.

10.4 Case study 2: SO model 2

Case study 2 is concerned with the pre- and post-clearance performance of SO model 2 (multiple bid model), as elaborated in Model 2: multiple bids and Model 2 with risk management. In this case study, $\beta = 0.0001$ is considered risk-neutral, and $\beta = 0.999$ is considered fully risk-averse. The Matlab code for the SO model 2 bidding model can be found on Github [104].

In Appendix E.1, the pre- and post-clearance performance of Examples 1, 2, and 3 with varying risk is represented, for both for and ten scenarios. The average pre- and post-clearance performance of simulations 1 - 10 are represented in Appendix E.2 and Appendix E.3. The visual representation of the pre- and post-clearance performance of simulations 1 - 10, for both four and ten scenarios, is represented in Figure 13 and Figure 14. Lastly, the expected costs and revenue of the simulation results are compared with the actual costs and revenue of the simulations. These results are represented in Figure 15a and Figure 15b, for four and ten scenarios, respectively.

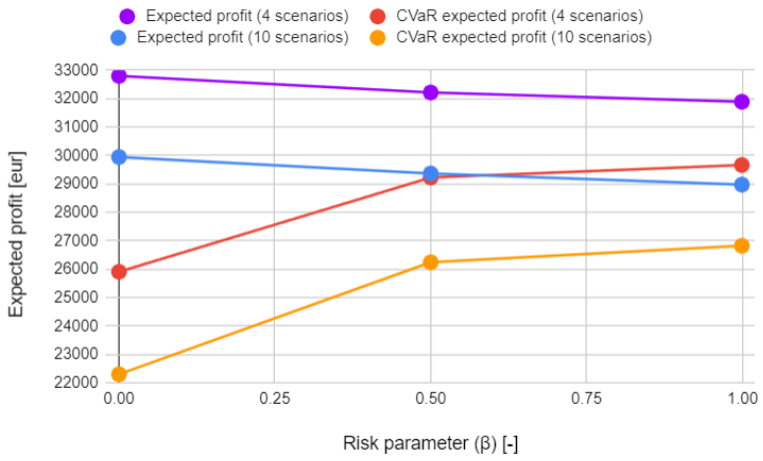

Figure 13: *Average pre-clearance performance simulations 1 - 10, case study 2, 4 and 10 scenarios*

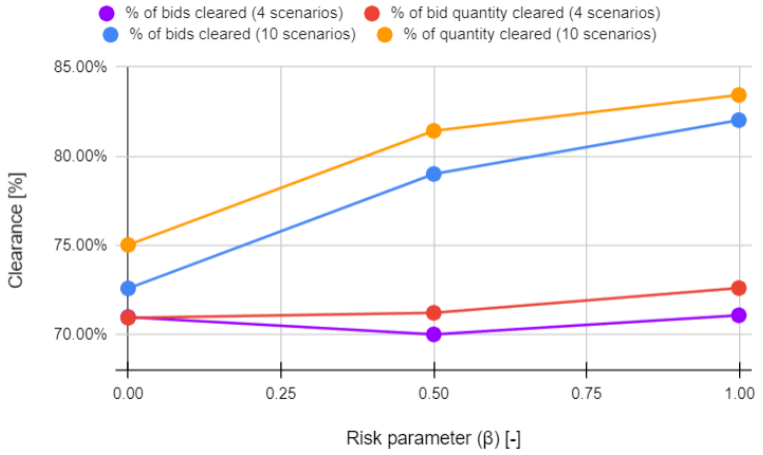

Figure 14: *Average post-clearance performance simulations 1 - 10, case study 2, 4 and 10 scenarios*

To illustrate the results of case study 2, the model specifications of risk-averse Example 1 ($\beta = 0.999$) are elaborated, in the case of four scenarios. The charge bid quantities ($x^c_{t,\omega}$) and the incremental charge quantities ($\Delta x^c_{t,\omega}$) of the risk-averse SO model 2 of Example 1, t = 15 until t = 24 are represented in Table 12a and Table 12b, respectively. The discharging bids are omitted in this visualization, but the methodology is the same. In Table 13, the corresponding scenario prices are represented, for each scenario ω. By analysing Table 13 and Table 12a, the incremental quantities in Table 12b can be derived. Namely, when multiple charging bids are submitted at the same time step, with equal bid quantity, the charging bid with the highest scenario price is represented as incremental quantity. In the case of different charge bid quantities, as is the case for t = 20, the (decision) variables $x^c_{t,\omega}$ and $\Delta x^c_{t,\omega}$ are constructed via the principles of the monotonic bidding curve, as elaborated in Model 2: multiple bids.

Furthermore, the incremental quantities ($\Delta x^c_{t,\omega}$) together with the corresponding scenario price construct the (active) charge price-quantity points that are submitted to the market operator. Hence, for time t = 20, the submitted charge price-quantity points ($c_{t,\omega}, \Delta x^c_{t,\omega}$) are: (46.01, 253.8) and (43.9, 82.33).

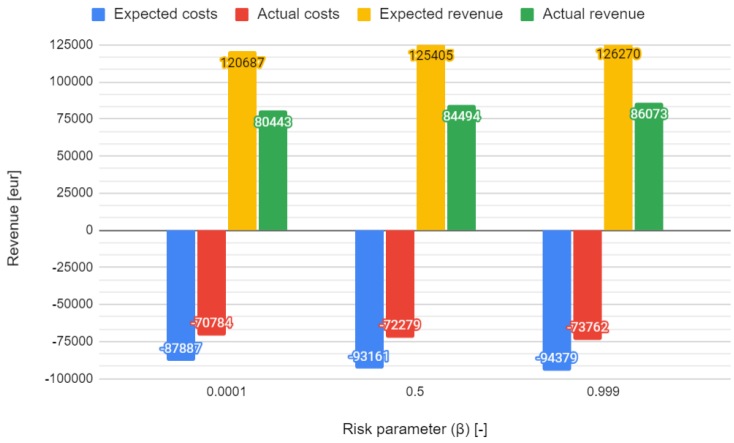

(a) 4 scenarios

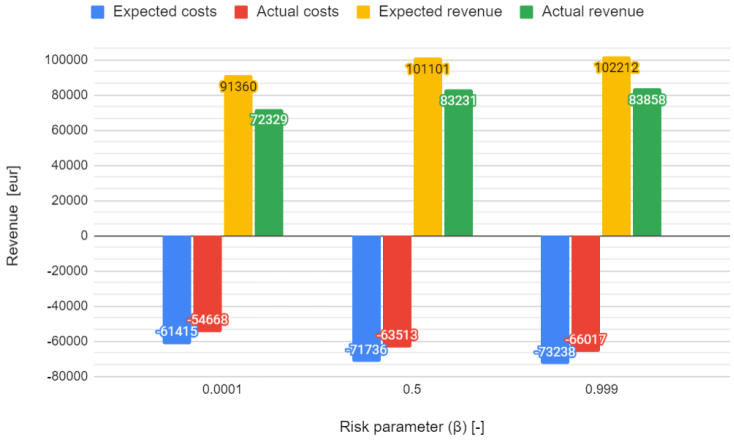

(b) 10 scenarios

Figure 15: *Comparison of expected costs/revenue (pre-clearance) and actual costs/revenue (post-clearance), case study 2*

Table 12: *(Decision) Variables Example 1 time 15-24, case study 2*

(a) Charge bid quantities $x^c_{t,\omega}$

time [h]	$x^c_{t,1}$ [kW]	$x^c_{t,2}$ [kW]	$x^c_{t,3}$ [kW]	$x^c_{t,4}$ [kW]
15	82.33	0	82.33	82.33
16	367.67	367.67	367.67	367.67
17	0	0	0	0
18	0	0	0	0
19	0	0	0	0
20	336.12	336.12	253.8	336.12
21	113.88	113.88	113.88	113.88
22	0	0	0	0
23	158.26	158.26	158.26	158.26
24	0	0	0	0

(b) Incremental quantities $\Delta x^c_{t,\omega}$

time [h]	$\Delta x^c_{t,1}$ [kW]	$\Delta x^c_{t,2}$ [kW]	$\Delta x^c_{t,3}$ [kW]	$\Delta x^c_{t,4}$ [kW]
15	82.33	0	0	0
16	0	0	0	367.67
17	0	0	0	0
18	0	0	0	0
19	0	0	0	0
20	0	0	253.8	82.33
21	0	0	0	113.88
22	0	0	0	0
23	0	0	0	158.26
24	0	0	0	0

Table 13: *Scenario prices Example 1 [€/kWh], case study 2, 4 scenarios*

Time	$\omega = 1$	$\omega = 2$	$\omega = 3$	$\omega = 4$
15	44.32	45.35	34.01	43.76
16	41.99	40.21	34.21	45.36
17	41.39	42.62	32.94	48.72
18	51.16	37.78	38.74	54.29
19	45.8	37.49	38.37	49.95
20	41.25	36.11	46.01	43.9
21	40.14	39.66	39.22	46.62
22	44.18	49.36	47.9	51.11
23	41.34	36.97	42.29	49.97
24	46.06	38.06	44.31	46.06

10.4.1 Analysis case study 2

Pre-clearance performance

Regarding the pre-clearance performance of SO model 2 with four and ten scenarios, it is observed that the expected profit of the bid model decreases as the risk aversion of the agent increases. This is both observed for Examples 1, 2, and 3 in Appendix E.1 and for simulations 1 - 10 in Figure 13, Appendix E.2 and Appendix E.3.

For the average performance of simulations 1 - 10 as represented in Figure 13, the magnitude of the decrease in expected profit is low when changing β, with a total deduction between the risk-neutral and risk-averse model of around 1000 € for both four and ten scenarios. For the CVaR expected profit metric, it is observed that CVaR increases when the agent becomes more risk-averse. This is the case for both Examples 1, 2, and 3 and simulations 1 - 10, for both four and ten scenarios. This means that when becoming more risk-averse, the worst 5% cases of the profit increase. As represented in Figure 13, the gap between CVaR and the expected profit is the smallest for the fully risk-averse agent.

Investigating Figure 13, a difference in magnitude for the expected profit and CVaR between four and ten scenarios is observed. When looking at the average pre-clearance performance of simulations 1- 10, in the case of four scenarios, the expected profit lies in the range of 32800-31891 € (purple line), depending on the risk attitude of the agent. In the case of ten scenarios, the expected profit lies in the range of 29945 - 28974 € (blue line), again depending on the risk-attitude of the agent. Since the same SARIMA model is used to establish the coefficients for the scenario generation, it becomes apparent that having more scenarios decreases the expected profit, for all risk-attitudes of the agent. When observing the difference in magnitude of CVaR for simulations 1 - 10, four scenarios represent a CVaR expected profit between 25906 - 29664 € (red line). When having ten scenarios, a range of 22298 - 26821€ is observed (yellow line). The profit obtained in the worst 5% of the cases is lower in the case of ten scenarios (yellow line) compared to having four scenarios (red line).

Post-clearance performance

In the case of four scenarios for simulations 1 - 10, the post-clearance performance remains stable at around 71% clearance when varying the risk attitude, for both the % of bids cleared and % of bid quantity cleared. This can be seen in Figure 14. For Examples 1, 2, and 3 in Appendix E.1, it is observed that the clearance performance increases when becoming more risk-averse. However, since the sample size of the simulations is larger, the pattern observed in simulations 1 - 10 is more reliable.

For the individual simulations 1 - 10 with four scenarios, it is observed that for simulations 6, 8, 9, and 10, clearance performance does not improve when becoming more risk-averse. This can be attributed to the fact that the scenario forecasts of these simulations do not comprise a consistent upper and lower bound surrounding the actual LEM price, and the peaks and troughs of the

scenarios do not properly align with each other as well as the actual LEM price. Exploring all scenario forecasts of simulations 1 - 10, in the case of four scenarios, it becomes apparent that aligned peaks and troughs of the scenarios contribute to higher % clearance performance. In addition, a forecast where the actual price is within the bounds of the scenario prices contributes to the clearing performance of the model. In other words, having at least one scenario price below and above the actual LEM price.

Each individual scenario creates a bidding schedule. However, the battery capacity constraints concern the *aggregate* of the incremental quantities ($\Delta x^c_{t,\omega}$ and $\Delta x^d_{t,\omega}$) of the price-quantity points. Hence, the overall bid schedule is interconnected across all scenarios. This results in the fact that not every peak and trough of an individual scenario can be exploited. If for three out of four scenarios, a trough occurs (meaning the battery wants to charge), and the fourth scenario prefers to charge a time step later, it is more beneficial for the fourth scenario schedule to align with the other three scenario schedules. This is because the incremental quantity of the three aligned scenario bids increases the state of charge of the battery. As a result, the fourth scenario cannot always charge again one time step later, since this might violate the capacity of the battery. This 'alignment' of the bidding schedule is preferable because more *equal* bid quantities at one time step increase the chance of clearance. If on top of the bid quantity alignment, the actual LEM price realization is within the bounds of the scenario prices, the model submits the most conservative scenario bid price that has the most chance of clearance.

This phenomenon is observed in risk-averse Example 1 (with four scenarios), as illustrated in Table 12 and Table 13. The scenario price realization of Example 1 is represented in Figure 5. At time t = 23, four equal bid quantities are obtained, namely $x^c_{23,1} = x^c_{23,2} = x^c_{23,3} = x^c_{23,4} = 158.26$. For scenarios 1, 2, and 3, the price realization at t = 23 is a price trough. For scenario 4, this is not the case, because the price at t = 24 is lower than t = 23. Still, it is most profitable for the model to charge at time t = 23, and discharge at t = 24. The actual price at t = 23 is equal to 47.44 [€/kWh], and the final active price-quantity point that is submitted to the market operator has a bid price of 49.97 [€/kWh]. Hence, this charge price-quantity point is cleared in the LEM. Without the alignment of $x^c_{23,\omega}$, this price-quantity point would not have been cleared since the other three scenario prices are below the actual LEM price.

For the case of having ten scenarios, the % of bids cleared and the % of bid quantity cleared has improved compared to having four scenarios, both in magnitude and risk-attitude pattern. When investigating the clearance performance of simulations 1 - 10 in Appendix E.3 and Figure 14, it is observed that the clearance metrics improve when becoming more risk-averse. The % of bid cleared improves in the range of 72.58 % to 82.02 %, when moving from risk-neutral to risk-averse. The % bid quantity cleared improves in the range of 75.02 % to 83.43 %. Comparing the post-clearance % performance metrics with four and ten scenarios, the % clearance with ten scenarios outperforms having four scenarios. This improvement can be attributed to the fact that ten scenarios can more comprehensively construct an upper and lower bound surrounding the actual LEM price. However, still, the peaks and troughs among the scenarios should align as much as possible to obtain a perfect clearance performance.

Lastly, the actual costs/revenue is compared with the expected costs/revenue in Figure 15. In the case of four scenarios, the expected costs and revenue both increase when becoming more risk-averse. The actual costs and revenue remain stable fractions of the expected costs and revenue, respectively, when becoming more risk-averse. Hence, as can be observed in Figure 15a, the magnitude of actual costs/revenue also increases when becoming more risk-averse. In addition, the gap between the expected and actual costs is smaller than the gap between the expected and actual revenue. In the case of ten scenarios, the magnitude of the gap between the actual and expected costs/revenue is smaller than for four scenarios. Besides, similar to the case of the four scenarios, the gap between the expected and actual costs is smaller than the gap between the expected and actual revenue.

Overall, the magnitude of the actual costs and revenue in the case of ten scenarios is lower than for four scenarios, following the pattern of the expected costs and revenue. However, the pattern of

increasing actual revenue and costs when becoming more risk-averse is observed more significantly in the case of ten scenarios. This pattern is correlated with the increasing % clearance for ten scenarios in SO model 2, and can additionally be influenced by the use of the actual LEM prices instead of the scenario LEM prices.

10.5 Case study 3: Comparing SO models 1 and 2

Case study 3 is concerned with comparing the pre-clearance and post-clearance performance of SO model 1 (single bid model/base model) with SO model 2 (multiple bids). This is done for both four and ten scenarios, similar to Case study 1: SO model 1 and Case study 2: SO model 2.

Starting with four scenarios, the pre-clearance performance results of simulations 1 - 10 of SO models 1 and 2 are combined in Figure 16. The expected profit of SO model 2 is higher than the expected profit for SO model 1, for all risk attitudes of the agent. However, the CVaR expected profit (worst 5% of the uncertainty realizations) is less for SO model 2 compared to SO model 1, for all risk attitudes of the agent. Similar patterns are observed for Examples 1, 2, and 3, in the case of four scenarios (Appendix D.1 and Appendix E.1).

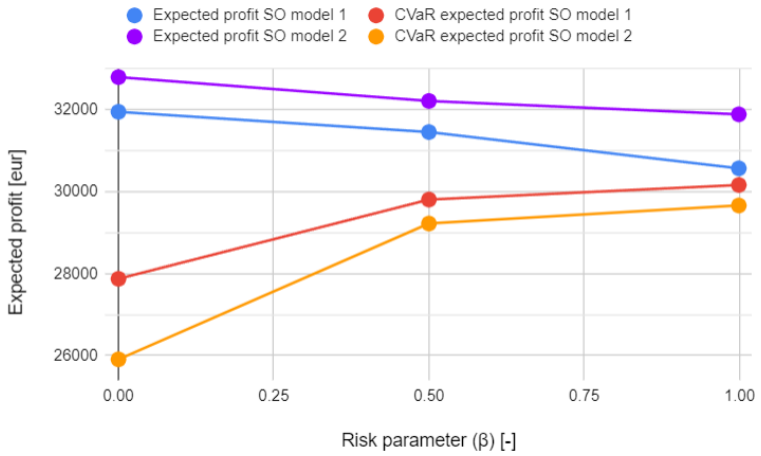

Figure 16: *Pre-clearance performance simulations 1 - 10, case study 3, 4 scenarios*

The % of bids cleared and % of bid quantity cleared for simulations 1 - 10, for four scenarios is visualized in Figure 17. Here, a substantial difference of around 30 % is observed between SO models 1 and 2. Both post-clearance % performance metrics of SO model 1 are observed around 41%, while the post-clearance % performance metrics of SO model 2 are observed around 71%. For both SO model 1 and SO model 2 with four scenarios it is observed that the % clearances remain stable when increasing the risk-aversiveness of the agent owning the BESS. No significant pattern is observed between a high clearance % for individual simulations of SO model 1 and a high clearance % for SO model 2. For example, simulation 1 has 100 % clearance performance for SO model 2, while for SO model 1, the % clearance performance is around average. A larger sample size is required to investigate the potential correlation between the % clearance between the two models.

Lastly, the expected and actual revenue/costs of SO models 1 and 2 in the case of four scenarios are compared (Figure 10a and Figure 15a). In line with the comparison of the bid clearance between SO models 1 and 2, it is observed that the gap between the expected and actual costs/revenue of the models is smallest for SO model 2. In other words, the actual costs and revenue of SO model 2 follow the expected costs and revenue more closely. Besides, the magnitude of actual costs and revenue of SO model 2 is higher than for SO model 1. Overall, more bids are cleared in SO model 2, resulting in higher actual costs/revenue. This result is closely connected to the clearance performance as previously mentioned.

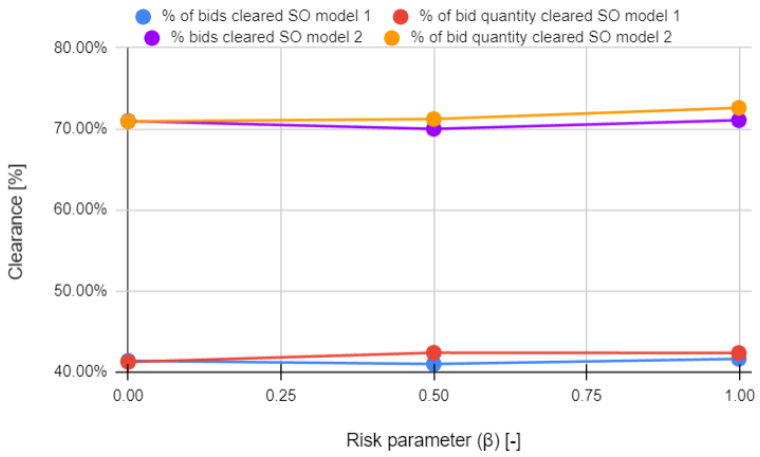

Figure 17: *Post-clearance performance simulations 1 - 10, case study 3, 4 scenarios*

For ten scenarios, the pre-clearance and post-clearance performance are represented in Figure 18 and Figure 19, respectively. For the pre-clearance performance, similar patterns are observed compared to having four scenarios. SO model 2 outperforms SO model 1 in terms of expected profit, for all risk-attitudes of the agent. Additionally, the CVaR expected profit is less for SO model 2 compared to SO model 1, for all risk-attitudes of the agent. This observation is in line with the results of Examples 1, 2, and 3, in the case of ten scenarios (Appendix D.1 and Appendix E.1).

It can be observed that both the expected profit and the CVaR expected profit are reduced in magnitude when having ten scenarios, compared to having four scenarios. This is already elaborated in Case study 1: SO model 1 and Case study 2: SO model 2.

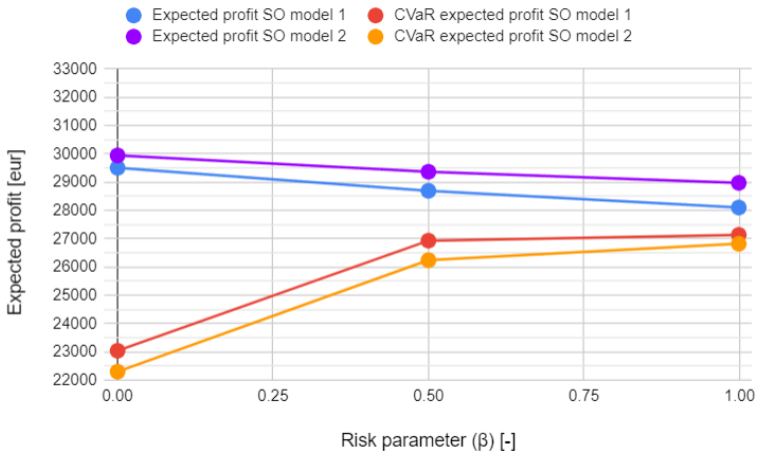

Figure 18: *Pre-clearance performance simulations 1 - 10, case study 3, 10 scenarios*

As represented in Figure 19, the substantial gap between the % clearance performance of SO models 1 and 2 again becomes apparent in the case of ten scenarios. The post-clearance performance of SO model 1 lies in the range of 46 - 52 %, while the post-clearance performance of SO model 2 lies in the range of 72 - 84 %. As elaborated in Case study 2: SO model 2, the post-clearance performance of SO model 2 also improves as the agent becomes more risk averse. This improvement is not observed for SO model 1. For the post-clearance performance of Examples 1, 2, and 3,

this significant clearance performance gap is also observed. Similar to having four scenarios, no significant pattern is observed that correlates high clearance in SO model 1 with high clearance in SO model 2.

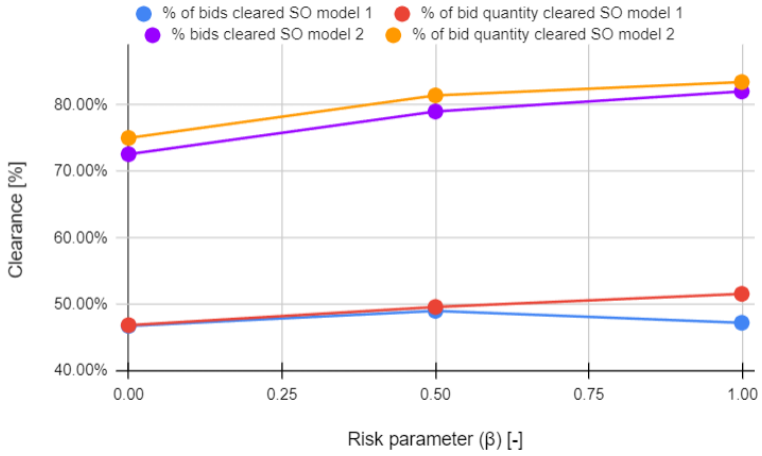

Figure 19: *Post-clearance performance simulations 1 - 10, case study 3, 10 scenarios*

Lastly, the comparison between the expected costs/revenue and the actual costs/revenue of SO models 1 and 2 has been made in the case of ten scenarios (Figure 10b and Figure 15b). The observations align with the case of having four scenarios. The magnitude of the actual revenue and costs of SO model 2 is higher than for SO model 1. In addition, the gap between expected costs/revenue and actual costs/revenue is smaller for SO model 2. This is again correlated with the higher % clearance performance of SO model 2.

10.6 Case study 4: Comparing SO model 1 and RO model

Case study 4 is concerned with comparing the pre-clearance and post-clearance performance of SO model 1 (single bid model/base model) with the RO model. The pre- and post-clearance performance of SO model 1 are represented in Case study 1: SO model 1. First, the results of the RO model are represented and afterward, the two bidding models are compared. As elaborated in Numerical investigations of the models, for the RO model, Γ_0 is specified for the range 0 - 8. $\Gamma_0 = 0$ represents risk-neutral, and $\Gamma_0 = 8$ represents the risk-averse agent. The Matlab code for the RO model can be found on Github [104].

10.6.1 RO model results

For the pre-clearance performance metrics of the RO model, the expected profit is obtained as well as the envisioned profit. For the *expected* profit, the *mean* bid price is used, and the expected profit is directly obtainable from the bidding model. On the other hand, the *robust* bid prices are the bid prices that are submitted to the market operator, meaning that the *envisioned* profit calculated via the robust bid prices is the most interesting to investigate. However, since the expected profit is the result directly obtained from the RO model, it is important to also look at the pattern of the expected profit.

The RO model pre- and post-clearance performance metrics of Examples 1, 2, and 3, are represented in Appendix F.1, for both four and ten scenarios. In addition, the average pre- and post-clearance performance of simulations 1 - 10 are represented in Appendix F.2 and Appendix F.3. The average results of the simulations are visualized in Figure 20 and Figure 21. Lastly, the comparison between the envisioned costs/revenue and the actual costs/revenue has been visualized for both four and ten scenarios in Figure 22a and Figure 22b, respectively.

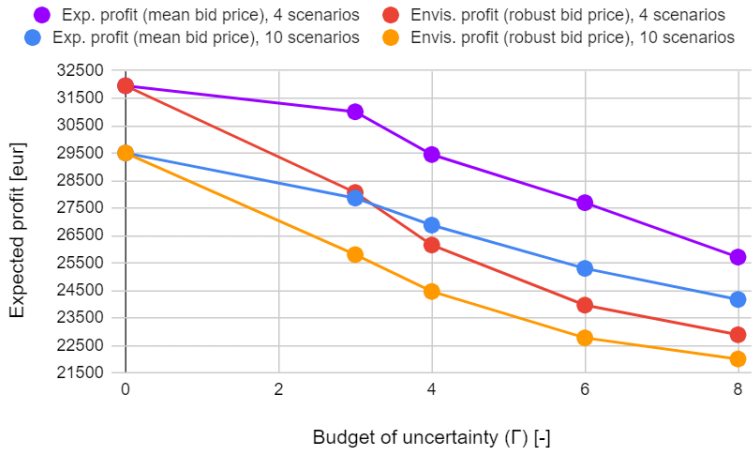

Figure 20: *Pre-clearance performance simulations 1 - 10, case study 4, 4 and 10 scenarios*

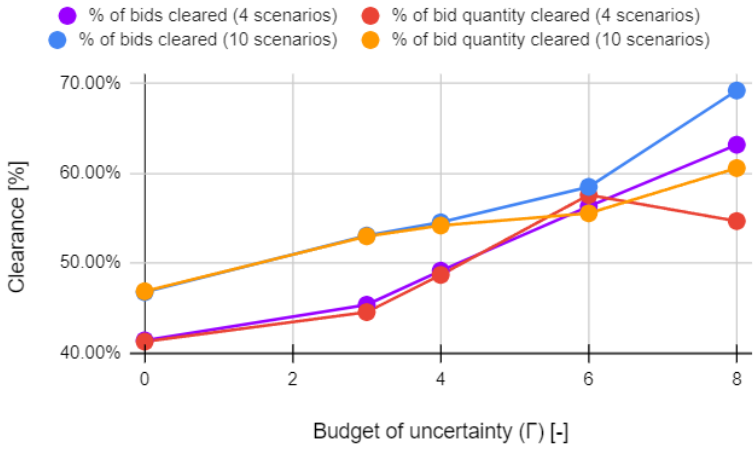

Figure 21: *Post-clearance performance simulations 1 - 10, case study 4, 4 and 10 scenarios*

To illustrate the performance of the RO model in comparison with SO model 1, risk-neutral Example 1 ($\Gamma_0 = 0$) is compared with risk-averse Example 1 ($\Gamma_0 = 8$), from t = 18 until t = 24. For SO model 1, the results of this same example are visualized in Table 11. For the RO model results, the bidding schedule is represented in Table 14. For the risk-neutral attitude, the same result is obtained for both models (RO model and SO model 1), charging at the lowest mean expected price $\bar{c}_t$ and discharging at the highest mean expected price $\bar{c}_t$. For $\Gamma_0 = 0$, the RO model does not take into account deviation from the mean expected price $\bar{c}_t$. When looking at the results for $\Gamma_0 = 8$, a more conservative bidding strategy is observed. Instead of charging the BESS fully at time t = 21, where the expected price is the lowest, the risk-averse model wants to charge equally at t = 19, 20, 21. As can be seen in the expected price table (Table 15), the predicted prices of times t = 19, 20, 21 are very close to each other. Due to $\Gamma_0 = 8$, the conservative model allows the prices to deviate from the expected prices, taking t = 19, 20, and 21 equally beneficial to charge the BESS.

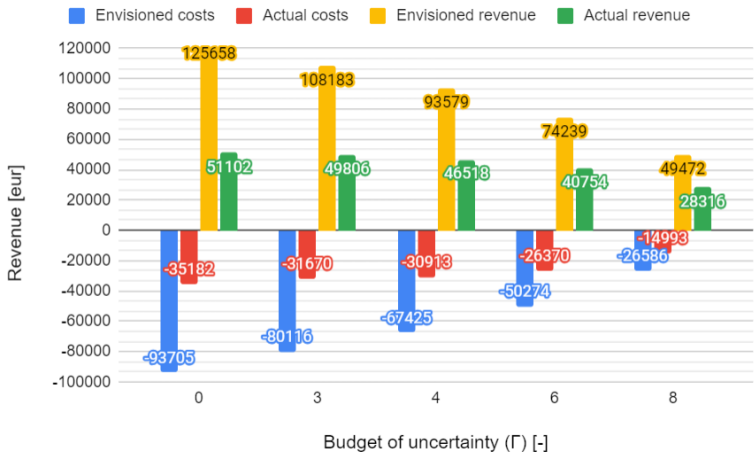

(a) 4 scenarios

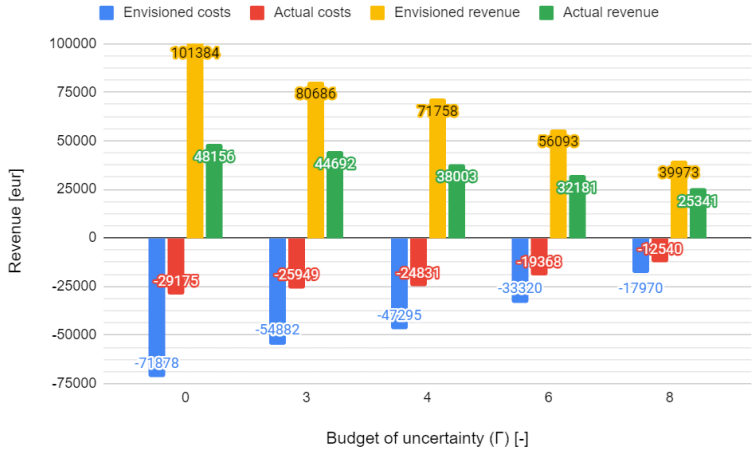

(b) 10 scenarios

Figure 22: *Comparison of expected costs/revenue (pre-clearance) and actual costs/revenue (post-clearance), case study 4*

Table 14: *Bidding schedule Example 1 time 18-24, case study 4*

(a) $\Gamma_0 = 0$

Time [h]	x_t^c [kW]	x_t^d [kW]	SoC [kWh]
18	0	450	0
19	0	0	0
20	0	0	0
21	450	0	450
22	0	450	0
23	450	0	450
24	0	450	0

(b) $\Gamma_0 = 8$

Time [h]	x_t^c [kW]	x_t^d [kW]	SoC [kWh]
18	0	75	150
19	75	0	225
20	75	0	300
21	75	0	375
22	0	375	0
23	75	0	75
24	0	75	0

Table 15: *Price specifications Example 1, case study 4, 4 scenarios*

Time [h]	$\bar{c}_t$ [€/kWh]	d_t [€/kWh]
18	46.19	4.94
19	43.53	4.94
20	42.31	4.94
21	42.00	4.94
22	48.59	4.94
23	43.60	4.94
24	43.93	4.94

10.6.2 Analysis case study 4

RO model performance analysis

In the case of four scenarios, it is observed for simulations 1 - 10 and Examples 1, 2, and 3 that the expected and envisioned profit of the RO model drops when the agent becomes more risk-averse. This can be seen in Figure 20, Appendix F.1 and Appendix F.2. In addition, the envisioned profit with the *robust* bid price is lower than the expected profit with the *mean* bid price, for all risk-attitudes except being risk-neutral. These same patterns are observed when having ten scenarios, for both the examples and simulations (Appendix F.1 and Appendix F.3). Furthermore, the expected and envisioned profit of the RO model is lower for ten scenarios than four scenarios, for every risk-attitude of the agent, for simulations 1 - 10.

Regarding the post-clearance performance (%), it is observed that for both four and ten scenarios, the clearance metrics of simulations 1 - 10 and Examples 1, 2, and 3 improve when moving to a more risk-averse attitude (Figure 21). In the case of four scenarios, the average % of cleared bids of simulations 1 - 10 improves from 41.39 % to 63.16 %, and the % cleared quantity improves from 41.25 % to 54.66 %. In the case of ten scenarios, the average % of cleared bids of simulations 1 - 10 improves from 46.74 % to 69.19 %, and the % cleared quantity improves from 46.85 % to 60.56 %. As can be seen in Figure 21, the clearance performance of ten scenarios outperforms having four scenarios.

When observing Figure 22, it is observed that the envisioned and actual costs and revenue both reduce in magnitude when the agent becomes more risk-averse. Similar to before, the actual costs and revenue follow the behavior of the envisioned costs and revenue. However, the envisioned costs/revenue decrease with greater magnitude compared to the actual costs/revenue. This can be mainly attributed to the increase in (%) clearance performance when the agent is more risk-averse, where the actual revenue/costs comprise a larger fraction of the envisioned revenue/costs for larger values of Γ_0. Furthermore, it is observed that the magnitude of the envisioned and actual revenue/costs of the four scenarios is higher compared to the ten scenarios, for all risk attitudes.

Investigating the results of the RO model, an important observation is made. For every testing set example, a 'threshold value' of Γ_0 arises from which onward the dual variable p equals zero. For both four and ten scenarios, the first Γ_0 that obtains p equal to zero lies in between 8 - 13. When this occurs, the performance metrics can show extraordinary patterns. For example, Example 1 with four scenarios exhibits $p = 0$ when $\Gamma_0 = 12$. Then, the bidding schedule comprises two time steps where the agent submits bid quantities over the whole time horizon, where only one of the bids is cleared. As a result, the clearing performance of Example 1 with $\Gamma_0 = 12$ drops to around 10 %, deviating from the pattern where high values of Γ_0 have better % clearance performance, as can be observed in Figure 21. For all simulations and examples, increasing Γ_0 beyond this 'threshold' does not alter the bidding schedule anymore, meaning that the most risk-averse bidding schedule has been obtained. The Numerical investigations of the models elaborates that Γ_0 in the range of 0 - 8 is assessed since Γ_0 should be of the order $\sqrt{24}$. Hence, the results above show the patterns observed only in the range Γ_0 in 0-8.

RO and SO model 1 comparison analysis

A note must be made before comparing the RO model and SO model 1, since the risk parameters used for both models are not 1-on-1 equivalent. For SO model 1, β is varied between 0 - 1, where 0 means a risk-neutral attitude and 1 means fully risk-averse. For the RO model, Γ_0 is varied between 0 - 8. Hence, for this comparison, the risk-attitude of $\Gamma_0 = 8$ is considered the most conservative bidding schedule in the case of the RO model.

Comparing Examples 1, 2, and 3, with four scenarios, it is observed that in the case of a risk-neutral attitude, the expected profit is equal for SO model 1 and the RO model. This also holds for the envisioned profit of the RO model and the expected profit of SO model 1. For the analysis, the envisioned profit for the RO model is used, since this resembles the profit with the robust bid price that is submitted to the market operator. When increasing the risk-aversiveness of the agent, it is observed that the envisioned profit of the RO model decreases with greater magnitude compared to the expected profit of SO model 1. For simulations 1 - 10, the average range of envisioned profit of the RO model reduces from 31953€ to 22887€. For SO model 1, this reduction stretches from 31953€ to 30572€. This pattern aligns with the Example results and holds for both four and ten scenarios. Overall, the RO model envisioned profit reduces with greater magnitude when becoming more risk-averse compared to SO model 1 expected profit.

Similar to the pre-clearance performance, the % post-clearance performance in risk-neutral SO model 1 and RO model are equal (% of bids cleared and % of bid quantity cleared). As described in Case study 1: SO model 1, the clearance performance of SO model 1 remains stable when increasing the risk-aversiveness of the agent. As represented in Figure 21, the clearance performance improves when the agent becomes more risk-averse. Hence, for all risk attitudes, RO model 2 outperforms SO model 1 in terms of clearance performance, except for the risk-neutral models. This pattern is also observed for Examples 1, 2, and 3, for both four and ten scenarios.

When observing Figure 10 and Figure 22, different patterns are observed for the SO model 1 and the RO model. As elaborated above, the actual costs and revenue of the RO model decrease as the agent becomes more risk-averse. This is due to the conservative bidding schedule obtained in the RO model, for high values of Γ_0. However, for SO model 1 the actual revenue and costs remain stable when varying β. As a result, the magnitude of the actual costs and revenue is greater for SO model 1, for all risk attitudes except being risk-neutral. In the risk-neutral models, the actual revenue and costs are equal.

11 Discussion

This chapter discusses the limitations of the research and elaborates on the main findings. The main findings are compared with existing theory and remarkable observations of the case studies are discussed. Afterward, three interesting future directions of research are described, where the last future direction is elaborated in more detail.

Scenario-based modeling of price uncertainty elaborates on the theoretical framework for deriving a representative reduced set of scenarios, used as input into the developed SO models. First, as stated in the Numerical investigations of the models section, the lack of accurate historical data on LEM prices prevented the use of the specified SARIMAX model in this research. The envisioned methodology to obtain an accurate forecast of the LEM price was to incorporate an historical LEM price data time series and to use an (accurate) WSM price data time series as an exogenous variable to capture the correlation between the WSM and the LEM. An attempt was undertaken to construct LEM data based on bids submitted by dummy agents, meaning that the agents submit bids based on simple, unsophisticated bidding mechanisms. By aggregating the bids from local participants in the LEM day-ahead market, the determination of the local market's short or long state becomes feasible. Subsequently, according to the proposed market clearing mechanism in Appendix A, the local market price could be forecasted, and local market price data could be generated. Hence, it is required to have insight into the local demand and supply ratio to ascertain deviations of the local market price from the wholesale market price. The Matlab code on Github [104] was created to determine the local market clearing price based on the local bids submitted, and to determine which of the submitted bids are cleared in the LEM. The market clearance was determined by carrying out the proposed market clearing mechanism in Appendix A. Regrettably, due to time limitations and the lack of accuracy of the dummy agents in the LEM, the generated LEM price data could not be effectively integrated into this research.

As mentioned throughout the research, the models developed in this research are tailored to the LEM day-ahead market. Nonetheless, the methodology permits the generation of price scenarios for different energy markets provided accurate price data is available. Then, with a set of price scenarios generated according to the methodology elaborated in Scenario-based modeling of price uncertainty, the developed bidding models to determine the optimal bidding schedules can be applied across various energy markets.

In this research, the publicly available WSM price data [32] is set equal to the LEM price data, with a SARIMA point forecast model employed for stage 1 of the scenario generation methodology described in Scenario-based modeling of price uncertainty. However, there are some limitations in the methodology of the SARIMA model used in this research. First, the daily seasonality of the electricity prices is captured in the SARIMA model (S = 24), excluding other price seasonalities, such as weekly and yearly seasonality [107]. Additionally, the order parameters p, d, q, P, D, Q are determined by investigating the training set of Example 1 and are subsequently applied to the other examples/simulations. This approach, while promoting coherence between the scenario generation algorithm and case studies, may not yield optimal order parameter combinations for different datasets, potentially comprising the goodness of fit of other forecasts. Furthermore, a limited number of combinations of the order parameters is investigated in this research, resulting in a possible sub-optimal order parameter combination for Example 1. As elaborated in Numerical results, residual auto-correlation persists in Example 1's prediction error, indicating potential improvements in capturing time series correlations through an alternative order parameter set. Moreover, the (S)AR(I)MA(X)-type models make certain simplifying assumptions, for example, the prediction error (residuals) conforming to white noise characteristics (e.g. zero mean, constant variance) [107]. In literature, more sophisticated models exist which relax this assumption. For example, the Generalized Auto-regressive Conditional Heteroskedasticity (GARCH) model enables varying prediction errors (residuals) over the forecast horizon [27]. Combining the (S)AR(I)MA(X)-model with the GARCH model, similar to [27] can lead to more sophistication in the LEM price forecast.

11.1 Main findings

Analyzing the results of the stochastic optimization models, the pre-clearance performance of SO models 1 and 2 align with existing theory. First of all, existing literature states that expected profit diminishes with increasing levels of risk aversion [23]. This pattern is also observed in the case studies carried out in this research. On the other hand, the CVaR expected profit increases when becoming more risk-averse, as elaborated in [23]. This pattern is also observed in Case study 1: SO model 1 and Case study 2: SO model 2. Furthermore, [37] finds that allowing more price-quantity points per time step have resulted in enhanced expected profit performance compared to a single price-quantity point submission per time step [50]. This statement is supported by the results of Case study 3: comparing SO models 1 and 2, where the comparison between SO models 1 and 2 demonstrates superior expected profit performance for SO model 2 across varying risk attitudes.

Furthermore, in Case study 3: comparing SO models 1 and 2 it has been found that the % clearance performance of SO model 2 outperforms the % clearance performance of SO model 1, for all risk attitudes. While SO model 1 exhibits constant % clearance regardless of the agent's risk attitude, SO model 2 displays an increasing pattern, only evident in the case of ten scenarios. The essence of risk management in this context revolves around mitigating the potential for high charging costs when buying energy and avoiding negative revenue when selling energy. In the SO models, the price scenarios comprise the only information about the day-ahead prices. Consequently, the optimization model mitigates the risk associated with the *forecasted* day-ahead prices, operating under the assumption that the price scenarios accurately reflect the probability distribution of the day-ahead window. Hence, discrepancies between forecasted and actual day-ahead market prices can introduce misalignments in the risk the model wants to reduce and the risk the actual day-ahead market represents. In the end, having a good price forecast is essential in creating an optimal bidding schedule for an agent participating in the LEM.

Overall, the findings from the simulations were consistent with those from the examples. However, there were some deviations noted in terms of the % of bids cleared and the % of bid quantity cleared, which did not coincide with the patterns observed in the simulations. Notably, these two metrics exhibited significant variability across both simulations and examples, emphasizing the importance of a large sample size. In this research, more credibility is given to the simulation observations compared to the example observations, due to its larger sample size. Given that the % clearance of SO model 2 with ten scenarios outperforms that of four scenarios, further investigation with an increased sample size can provide a more comprehensive insight into these patterns. Since the % clearance of SO model 2 with ten scenarios outperforms four scenarios, additional research with a larger sample size can provide more insight into these observed patterns.

Analyzing the performance of the RO model, with varying Γ_0, the distinction is made between the expected profit and the envisioned profit of the bidding schedule. The expected profit is directly derived from the model results, while the envisioned profit manipulates the bid price of the bidding schedule after obtaining the optimal schedule. Consequently, comparing the envisioned profit of the RO model with the expected profit of SO model 1 is not 1-on-1 equivalent. Moreover, as highlighted in Case study 4: Comparing SO model 1 and RO model, distinct risk parameters are employed for the RO and SO models, making the comparison between the two models complex. A proposed solution to make a more fair comparison between these two models is outlined in Further research.

In the RO model results, $\Gamma_0 = 8$ is identified as the most conservative risk-attitude of the agent. In the case of four scenarios, simulations 2, 8, and 10 have reached their most risk-averse bidding schedule with $\Gamma_0 = 8$. For ten scenarios, simulations 3, 8, and 10 also obtain their most risk-averse bidding schedule when $\Gamma_0 = 8$. Increasing Γ_0 beyond this value does not alter their bidding schedule. Moreover, the dual parameter p equals zero when the most risk-averse bidding schedule has been obtained. In the most risk-averse bidding schedules, % clearing patterns can deviate from the observed increasing clearance patterns, because the number of price-quantity points in these bidding schedules reduces compared to a risk-neutral bidding schedule. Consequently, if the reduced number of price-quantity point fails to clear in the LEM, the % clearance declines significantly, deviating from the observed pattern.

Using a similar argument as for the SO model % clearance behavior, the RO model uses the mean price forecast and its standard deviation forecast as input. The RO model becomes more risk-averse using its uncertainty set as reliable information. However, in reality, assuming a constant standard deviation over the day-ahead timeframe, as presumed by the (S)AR(I)MA(X)-type models, is unrealistic [27]. Consequently, the upper and lower bounds of the box interval may misalign with the actual LEM price. To mitigate the risk of high charging costs during battery charging and negative revenue in the case of battery discharge, an accurate box interval uncertainty set is essential.

Furthermore, the post-clearance performance metrics, actual revenue/costs, are analyzed. Comparing the actual revenue/costs with the expected (envisioned) revenue/costs derived from the bidding models, a note should be made. Moving from the expected (envisioned) costs/revenue to the actual costs/revenue, the bid price has been changed into the *actual* LEM price and only the *cleared* bids are considered. Hence, a pattern observed in the actual revenue/costs when varying the risk attitude of the agent can be caused by the changing clearance performance (%) and changing bidding schedules using different *actual* price realizations. Notably, the actual revenue and costs may present a skewed perspective as uncleared bids are disregarded. This research does not incorporate a penalty or fine system for the agent to compensate for the uncleared bids, and a balancing market is out of the scope of this research. Hence, relying on the actual revenue and cost results and the patterns observed when varying the risk is not very reliable. For instance, low actual charging costs do not necessarily indicate a profitable bidding schedule but could result from a low % charging clearance performance. Nevertheless, the actual revenue/costs of SO model 2 exhibit the largest magnitude across all risk attitudes of the agent. The gap between the actual revenue and actual costs and the expected revenue and expected costs is the smallest for SO model 2. This aligns with the good % clearance results obtained for SO model 2.

While the RO model requires solely an upper and lower bound of the uncertainty (using the box interval uncertainty set), the SO models require explicit scenario price generation to obtain the bidding schedules. Given the complexity inherent in forecasting energy prices, employing the RO model with *accurate* upper and lower bounds of the uncertainty set offers a simpler alternative. Still, when exploiting RO, using a point forecast model is required to determine an accurate mean and standard deviation of the LEM prices. When limited information is available on day-ahead prices, the RO model emerges as a viable choice. However, when enough historical data exists to obtain an accurate set of scenarios, the superiority of SO model 2 over the RO model in terms of % clearance and expected profit becomes evident, as demonstrated in this research. In this case, opting for SO model 2 proves more advantageous than exploiting the RO model developed in this research.

11.2 Future research

This section is concerned with outlining multiple interesting future research directions in the field of optimizing bidding schedules for agents in energy markets. The last research direction outlined in this section is elaborated in more detail.

CVaR uncertainty set in robust optimization model

First, the RO model developed in this research has a simple, straightforward uncertainty set, namely the box interval $[\bar{c}_t - d_t, \bar{c} + d_t]$ [26]. As carried out in this research, this uncertainty set can be integrated into the robust optimization model of an agent owning the BESS asset. As elaborated in the Discussion, comparing the performance of SO model 1 with risk management and the RO model developed in this research is complex, since the risk parameters used in the two models are not 1-on-1 equivalent. However, Uncertainty set construction via risk measures derives a different uncertainty set in robust optimization, representing the CVaR risk measure as the uncertainty set in robust optimization. Future research can investigate implementing the uncertainty set represented in Equation 6.24 into the robust optimization problem and obtain the optimal bidding schedule of the agent. Then, more emphasis can be put on comparing SO model 1 with CVaR as risk management and the RO model with an uncertainty set as represented in Equation 6.24.

Other energy markets

Existing papers focus on exposure to the real-time market besides the day-ahead market, enabling the agent to bid in both markets. Hence, the bidding schedule of the agent for the day-ahead market can be corrected in the real-time market [59]. This makes the optimization of the bidding schedules more complex, but also more realistic. In this research, the bids that are not cleared in the LEM day-ahead market cannot be compensated or corrected in other markets.

Besides the future direction of incorporating another market to compensate for the uncleared bids in the day-ahead market, the optimization models developed in this research can be applied to whole other markets in general. An example of this is the hydrogen market. The only requirement to use the developed bidding models is to acquire enough data to forecast energy prices, which have to be used as input in the (stochastic and robust) optimization models.

Multiple asset expansion

This section provides an outline of how to expand the developed optimization models to account for multiple assets. The scope of this research was to maximize the profit of a single agent operating within the day-ahead market. The asset collection of the agent in this research consisted of owning a BESS asset. However, an interesting expansion of the optimization models developed in this research, especially SO model 2, is to add multiple assets to the asset collection of the single agent, and again determine the optimal bidding schedule of the agent participating in the day-ahead market. The guidelines on how to carry out this expansion of assets for SO model 2 are provided next.

In SO model 2 (Model 2: multiple bids, different types of constraints are constructed. These types of constraints are categorized into Battery constraints, Monotonicity constraints, Non-anticipativity constraints, Active price-quantity point constraints, and State of charge of active price-quantity points constraint. The Battery constraints and State of charge of active price-quantity points constraint are BESS specific constraints. The other constraint types are general constraints, required to construct the (monotonic) buying and selling bidding curve of SO model 2.

When adding another asset to the optimization problem, adjustments are made to the constraints and the objective function. New asset-specific constraints are required, for example, specifications of PV-panel electricity generation in case of adding PV panels or generator electricity generation in case of adding a generator. An example of an asset-specific constraint for a generator is that the electricity output of the generator should remain within the capacity bounds of the generator [50].

Importantly, the distinction between the different electricity outputs of the assets needs to be made. In this research $x^c_{t,\omega}$ and $x^d_{t,\omega}$ represent the (dis)charge quantities of the BESS asset, directly bidding into the day-ahead market. These quantities are the only electricity quantities incorporated in this research because the (dis)charge rate of the battery is equal to the electricity that is bid into the day-ahead market. When adding another asset to the optimization model, constructing an *internal energy balance* becomes an essential additional element of the optimization problem. For example, in [50], an internal energy balance is constructed in the constraints, balancing the day-ahead market quantity sold/bought (macro grid), the real-time market quantity sold/bought (macro grid), the battery (dis)charge rates, electricity generated by the generator, electricity generated by the PV system, and electricity demand of the agent (comprising the microgrid). When having multiple assets in the optimization problem, the supply elements and the consumption of energy need to be balanced. Focusing on the day-ahead market only, the actual bids that the agent submits are the electricity quantities sold/bought in the day-ahead market. These bid quantities that are submitted to the day-ahead market cover the electricity patterns of all assets, not just the battery asset, as is the case in this research.

Hence, adding additional assets requires the addition of asset-specific constraints and the internal energy balance of the agent, balancing the electricity usage patterns of all assets. In the objective function, when only taking into account the day-ahead market costs, the battery charge/discharge quantities in the objective function ($x^c_{t,\omega}$ and $x^d_{t,\omega}$) are replaced by the bid quantities to buy/sell

electricity in the day-ahead market ($x_{t,\omega}^{buy,DA}$ and $x_{t,\omega}^{sell,DA}$). As mentioned before, these new bid quantities comprise the aggregate electricity usage of all assets and bid electricity in the day-ahead market when it is convenient for all assets, not only the BESS asset. Besides, additional costs can arise when having multiple assets, for example from a generator asset that uses fuel. Hence, multiple cost terms can arise in the new objective function, targeting cost elements of the different asset collections of the model.

Adding risk management to SO model 2 with multiple assets is expected to have a similar methodology as described in Model 2 with risk management. The same risk can be targeted, namely the risk of the day-ahead market price being uncertain. Still, the goal of the agent is to sell (buy) electricity in the day-ahead market when the price is high (low). The risk connected is that the price can deviate from the expected price, resulting in high costs (or negative revenue). However, care should be given to the decision variables that are incorporated into the CVaR constraints. In this research, the expected costs in the objective function (including $x_{t,\omega}^{c}$ and $x_{t,\omega}^{d}$) are used in the CVaR constraints to measure the risk of the worst 5% of the cases. When having multiple assets, these decision variables also change to ($x_{t,\omega}^{buy,DA}$ and $x_{t,\omega}^{sell,DA}$), as introduced above.

Lastly, the models developed in this research could expand to also incorporate the real-time market, which is used when the bid quantity in the day-ahead market is not cleared [59]. When also incorporating risk management in the real-time market, the complexity of the model grows significantly.

12 Conclusion

This research focused on developing the optimal bidding schedule for an agent owning a BESS asset, participating in the LEM day-ahead market. The agent aims to exploit energy arbitrage of the LEM, by buying energy at low prices and selling energy when the price is high [59]. To cope with the uncertainty of the LEM day-ahead prices, both stochastic and robust optimization domains were investigated.

This research commenced by providing the reader with a theoretical foundation regarding scenario-based modeling. Scenario-based modeling was used in the modeling domain of stochastic optimization to represent the LEM price uncertainty. Afterward, the outline to add risk management to a stochastic optimization problem was provided. Risk management is added to the stochastic optimization models in this research by using the Conditional Value at Risk (CVaR) risk measure [74]. CVaR represents the expected profit of the (1-α)% worst cases of the profit realizations [72], where the aim is to minimize these worst cases.

In terms of robust optimization, a general robust problem was firstly derived by specifying the uncertainty set used in this research. The box interval uncertainty set is constructed, which is obtained by specifying the mean price forecast and its standard deviation. By using a polyhedral box interval uncertainty set, the robust counterpart of the original problem could be constructed. Afterward, by constructing its dual problem, a general, linear robust optimization problem was derived that could later be scoped to the battery asset specifications.

After the theoretical background has been provided for both stochastic and robust optimization domains, two stochastic models have been developed in the application of the agent owning the BESS asset. The risk-neutral SO model 1 serves as a benchmark model, where the agent is allowed to submit a single bid to the market operator per time step. SO model 2 allows the submission of multiple bids per time step, resulting in a monotonic bidding curve construction for both charging and discharging bids [36]. Despite monotonicity constraints, non-anticipativity constraints, and active price-quantity point constraints are developed for SO model 2 [50]. Both of the stochastic optimization models are extended to incorporate the risk attitude of the agent. This is done separately for charging risk, discharging risk, and simultaneous charging and discharging risk of the battery. However, the case studies are carried out only with simultaneous charging and discharging risk.

Applying the general robust problem derived in the theoretical background to the agent owning the BESS asset participating in the day-ahead market, the robust optimization model is developed. The developed RO model can submit a single price-quantity point per time step. For the robust optimization model, the budget of uncertainty is used to adjust the risk attitude of the agent.

Transitioning to the numerical investigations of the models, three example training sets and ten simulation training sets of LEM price data are constructed to develop the LEM day-ahead forecasts. The SARIMA$(1,0,1)(1,0,1)_{24}$ model was used as a point forecast model to forecast the LEM day-ahead prices. Then, based on the found model coefficients, 100 LEM day-ahead price scenarios were generated via the developed scenario generation algorithm. Afterward, these scenarios were reduced to a tractable number of four and ten scenarios, by using the forward selection algorithm based on the Kantorovich Distance [73, 23]. This optimal reduced set of scenarios served as input in the developed stochastic optimization models. The mean and standard deviation obtained from the SARIMA$(1,0,1)(1,0,1)_{24}$ model were similarly used as input in the robust optimization model.

The three examples have different training set durations. Example 3 obtained the lowest MAPE value, constructing the most accurate price forecast. Consequently, the simulations are constructed with a training set duration of one week, similar to Example 3. Then, four case studies are conducted to assess the performance of the bidding models, assessing the performance of having four and ten scenarios. These case studies assess the performance of SO models 1, 2, and the RO model separately, varying the risk attitude of the agent. In addition, the performance comparison has been made between SO models 1 and 2, and between SO model 1 and the RO model.

The performance metrics are divided into pre-clearance performance metrics and post-clearance performance metrics. In terms of pre-clearance performance, it is observed for all three models that the expected profit decreases as the agent becomes more risk-averse. On the other hand, the CVaR expected profit in SO models 1 and 2 increases when becoming more risk-averse. The gap between the expected profit and the CVaR expected profit decreases as the agent becomes more risk-averse.

In terms of expected profit, SO model 2 outperforms the other two models, for all risk attitudes of the agent. In addition, it is observed that the expected (envisioned for the RO model) profit has a smaller magnitude in the case of ten scenarios compared to four scenarios, for all three models and all risk attitudes. From the three models, the RO model envisioned profit reduces with the greatest magnitude when becoming more risk-averse. In all cases, the agent faces the tradeoff between a higher expected profit and risk aversion. When comparing the CVaR expected profit of SO models 1 and 2, SO model 2 shows a lower CVaR expected profit, for all risk attitudes. In other words, the 5% worst-case realizations in SO model 2 result in a lower expected profit compared to the benchmark model.

Besides investigating the pre-clearance performance (expected profit and CVaR), this research assesses the post-clearance performance of the models in the LEM day-ahead market in terms of actual costs/revenue, % of bids cleared, and % of bid quantity cleared. The post-clearance performance metrics require the additional step of checking whether the price-quantity points submitted to the market operator are cleared in the LEM day-ahead market. In terms of % clearance (% of bids cleared and % of bid quantity cleared), SO model 2 gives the best results, for all risk-attitudes. Comparing SO models 1 and 2, the % clearance performance of SO model 1 remains constant around 41% (48%) for four (ten) scenarios, while the % clearance performance of SO model 2 remains constant around 71% for four scenarios, and increases in the range of 72-84% for ten scenarios. It is observed that for ten scenarios, the % clearance performance of SO model 2 shows an increasing pattern when becoming more risk-averse. This increasing pattern is not significantly observed for SO model 1 (four and ten scenarios) and SO model 2 with four scenarios.

Considering the % clearance performance of the RO model, an increasing % clearing pattern is observed when becoming more risk-averse. Comparing the RO model with SO model 1, the RO model outperforms SO model 1 in terms of % clearance, except for a risk-neutral attitude. Overall, the magnitude of % clearance of SO model 2 outperforms the other two models, for all risk-attitudes of the agent. To strengthen the results, a larger sample size would improve the credibility and reliability of the % clearance patterns observed. The performance of SO model 2 is further strengthened by investigating the actual costs of the charging bids and the actual revenue of the discharging bids of the bidding models. Correlated with the high % clearance of SO model 2, the actual costs and revenue of SO model 2 have greater magnitude compared to the other two models, for all risk attitudes. In other words, the gap between the actual costs and revenue and the expected costs and revenue is the smallest for SO model 2, indicating its effectiveness in the local day-ahead market.

The results of the stochastic bidding models indicate that having a good set of price scenarios contributes to good post-clearance performance of the bidding models, especially for SO model 2. In this case, when the actual LEM price realization lies within the bandwidth of the scenario prices, and the peaks and troughs of the price scenarios align, the best clearance performance is obtained. When limited historical price data is available, robust optimization can be used since this only requires the specification of an uncertainty set, without explicitly modeling the probability distribution of the uncertainty.

13 Appendix

13.1 Appendix A: Proposed market clearing mechanism

This section provides an elaboration of the market clearing mechanism proposed by the market parties involved, to incentivize the LEM, as visualized in Figure 25. The corresponding Matlab code is located on Github [104].

- After all bids are submitted to the LEM, a merit order of both demand and supply bids is established. These bids exclude the extra transport fee.
  - Local supply bids with a higher price than p_{wsm} are outside of the market. These local supplier bids would not be cleared in both the LEM and WSM, since no consumer is willing to pay such a high price. The organization of these bids in the merit order can be seen in Figure 23.

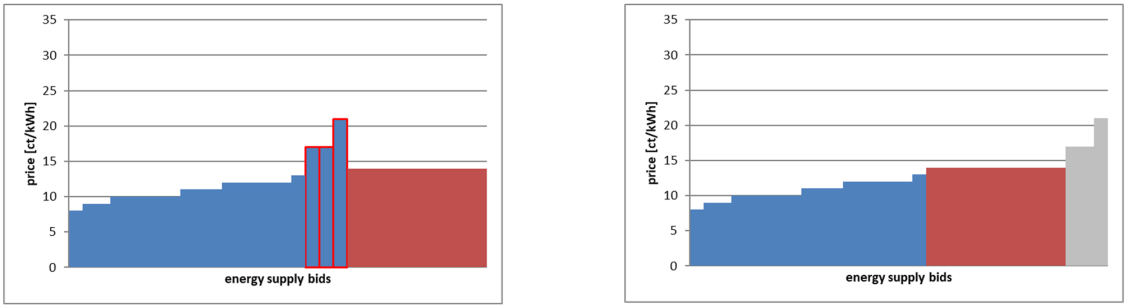

(a) *Local energy supply bids with some local bids (blue) at a higher price than WSM (spot) price (red).*

(b) *Local energy supply bids higher than WSM price (red) are considered out of the merit order (grey).*

Figure 23: *Local Energy supply bid merit order*

  - Local demand bids with the transport fee on top that are lower than p_{wsm} are outside of the market. Any supplier will sell energy to the wholesale trader in this case, and these local demand bids will not be cleared in both the LEM and the WSM. These local demand bids are visualized in grey in Figure 24.

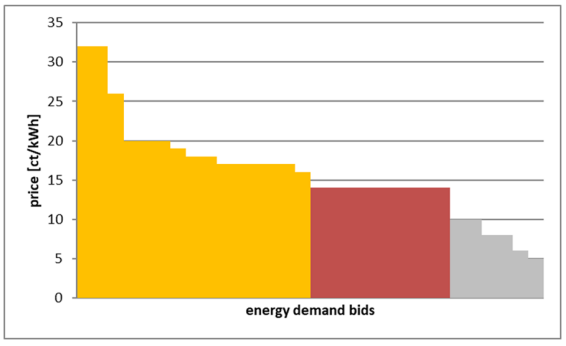

Figure 24: *Merit order of local demand bids (yellow) and wholesale trader bids at WSM price (red), and the local demand bids outside of the merit order (grey).*

- The provisional local market price is determined which is the market price where local demand and supply meet.

- There are two scenarios, namely when the local market is long or short. There is a different market clearing procedure for both scenarios, these procedures are described in the following two sections.

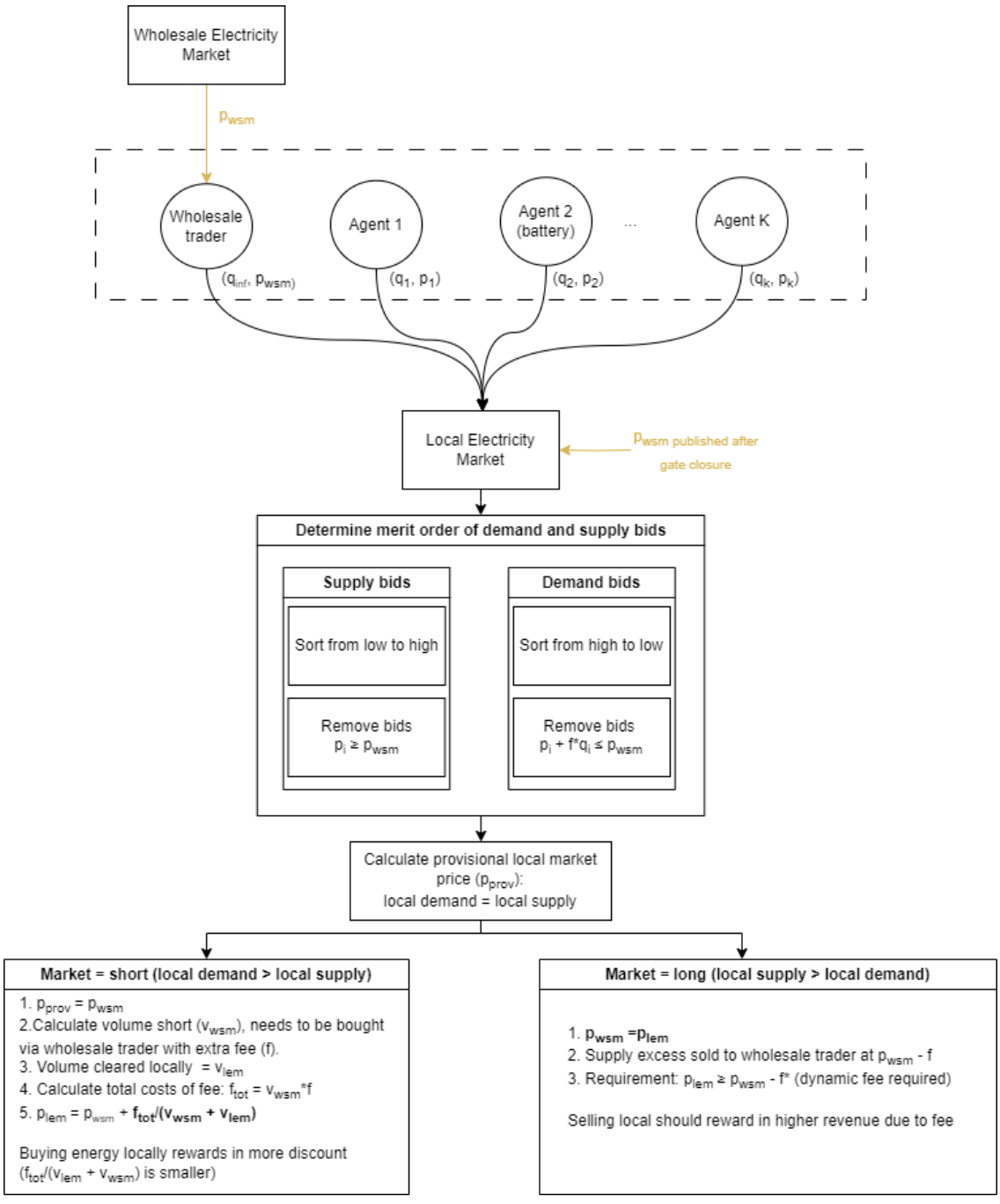

Figure 25: *Local Electricity Market Clearing Mechanism*

13.1.1 Short local market (local demand > local supply)

1. As can be seen in Figure 26, the provisional local market price is equal to the WSM price:

$$p_{prov} = p_{wsm} \tag{13.1}$$

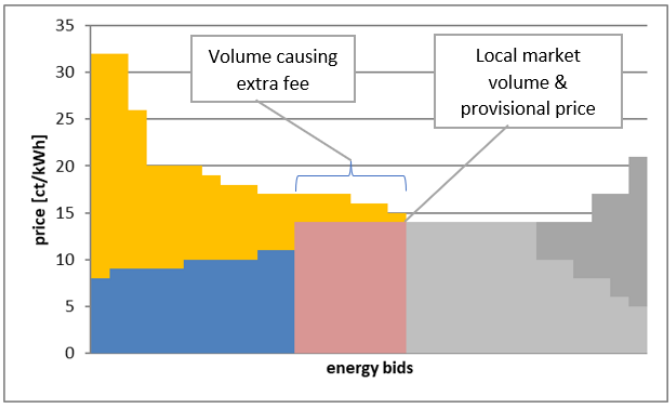

Figure 26: *Short local market, with the wholesale volume that is subject to extra transport fee*

2. As indicated in Figure 26, the volume of wholesale energy to fulfill the local demand is determined (v_{wsm}). This volume needs to be bought via the wholesale trader with the additional transport fee (f). The rest of the local volume can be fulfilled locally (v_{lem}). The local market volume is equal to $v = v_{wsm} + v_{lem}$. When the market is short, the consumers have to pay an additional fee on top of the WSM price. This fee is socialized over all local demand participants.

3. The total fee for the wholesale volume is calculated. Here, f_{tot} is in [cents], v_{wsm} is in [kWh], f is in [cents/kWh].

$$f_{tot} = v_{wsm} \cdot f \tag{13.2}$$

4. The cleared local market price (p_{lem}) is equal to the provisional local market price plus the total wholesale fee divided by the whole local volume. This is the final market price that will be paid by the local consumers and is received by the local suppliers.

$$p_{lem} = p_{prov} + \frac{f_{tot}}{v_{wsm} + v_{lem}} \tag{13.3}$$

$$= p_{wsm} + \frac{v_{wsm} \cdot f}{v_{wsm} + v_{lem}} \tag{13.4}$$

$$= p_{wsm} + \frac{f_{tot}}{v} \tag{13.5}$$

Hence, the cleared local market price (p_{lem}) for the consumers is equal to or larger than the WSM price (p_{wsm}), depending on how much energy needs to be bought via the wholesale trader. The term $\frac{f_{tot}}{v_{wsm}+v_{lem}}$ becomes smaller when less energy is bought via the wholesale trader, resulting in less additional costs for the local demand participants. When all energy is bought via the wholesale trader, this additional term becomes large, making the cleared local market price relatively high. Hence, the more energy is traded locally, the more 'discount' the local demand participants get. Note here that f_{tot} is divided over all local demand participants, meaning that the transport fee is socialized over all local demand participants. This can be seen in the dark green box in Figure 27b. Local suppliers also receive p_{lem}, as they receive some additional revenue from clearing locally.

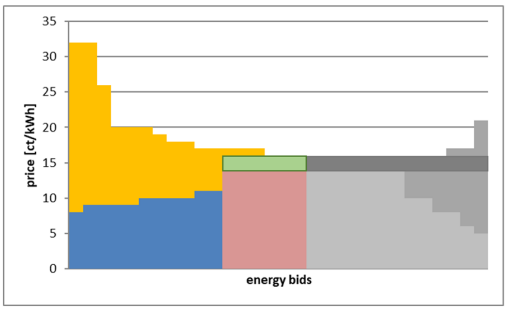

(a) Total transport fee is calculated (light green)

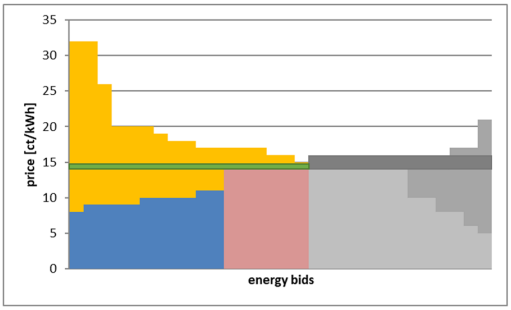

(b) Transport fee is divided over all local demand participants (dark green)

Figure 27: *Transport fee representation in a short market*

13.1.2 Long local market (local supply > local demand)

1. In this scenario, the provisional local market price is lower than or equal to the WSM price (see Figure 28) and is equal to the cleared local market price. In this case, all consumers are fulfilled in the local market and pay the cleared local market price. Some supply shall be cleared on the WSM, wherefore the suppliers corresponding to the local supply bids that are cleared via the wholesale trader have to pay the transport fee to the grid operator. This is different compared to the short market, where the transport fee is divided over all local demand participants instead.

$$p_{prov} = p_{lem} \tag{13.6}$$

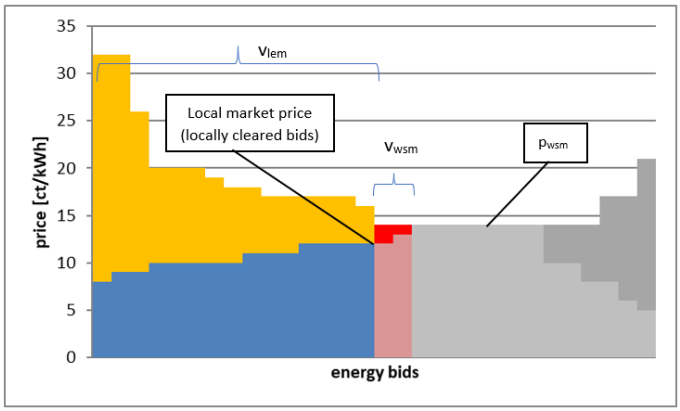

Figure 28: *Long local market, with the local supply bids that are cleared via the wholesale trader*

2. The supply bids that are not cleared locally are sold to the wholesale trader (dark red in Figure 28). This volume is equal to v_{wsm}. In this case, that particular supplier needs to pay the transport fee to the grid operator.

    - As can be seen in Figure 29, the price the supplier that is cleared via the wholesale trader receives [ct/kWh], is equal to the WSM price [ct/kWh] minus the transport fee f [ct/kWh] of the bidding agent:

$$p_{wsm} - f \tag{13.7}$$

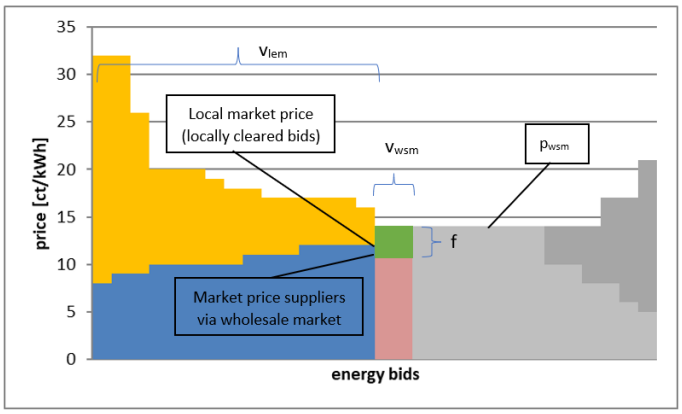

Figure 29: *Long local market, with the transport fee indicated in green.*

The revenue of the supplier i [ct] that is cleared via the wholesale trader is equal to:

$$revenue_i = (p_{wsm} - f) \cdot q_i \tag{13.8}$$

- The revenue of the supplier i that is cleared locally is equal to the local market clearing price (p_{lem}) multiplied with the quantity of the supply bid.

$$revenue_i = p_{lem} \cdot q_i \tag{13.9}$$

3. Note that the transport fee should be dynamic to make selling to the local market more beneficial for a local supplier.

   The following relation should hold in a long local market: the revenue of supplying in LEM is greater than or equal to supplying energy in WSM. Otherwise, the situation arises where bidding supply below the WSM price is not beneficial, and clearing via the wholesale trader is more beneficial than remaining local. In a long market, supply agents should respond competitively with other supply agents to be cleared locally. This drives the market price down. However, the transport fee should remain a proper incentive for the supply agents. Hence, the transport fee should be dynamic. The following equation should hold, where p_{lem} is in [ct/kWh], p_{wsm} is in [ct/kWh], and f is in [ct/kWh]. This way, the p_{lem} lies within the range of the transport fee. Hence, clearing locally is more beneficial compared to obtaining a lower price when selling energy via the wholesale trader (namely p_{wsm} - f). The upper bound of the equation below is due to the fact that the market is long and there is excess local supply. Hence, the local market price is smaller or equal to the wholesale market price.

$$p_{wsm} - f \leq p_{lem} \leq p_{wsm} \tag{13.10}$$

13.2 Appendix B.1: Example 1 scenarios

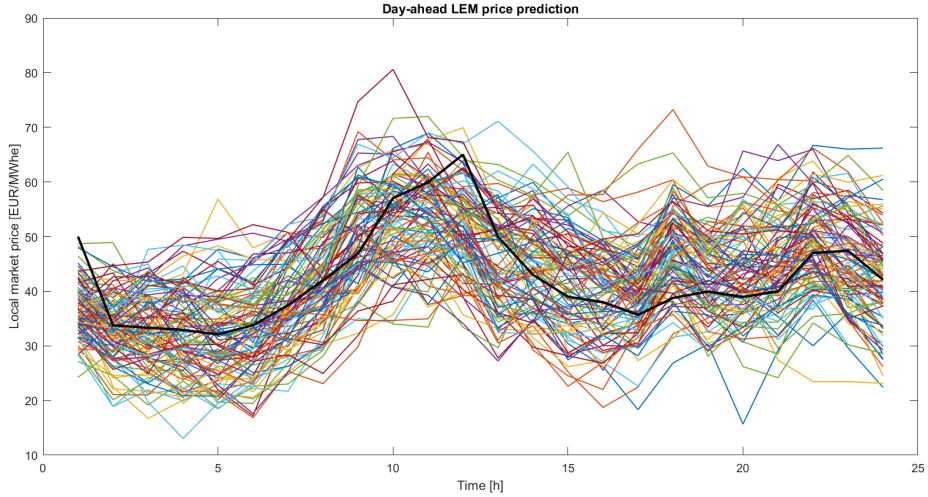

Figure 30: *Example 1 day-ahead price scenarios 1st of May 2015. Black: actual price 1st of May 2015. Colors: 100 scenario realizations*

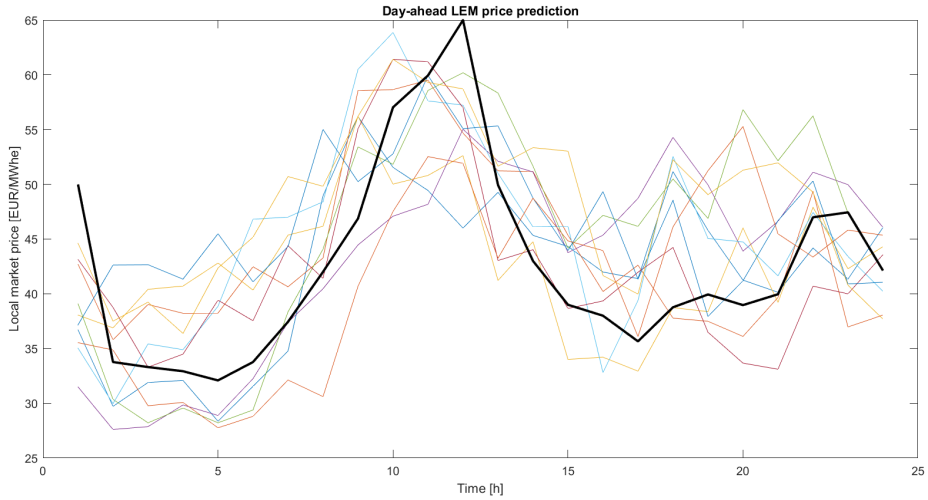

Figure 31: *Example 1 day-ahead price scenarios 1st of May 2015. Black: actual price 1st of May 2015. Colors: 10 scenario realizations*

13.3 Appendix B.2: Example 2 scenarios

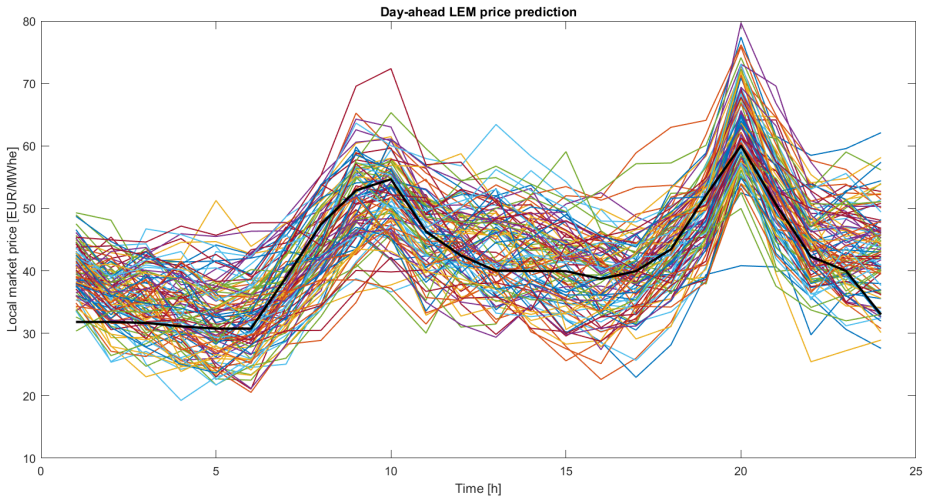

Figure 32: *Example 2 day-ahead price scenarios 18th of March 2015. Black: actual price 18th of March 2015. Colors: 100 scenario realizations*

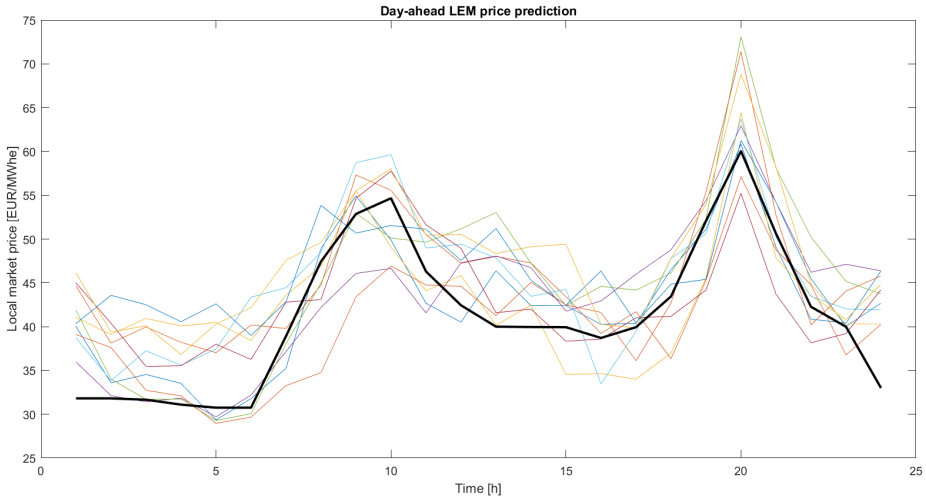

Figure 33: *Example 2 day-ahead price scenarios 18th of March 2015. Black: actual price 18th of March 2015. Colors: 10 scenario realizations*

13.4 Appendix B.3: Example 3 scenarios

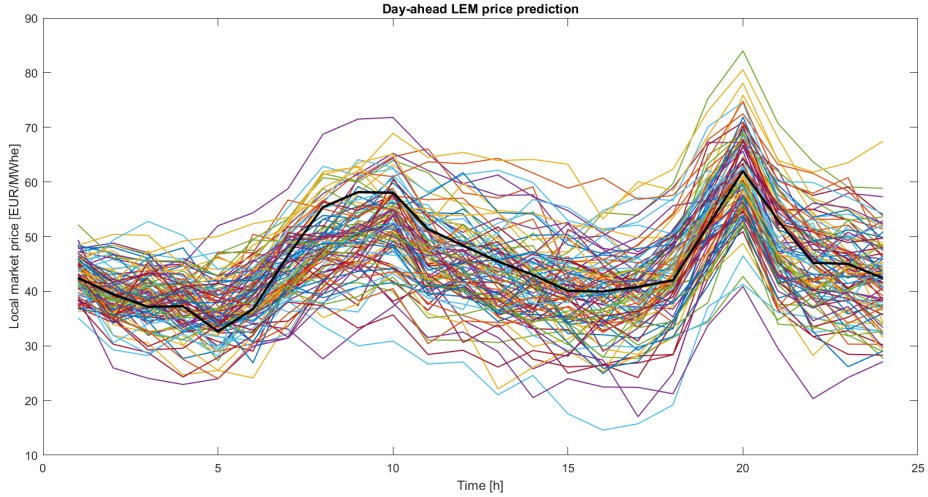

Figure 34: *Example 3 day-ahead price scenarios 12th of March 2015. Black: actual price 12th of March 2015. Colors: 100 scenario realizations*

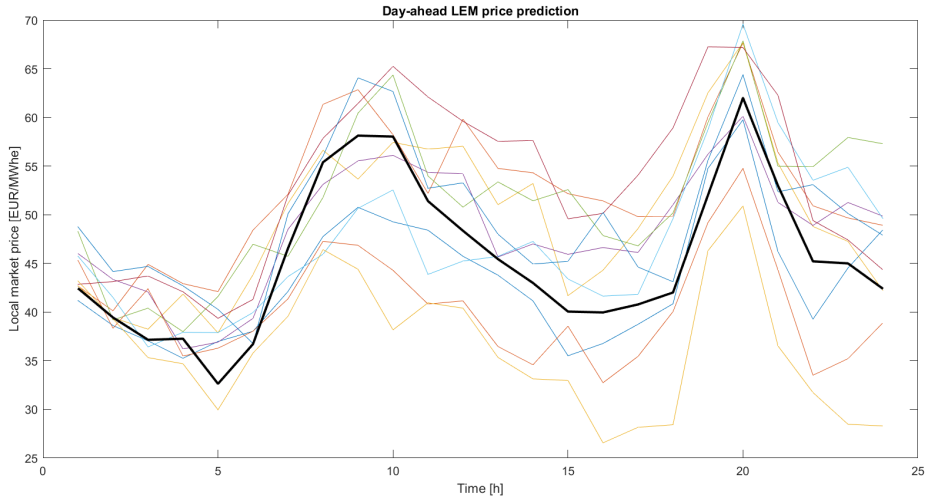

Figure 35: *Example 2 day-ahead price scenarios 12th of March 2015. Black: actual price 12th of March 2015. Colors: 10 scenario realizations*

13.5 Appendix C: Example 3 ACF plot

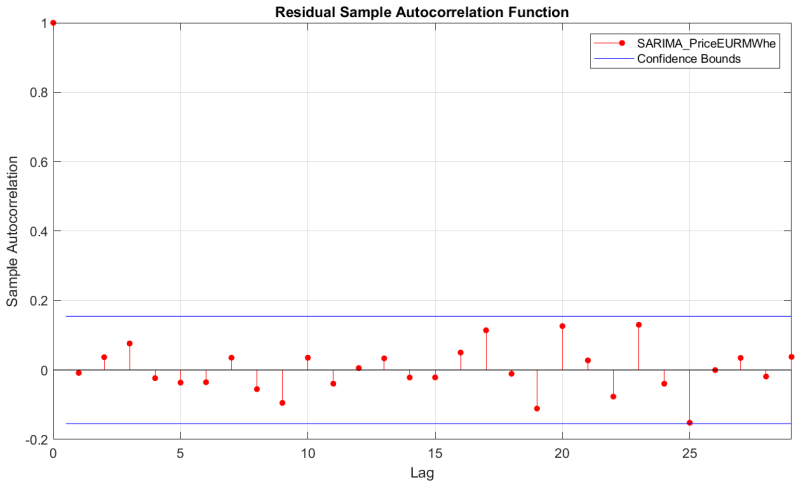

Figure 36: *Autocorrelation Function plot of Example 3*

13.6 Appendix D.1: Pre- and post-clearance performance Examples 1, 2, 3, case study 1

Table 16: *Pre-clearance performance examples 1 - 3, case study 1, 4 scenarios*

	β	Exp. profit [€]	Exp. costs [€]	Exp. revenue [€]	CVaR [€]
Example 1					
	0.0001	30320	109795	140114	28467
	0.5	30057	118827	148884	29987
	0.999	30015	115816	145831	30015
Example 2					
	0.0001	36511	87866	124377	33036
	0.5	36142	88235	124377	33558
	0.999	34725	72072	106797	33846
Example 3					
	0.0001	36553	53380	89934	31121
	0.5	35269	64969	100238	34354
	0.999	34803	83393	118196	34803

Table 17: *Post-clearance performance examples 1 - 3, case study 1, 4 scenarios*

	β	Actual costs [€]	Actual revenue [€]	Cleared bids [%]	Cleared quantity [%]
Example 1					
	0.0001	49523	49246	38.46 %	37.93 %
	0.5	49230	49246	37.50 %	36.02 %
	0.999	47031	49246	37.50 %	35.88 %
Example 2					
	0.0001	63567	23792	45.45 %	45.92 %
	0.5	64121	23792	45.45 %	45.92 %
	0.999	49513	24574	54.55 %	45.00 %
Example 3					
	0.0001	0	71035	42.86 %	41.94 %
	0.5	7264	71035	40.00 %	42.87 %
	0.999	19341	71035	41.67 %	40.76 %

Table 18: *Pre-clearance performance examples 1 - 3, case study 1, 10 scenarios*

	β	Exp. profit [€]	Exp. costs [€]	Exp. revenue [€]	CVaR [€]
Example 1					
	0.0001	30072	72832	102904	25200
	0.5	29614	77526	107141	27070
	0.999	28886	63322	92209	27410
Example 2					
	0.0001	36795	73019	109813	29313
	0.5	35623	83860	119483	32089
	0.999	35121	85033	120154	32275
Example 3					
	0.0001	35126	53485	88612	31885
	0.5	348896	50936	85833	33581
	0.999	34793	52752	87544	33587

Table 19: *Post-clearance performance examples 1 - 3, case study 1, 10 scenarios*

	β	Actual costs [€]	Actual revenue [€]	Cleared bids [%]	Cleared quantity [%]
Example 1					
	0.0001	66992	49246	66.67%	66.25 %
	0.5	71583	48819	64.29%	65.22 %
	0.999	55905	47626	61.54 %	66.39 %
Example 2					
	0.0001	52668	23792	44.44 %	45.00 %
	0.5	63080	24597	41.67 %	45.60 %
	0.999	70289	24597	53.85 %	49.33 %
Example 3					
	0.0001	14684	540059	42.86 %	43.55 %
	0.5	14684	69268	50.00 %	56.64 %
	0.999	14684	71204	41.67 %	56.47 %

13.7 Appendix D.2: Pre- and post-clearance performance simulation 1 - 10, case study 1, 4 scenarios

Table 20: *Average pre-clearance performance simulations 1 - 10, case study 1, 4 scenarios*

β	Exp. profit [€]	Exp. costs [€]	Exp. revenue [€]	CVaR [€]
0.0001	31953	93705	125658	27873
0.5	31458	95103	126561	29808
0.999	30572	94399	124971	30165

Table 21: *Average post-clearance performance simulations 1 - 10, case study 1, 4 scenarios*

β	Actual costs [€]	Actual revenue [€]	Cleared bids [%]	Cleared quantity [%]
0.0001	35182	51102	41.39 %	41.25 %
0.5	39953	50254	41.00 %	42.39 %
0.999	40117	49680	41.63 %	42.36 %

13.8 Appendix D.3: Pre- and post-clearance performance simulation 1 - 10, case study 1, 10 scenarios

Table 22: *Average pre-clearance performance simulations 1 - 10, case study 1, 10 scenarios*

β	Exp. profit [€]	Exp. costs [€]	Exp. revenue [€]	CVaR [€]
0.0001	29506	71878	101384	23037
0.5	28693	75220	103913	26931
0.999	28102	70272	98375	27136

Table 23: *Average post-clearance performance simulations 1 - 10, case study 1, 10 scenarios*

β	Actual costs [€]	Actual revenue [€]	Cleared bids [%]	Cleared quantity [%]
0.0001	29175	48156	46.74 %	46.85 %
0.5	35733	50270	49.00 %	49.59 %
0.999	36149	48970	47.21 %	51.56 %

13.9 Appendix E.1: Pre- and post-clearance performance Examples 1, 2, 3, case study 2

Table 24: *Pre-clearance performance examples 1 - 3, case study 2, 4 scenarios*

	β	Exp. profit [€]	Exp. costs [€]	Exp. revenue [€]	CVaR [€]
Example 1					
	0.0001	31877	84878	116755	25842
	0.5	31233	102099	133332	28765
	0.999	30256	117334	147589	29808
Example 2					
	0.0001	36893	74316	111209	31103
	0.5	36511	87866	124377	33036
	0.999	36142	88235	124377	33558
Example 3					
	0.0001	36553	53380	89934	31121
	0.5	35679	61470	97419	33805
	0.999	35269	64969	100238	34354

Table 25: *Post-clearance performance examples 1 - 3, case study 2, 4 scenarios*

	β	Actual costs [€]	Actual revenue [€]	Cleared bids [%]	Cleared quantity [%]
Example 1					
	0.0001	86072	125256	84.62 %	84.48 %
	0.5	112686	117008	86.67 %	88.74 %
	0.999	120113	127222	89.47 %	91.30 %
Example 2					
	0.0001	63567	65057	63.64 %	64.29 %
	0.5	84402	65057	72.73 %	73.47 %
	0.999	84956	65057	72.73 %	73.47 %
Example 3					
	0.0001	55134	90110	100.00 %	100.00 %
	0.5	61173	98185	100.00 %	100.00 %
	0.999	65719	102211	100.00 %	100.00 %

Table 26: *Pre-clearance performance examples 1 - 3, case study 2, 10 scenarios*

	β	Exp. profit [€]	Exp. costs [€]	Exp. revenue [€]	CVaR [€]
Example 1					
	0.0001	30096	70201	100296	23573
	0.5	29938	75881	105819	26609
	0.999	29614	77526	107141	27070
Example 2					
	0.0001	36795	73019	109813	29313
	0.5	36285	83479	119764	31163
	0.999	35623	83860	119483	32089
Example 3					
	0.0001	35126	53485	88612	31885
	0.5	35071	54161	89232	33257
	0.999	34900	51001	85901	33572

Table 27: *Post-clearance performance examples 1 - 3, case study 2, 10 scenarios*

	β	Actual costs [€]	Actual revenue [€]	Cleared bids [%]	Cleared quantity [%]
Example 1					
	0.0001	66992	103098	100.00 %	100.00 %
	0.5	69948	108036	100.00 %	100.00 %
	0.999	71583	109404	100.00 %	100.00 %
Example 2					
	0.0001	70641	69908	77.78 %	78.75 %
	0.5	80570	79320	75.00 %	81.00 %
	0.999	81053	66272	75.00 %	73.68 %
Example 3					
	0.0001	53010	90110	100.00 %	100.00 %
	0.5	53751	91981	100.00 %	100.00 %
	0.999	50513	88548	100.00 %	100.00 %

13.10 Appendix E.2: Pre- and post-clearance performance simulation 1 - 10, case study 2, 4 scenarios

Table 28: *Average pre-clearance performance simulations 1 - 10, case study 2, 4 scenarios*

β	Exp. profit [€]	Exp. costs [€]	Exp. revenue [€]	CVaR [€]
0.0001	32800	87887	120687	25906
0.5	32217	93161	125405	29223
0.999	31891	94379	126270	29664

Table 29: *Average post-clearance performance simulations 1 - 10, case study 1, 10 scenarios*

β	Actual costs [€]	Actual revenue [€]	Cleared bids [%]	Cleared quantity [%]
0.0001	70784	80443	70.97 %	70.93 %
0.5	72279	84494	70.00 %	71.21 %
0.999	73762	86073	71.07 %	72.60 %

13.11 Appendix E.3: Pre- and post-clearance performance simulation 1 - 10, case study 2, 10 scenarios

Table 30: *Average pre-clearance performance simulations 1 - 10, case study 2, 10 scenarios*

β	Exp. profit [€]	Exp. costs [€]	Exp. revenue [€]	CVaR [€]
0.0001	29945	61415	91360	22298
0.5	29366	71736	101101	26239
0.999	28974	73238	102212	26821

Table 31: *Average post-clearance performance simulations 1 - 10, case study 2, 10 scenarios*

β	Actual costs [€]	Actual revenue [€]	Cleared bids [%]	Cleared quantity [%]
0.0001	54668	72329	72.58 %	75.02 %
0.5	63513	83281	79.00 %	81.42 %
0.999	66017	83858	82.02 %	83.43 %

13.12 Appendix F.1: pre- and post-clearance performance Examples 1, 2, 3, case study 4

Table 32: *Pre-clearance performance Examples 1 - 3, case study 4, 4 scenarios*

	Γ_0	Obj.	Exp. profit [€] (mean price)	Envis. profit [€] (robust price)	Envis. costs [€] (robust price)	Envis. revenue [€] (robust price)	p
Ex. 1							
	0	30320	30320	30320	109795	140114	2222
	3	23673	29845	26451	105080	131530	1975
	4	22225	27779	24405	77026	101431	1111
	6	20855	25854	23015	38747	61762	555
	8	19871	24315	21270	30079	51349	370
Ex. 2							
	0	36511	36511	36511	87866	124377	1721
	3	31349	36511	34169	88941	123110	1721
	4	29707	36016	33084	83224	116309	1529
	6	27726	33845	30881	53401	84283	574
	8	26725	31982	29943	24322	54265	96
Ex. 3							
	0	36553	36553	36553	53380	89934	1685
	3	31500	36553	35103	54012	89115	1684
	4	29972	34183	32530	44912	77442	842
	6	28288	34183	31704	45263	76967	842
	8	27104	32157	29568	34203	63771	421

Table 33: *Post-clearance performance examples 1 - 3, case study 4, 4 scenarios*

	β	Actual costs [€]	Actual revenue [€]	Cleared bids [%]	Cleared quantity [%]
Example 1					
	0	49523	49246	38.46 %	37.93 %
	3	49584	48993	50.00 %	40.00 %
	4	43970	39359	50.00 %	45.12 %
	6	26830	26096	61.11 %	51.09 %
	8	23970	38764	71.43 %	75.68 %
Example 2					
	0	63567	23792	45.45 %	45.92 %
	3	63567	23792	45.45 %	45.92 %
	4	60039	23881	57.14 %	46.74 %
	6	42449	24060	62.50 %	53.23 %
	8	21710	23836	64.71 %	64.06 %
Example 3					
	0	0	71035	42.86 %	41.94 %
	3	0	71035	42.86 %	41.94 %
	4	16333	70487	63.64 %	66.04 %
	6	33728	70487	81.82 %	83.02 %
	8	27815	62193	86.67 %	89.16 %

Table 34: *Pre-clearance performance Examples 1 - 3, case study 4, 10 scenarios*

	Γ_0	Obj.	Exp. profit [€] (mean price)	Envis. profit [€] (robust price)	Envis. costs [€] (robust price)	Envis. revenue [€] (robust price)	p
Ex. 1							
	0	30072	30072	30072	72832	102904	2222
	3	23781	27113	25694	38034	63727	1111
	4	22702	25664	24019	32535	56553	741
	6	21281	24613	22607	25087	47694	555
	8	20384	22935	21838	5277	27115	82
Ex. 2							
	0	36795	36795	36795	73019	109813	1721
	3	31793	36573	34757	69454	104211	1530
	4	30827	35798	33823	54183	88006	860
	6	29269	35387	32711	48102	80813	574
	8	28169	34860	31483	45526	77009	430
Ex. 3							
	0	35126	35126	35126	53485	88612	1685
	3	30256	34935	33531	51994	85526	1497
	4	29399	34265	32612	44741	77353	842
	6	27993	33420	31081	42205	73286	561
	8	26870	33420	30301	42532	72833	561

Table 35: *Post-clearance performance examples 1 - 3, case study 4, 4 scenarios*

	β	Actual costs [€]	Actual revenue [€]	Cleared bids [%]	Cleared quantity [%]
Example 1					
	0	66992	49246	66.67 %	66.25 %
	3	34748	39359	72.73 %	70.65 %
	4	29578	41843	78.57 %	77.50 %
	6	22606	31382	73.33 %	72.31 %
	8	4745	29566	76.47 %	90.00 %
Example 2					
	0	52668	23792	44.44 %	45.00 %
	3	66265	23881	66.67 %	56.79 %
	4	50949	24194	66.67 %	58.06 %
	6	44622	24060	71.43 %	58.93 %
	8	41916	23993	75.00 %	59.43 %
Example 3					
	0	14684	54059	42.86 %	43.55 %
	3	14915	54054	50.00 %	45.00 %
	4	15725	54036	50.00 %	50.94 %
	6	22064	53633	61.54 %	60.00 %
	8	34175	53633	76.92 %	72.00 %

13.13 Appendix F.2: pre- and post-clearance performance of simulations 1 - 10, case study 4, 4 scenarios

Table 36: *Average pre-clearance performance simulations 1 - 10, case study 4, 4 scenarios*

Γ_0	Obj.	Exp. profit [€] (mean price)	Envis. profit [€] (robust price)	Envis. costs [€] (robust price)	Envis. revenue [€] (robust price)	p
0	31953	31953	31953	93705	125658	2261
3	25411	31006	28067	80116	108183	1805
4	23831	29449	26154	67425	93579	1242
6	21890	27696	23965	50274	74239	766
8	20729	25715	22887	26586	49472	294

Table 37: *Average post-clearance performance simulations 1 - 10, case study 4, 4 scenarios*

Γ_0	Actual costs [€]	Actual revenue [€]	Cleared bids [%]	Cleared quantity [%]
0	35182	51102	41.39%	41.25%
3	31670	49806	45.35%	44.53%
4	30913	46518	49.14%	48.67%
6	26370	40754	56.30%	57.57%
8	14993	28316	63.16%	54.66%

13.14 Appendix F.3: pre- and post-clearance performance of simulations 1 - 10, case study 4, 10 scenarios

Table 38: *Average pre-clearance performance simulations 1 - 10, case study 4, 10 scenarios*

Γ_0	Obj.	Exp. profit [€] (mean price)	Envis. profit [€] (robust price)	Envis. costs [€] (robust price)	Envis. revenue [€] (robust price)	p
0	29506	29506	29506	71878	101384	2261
3	23573	27863	25803	54882	80686	1323
4	22447	26878	24462	47295	71758	940
6	20880	25302	22773	33320	56093	530
8	20149	24170	22003	17970	39973	230

Table 39: *Average post-clearance performance simulations 1 - 10, case study 4, 10 scenarios*

Γ_0	Actual costs [€]	Actual revenue [€]	Cleared bids [%]	Cleared quantity [%]
0	29175	48156	46.74 %	46.85 %
3	25949	44692	53.05 %	52.97 %
4	24831	38003	54.52 %	54.17 %
6	19368	32181	58.47 %	55.53 %
8	12540	25341	69.19 %	60.56 %

References

[1] Abdulqader, Q. M. (2023). Forecasting the ratio of the rural population in iraq using box-jenkins methodology. *Science Journal of University of Zakho*, 11(1):134–138.

[2] Abhinav, R. and Pindoriya, N. M. (2021). Risk-constrained optimal bidding strategy for a wind power producer with battery energy storage system using extended mathematical programming. *IET Renewable Power Generation*, 15(3):689–700.

[3] Artzner, P., Delbaen, F., Eber, J.-M., and Heath, D. (1999). Coherent measures of risk. *Mathematical finance*, 9(3):203–228.

[4] As' ad, M. (2012). Finding the best arima model to forecast daily peak electricity demand.

[5] Attarha, A., Amjady, N., Dehghan, S., and Vatani, B. (2018). Adaptive robust self-scheduling for a wind producer with compressed air energy storage. *IEEE Transactions on Sustainable Energy*, 9(4):1659–1671.

[6] Banaś, J. and Utnik-Banaś, K. (2021). Evaluating a seasonal autoregressive moving average model with an exogenous variable for short-term timber price forecasting. *Forest Policy and Economics*, 131:102564.

[7] Barbry, A., Anjos, M. F., Delage, E., and Schell, K. R. (2019). Robust self-scheduling of a price-maker energy storage facility in the new york electricity market. *Energy Economics*, 78:629–646.

[8] Bertsimas, D. and Brown, D. B. (2009). Constructing uncertainty sets for robust linear optimization. *Operations research*, 57(6):1483–1495.

[9] Bertsimas, D., Brown, D. B., and Caramanis, C. (2011). Theory and applications of robust optimization. *SIAM review*, 53(3):464–501.

[10] Bertsimas, D., Litvinov, E., Sun, X. A., Zhao, J., and Zheng, T. (2012). Adaptive robust optimization for the security constrained unit commitment problem. *IEEE transactions on power systems*, 28(1):52–63.

[11] Bertsimas, D. and Sim, M. (2003). Robust discrete optimization and network flows. *Mathematical programming*, 98(1-3):49–71.

[12] Bertsimas, D. and Sim, M. (2004). The price of robustness. *Operations research*, 52(1):35–53.

[13] Bertsimas, D. and Thiele, A. (2006). Robust and data-driven optimization: modern decision making under uncertainty. In *Models, methods, and applications for innovative decision making*, pages 95–122. INFORMS.

[14] Bjarghov, S., Löschenbrand, M., Saif, A. I., Pedrero, R. A., Pfeiffer, C., Khadem, S. K., Rabelhofer, M., Revheim, F., and Farahmand, H. (2021). Developments and challenges in local electricity markets: A comprehensive review. *IEEE Access*, 9:58910–58943.

[15] Bounitsis, G. L., Papageorgiou, L. G., and Charitopoulos, V. M. (2022). Data-driven scenario generation for two-stage stochastic programming. *Chemical Engineering Research and Design*, 187:206–224.

[16] Box, G. E., Jenkins, G. M., Reinsel, G. C., and Ljung, G. M. (2015). *Time series analysis: forecasting and control*. John Wiley & Sons.

[17] Brown, D. B. et al. (2006). *Risk and robust optimization*. PhD thesis, Massachusetts Institute of Technology.

[18] Cao, Y., Huang, L., Li, Y., Jermsittiparsert, K., Ahmadi-Nezamabad, H., and Nojavan, S. (2020). Optimal scheduling of electric vehicles aggregator under market price uncertainty using robust optimization technique. *International Journal of Electrical Power & Energy Systems*, 117:105628.

[19] Casla, I. M., Khodadadi, A., and Söder, L. (2022). Optimal day ahead planning and bidding strategy of battery storage unit participating in nordic frequency markets. *IEEE Access*, 10:76870–76883.

[20] Catalão, J., Pousinho, H., and Contreras, J. (2012). Optimal hydro scheduling and offering strategies considering price uncertainty and risk management. *Energy*, 37(1):237–244.

[21] Chang, D.-F., Zhu, W.-S., and Wu, S.-J. (2022). Predicting the enrollments in humanities and stem programs in higher education using arimax models. *International Journal of Online Pedagogy and Course Design (IJOPCD)*, 12(4):1–15.

[22] Chow, Y., Tamar, A., Mannor, S., and Pavone, M. (2015). Risk-sensitive and robust decision-making: a cvar optimization approach. *Advances in neural information processing systems*, 28.

[23] Conejo, A. J., Carrión, M., Morales, J. M., et al. (2010). *Decision making under uncertainty in electricity markets*, volume 1. Springer.

[24] Conejo, A. J., Contreras, J., Espínola, R., and Plazas, M. A. (2005). Forecasting electricity prices for a day-ahead pool-based electric energy market. *International journal of forecasting*, 21(3):435–462.

[25] Dai, T. and Qiao, W. (2015). Optimal bidding strategy of a strategic wind power producer in the short-term market. *IEEE transactions on sustainable energy*, 6(3):707–719.

[26] de Souza, M. Z., Bhattacharya, K., and Cañizares, C. A. (2021). Operation of a caes facility under price uncertainties using robust optimization. In *2021 IEEE Power & Energy Society General Meeting (PESGM)*, pages 01–05. IEEE.

[27] Diallo, A., Kácsor, E., and Vancsa, M. (2018). Forecasting the spread between hupx and eex dam prices the case of hungarian and german wholesale electricity prices. In *2018 15th International Conference on the European Energy Market (EEM)*, pages 1–5. IEEE.

[28] Dimoulkas, I. and Amelin, M. (2014). Constructing bidding curves for a chp producer in day-ahead electricity markets. In *2014 IEEE international energy conference (ENERGYCON)*, pages 487–494. IEEE.

[29] Duan, X., Hu, Z., and Song, Y. (2020). Bidding strategies in energy and reserve markets for an aggregator of multiple ev fast charging stations with battery storage. *IEEE Transactions on Intelligent Transportation Systems*, 22(1):471–482.

[30] Dupacová, J., Gröwe-Kuska, N., and Römisch, W. (2000). *Scenario reduction in stochastic programming: An approach using probability metrics*. Humboldt-Universität zu Berlin, Mathematisch-Naturwissenschaftliche Fakultät ....

[31] Dupačová, J., Gröwe-Kuska, N., and Römisch, W. (2003). Scenario reduction in stochastic programming. *Mathematical programming*, 95:493–511.

[32] Ewen, M. (2024). European wholesale electricity price data — Ember. https://ember-climate.org/data-catalogue/european-wholesale-electricity-price-data/.

[33] Fábián, C. I. (2008). Handling cvar objectives and constraints in two-stage stochastic models. *European Journal of Operational Research*, 191(3):888–911.

[34] Farahani, M., Samimi, A., and Shateri, H. (2023). Robust bidding strategy of battery energy storage system (bess) in joint active and reactive power of day-ahead and real-time markets. *Journal of Energy Storage*, 59:106520.

[35] Fernandes, B., Street, A., Valladão, D., and Fernandes, C. (2016). An adaptive robust portfolio optimization model with loss constraints based on data-driven polyhedral uncertainty sets. *European Journal of Operational Research*, 255(3):961–970.

[36] Ferruzzi, G., Cervone, G., Delle Monache, L., Graditi, G., and Jacobone, F. (2016). Optimal bidding in a day-ahead energy market for micro grid under uncertainty in renewable energy production. *Energy*, 106:194–202.

[37] Fleten, S.-E. and Pettersen, E. (2005). Constructing bidding curves for a price-taking retailer in the norwegian electricity market. *IEEE Transactions on Power Systems*, 20(2):701–708.

[38] Forcan, J. and Forcan, M. (2022). An overview of local electricity market designs. volume 2022-September. IEEE Computer Society.

[39] Fu, Y., Sun, Q., and Wennersten, R. (2020). Effectiveness of the cvar method in risk management in an integrated energy system. *Energy Reports*, 6:1010–1015.

[40] Gao, X. and Dowling, A. W. (2020). Making money in energy markets: Probabilistic forecasting and stochastic programming paradigms. In *2020 American Control Conference (ACC)*, pages 168–173. IEEE.

[41] Garcia, D. J., Gong, J., and You, F. (2016). Multi-stage adaptive robust optimization over bioconversion product and process networks with uncertain feedstock price and biofuel demand. In *Computer Aided Chemical Engineering*, volume 38, pages 217–222. Elsevier.

[42] Garcia, R. C., Contreras, J., Van Akkeren, M., and Garcia, J. B. C. (2005). A garch forecasting model to predict day-ahead electricity prices. *IEEE transactions on power systems*, 20(2):867–874.

[43] García-Martos, C., Rodríguez, J., and Sánchez, M. J. (2013). Modelling and forecasting fossil fuels, co2 and electricity prices and their volatilities. *Applied Energy*, 101:363–375.

[44] Goedegebure, N. and Hennig, R. (2022). Generating electricity price forecasting scenarios to analyze whether price uncertainty impacts tariff performance. In *2022 17th International Conference on Probabilistic Methods Applied to Power Systems (PMAPS)*, pages 1–6. IEEE.

[45] Gonzalez-Castellanos, A. and Pozo, D. (2021). An optimal scenario reduction method for stochastic power system problems. In *2021 IEEE Madrid PowerTech*, pages 1–6. IEEE.

[46] Growe-Kuska, N., Heitsch, H., and Romisch, W. (2003). Scenario reduction and scenario tree construction for power management problems. In *2003 IEEE Bologna Power Tech Conference Proceedings,*, volume 3, pages 7–pp. IEEE.

[47] Guan, Y. and Wang, J. (2013). Uncertainty sets for robust unit commitment. *IEEE Transactions on Power Systems*, 29(3):1439–1440.

[48] Haben, S., Voss, M., and Holderbaum, W. (2023). *Core Concepts and Methods in Load Forecasting: With Applications in Distribution Networks*. Springer Nature.

[49] Heitsch, H. and Römisch, W. (2003). Scenario reduction algorithms in stochastic programming. *Computational optimization and applications*, 24:187–206.

[50] Herding, R., Ross, E., Jones, W. R., Charitopoulos, V. M., and Papageorgiou, L. G. (2023). Stochastic programming approach for optimal day-ahead market bidding curves of a microgrid. *Applied Energy*, 336:120847.

[51] Jabr, R. A. (2005). Robust self-scheduling under price uncertainty using conditional value-at-risk. *IEEE Transactions on Power Systems*, 20(4):1852–1858.

[52] Karami, M., Shayanfar, H., Aghaei, J., and Ahmadi, A. (2013). Scenario-based security-constrained hydrothermal coordination with volatile wind power generation. *Renewable and Sustainable Energy Reviews*, 28:726–737.

[53] Kaut, M. (2021). Scenario generation by selection from historical data. *Computational Management Science*, 18(3):411–429.

[54] Kazemi, M., Zareipour, H., Amjady, N., Rosehart, W. D., and Ehsan, M. (2017). Operation scheduling of battery storage systems in joint energy and ancillary services markets. *IEEE Transactions on Sustainable Energy*, 8(4):1726–1735.

[55] Khodabakhsh, R. and Sirouspour, S. (2016). Optimal control of energy storage in a microgrid by minimizing conditional value-at-risk. *IEEE Transactions on Sustainable Energy*, 7(3):1264–1273.

[56] Kissi, E., Adjei-Kumi, T., Amoah, P., and Gyimah, J. (2018). Forecasting construction tender price index in ghana using autoregressive integrated moving average with exogenous variables model. *Construction Economics and Building*, 18(1):70–82.

[57] Korolko, N. and Sahinoglu, Z. (2015). Robust optimization of ev charging schedules in unregulated electricity markets. *IEEE Transactions on Smart Grid*, 8(1):149–157.

[58] Korstanje, J. (2021). *Advanced forecasting with Python*. Springer.

[59] Krishnamurthy, D., Uckun, C., Zhou, Z., Thimmapuram, P. R., and Botterud, A. (2017). Energy storage arbitrage under day-ahead and real-time price uncertainty. *IEEE Transactions on Power Systems*, 33(1):84–93.

[60] Lehna, M., Scheller, F., and Herwartz, H. (2022). Forecasting day-ahead electricity prices: A comparison of time series and neural network models taking external regressors into account. *Energy Economics*, 106:105742.

[61] Lezama, F., Soares, J., Faia, R., Vale, Z., Kilkki, O., Repo, S., and Segerstam, J. (2021). Bidding in local electricity markets with cascading wholesale market integration. *International Journal of Electrical Power and Energy Systems*, 131.

[62] Li, C. and Grossmann, I. E. (2021). A review of stochastic programming methods for optimization of process systems under uncertainty. *Frontiers in Chemical Engineering*, 2:34.

[63] Li, J., Zhou, J., and Chen, B. (2020). Review of wind power scenario generation methods for optimal operation of renewable energy systems. *Applied Energy*, 280:115992.

[64] Li, T., Shahidehpour, M., and Li, Z. (2007). Risk-constrained bidding strategy with stochastic unit commitment. *IEEE Transactions on Power Systems*, 22(1):449–458.

[65] Liang, J. and Tang, W. (2020). Scenario reduction for stochastic day-ahead scheduling: A mixed autoencoder based time-series clustering approach. *IEEE Transactions on Smart Grid*, 12(3):2652–2662.

[66] Liu, G., Xu, Y., and Tomsovic, K. (2015). Bidding strategy for microgrid in day-ahead market based on hybrid stochastic/robust optimization. *IEEE Transactions on Smart Grid*, 7(1):227–237.

[67] Lüth, A., Zepter, J. M., Del Granado, P. C., and Egging, R. (2018). Local electricity market designs for peer-to-peer trading: The role of battery flexibility. *Applied energy*, 229:1233–1243.

[68] Ma, X.-Y., Sun, Y.-Z., and Fang, H.-L. (2013). Scenario generation of wind power based on statistical uncertainty and variability. *IEEE Transactions on Sustainable Energy*, 4(4):894–904.

[69] Mavronicolas, M. and Monien, B. (2020). Conditional value-at-risk: structure and complexity of equilibria. *Theoretical Computer Science*, 807:266–283.

[70] Mayer, K. and Trück, S. (2018). Electricity markets around the world. *Journal of Commodity Markets*, 9:77–100.

[71] Mercère, G. (2023). *Data Driven Model Learning for Engineers: With Applications to Univariate Time Series*. Springer Nature.

[72] Mohsenian-Rad, H. (2015). Optimal bidding, scheduling, and deployment of battery systems in california day-ahead energy market. *IEEE Transactions on Power Systems*, 31(1):442–453.

[73] Morales, J. M., Pineda, S., Conejo, A. J., and Carrion, M. (2009). Scenario reduction for futures market trading in electricity markets. *IEEE Transactions on Power Systems*, 24(2):878–888.

[74] Natarajan, K., Pachamanova, D., and Sim, M. (2009). Constructing risk measures from uncertainty sets. *Operations research*, 57(5):1129–1141.

[75] Nogales, F. J., Contreras, J., Conejo, A. J., and Espínola, R. (2002). Forecasting next-day electricity prices by time series models. *IEEE Transactions on power systems*, 17(2):342–348.

[76] Nunez, A. C., Gutierrez, G., and Gil, E. (2018). Strategic generation bidding and scheduling under price uncertainty. *IEEE Latin America Transactions*, 16(5):1445–1453.

[77] Papavasiliou, A., He, Y., and Svoboda, A. (2014). Self-commitment of combined cycle units under electricity price uncertainty. *IEEE Transactions on Power Systems*, 30(4):1690–1701.

[78] Paraschiv, D. M., Bălăşoiu, N., Ben-Amor, S., and Bag, R. C. (2023). Hybridising neurofuzzy model and the seasonal autoregressive model for electricity price forecasting on germany's spot market. *The AMFITEATRU ECONOMIC journal*, 25(63):463–463.

[79] Parvar, S. S. and Nazaripouya, H. (2022). Optimal operation of battery energy storage under uncertainty using data-driven distributionally robust optimization. *Electric Power Systems Research*, 211:108180.

[80] Parvar, S. S., Nazaripouya, H., and Asadinejad, A. (2019). Analysis and modeling of electricity market for energy storage systems. In *2019 IEEE Power & Energy Society Innovative Smart Grid Technologies Conference (ISGT)*, pages 1–5. IEEE.

[81] Peter, Ď. and Silvia, P. (2012). Arima vs. arimax–which approach is better to analyze and forecast macroeconomic time series. In *Proceedings of 30th international conference mathematical methods in economics*, volume 2, pages 136–140.

[82] Petropoulos, F., Apiletti, D., Assimakopoulos, V., Babai, M. Z., Barrow, D. K., Taieb, S. B., Bergmeir, C., Bessa, R. J., Bijak, J., Boylan, J. E., et al. (2022). Forecasting: theory and practice. *International Journal of Forecasting*, 38(3):705–871.

[83] Pflug, G. C. (2000). Some remarks on the value-at-risk and the conditional value-at-risk. *Probabilistic constrained optimization: Methodology and applications*, pages 272–281.

[84] Plazas, M. A., Conejo, A. J., and Prieto, F. J. (2005). Multimarket optimal bidding for a power producer. *IEEE Transactions on Power Systems*, 20(4):2041–2050.

[85] Rios, I., Wets, R. J., and Woodruff, D. L. (2015). Multi-period forecasting and scenario generation with limited data. *Computational Management Science*, 12(2):267–295.

[86] Rockafellar, R. T. and Uryasev, S. (2002). Conditional value-at-risk for general loss distributions. *Journal of banking & finance*, 26(7):1443–1471.

[87] Rockafellar, R. T., Uryasev, S., et al. (2000). Optimization of conditional value-at-risk. *Journal of risk*, 2:21–42.

[88] Roos, E. and den Hertog, D. (2020). Reducing conservatism in robust optimization. *INFORMS Journal on Computing*, 32(4):1109–1127.

[89] Saber, H., Heidarabadi, H., Moeini-Aghtaie, M., Farzin, H., and Karimi, M. R. (2019). Expansion planning studies of independent-locally operated battery energy storage systems (besss): A cvar-based study. *IEEE Transactions on Sustainable Energy*, 11(4):2109–2118.

[90] Sarykalin, S., Serraino, G., and Uryasev, S. (2008). Value-at-risk vs. conditional value-at-risk in risk management and optimization. In *State-of-the-art decision-making tools in the information-intensive age*, pages 270–294. Informs.

[91] Sgarlato, R. and Ziel, F. (2022). The role of weather predictions in electricity price forecasting beyond the day-ahead horizon. *IEEE Transactions on Power Systems*, 38(3):2500–2511.

[92] Shah, D. and Chatterjee, S. (2020). A comprehensive review on day-ahead electricity market and important features of world's major electric power exchanges. *International Transactions on Electrical Energy Systems*, 30(7):e12360.

[93] Shah, I., Bibi, H., Ali, S., Wang, L., and Yue, Z. (2020). Forecasting one-day-ahead electricity prices for italian electricity market using parametric and nonparametric approaches. *IEEE Access*, 8:123104–123113.

[94] Shang, J., Jiang, X., Yin, W., Hou, Y., Yang, Z., and Liu, H. (2019). A robust operation strategy for energy storage considering uncertainty in electricity price. In *2019 IEEE Innovative Smart Grid Technologies-Asia (ISGT Asia)*, pages 3032–3036. IEEE.

[95] Sharma, K. C., Bhakar, R., Tiwari, H., and Chawda, S. (2017). Scenario based uncertainty modeling of electricity market prices. In *2017 6th International Conference on Computer Applications In Electrical Engineering-Recent Advances (CERA)*, pages 164–168. IEEE.

[96] Sharma, K. C., Jain, P., and Bhakar, R. (2013). Wind power scenario generation and reduction in stochastic programming framework. *Electric Power Components and Systems*, 41(3):271–285.

[97] Shikhina, A., Kochengin, A., Chrysostomou, G., and Shikhin, V. (2020). Investigation of autoregressive forecasting models for market electricity price. In *2020 IEEE 20th Mediterranean Electrotechnical Conference (MELECON)*, pages 570–575. IEEE.

[98] Soroudi, A. (2013). Robust optimization based self scheduling of hydro-thermal genco in smart grids. *Energy*, 61:262–271.

[99] Sun, X. A., Conejo, A. J., et al. (2021). *Robust optimization in electric energy systems*. Springer.

[100] Thatte, A. A., Xie, L., Viassolo, D. E., and Singh, S. (2013). Risk measure based robust bidding strategy for arbitrage using a wind farm and energy storage. *IEEE Transactions on Smart Grid*, 4(4):2191–2199.

[101] Tsaousoglou, G., Giraldo, J. S., and Paterakis, N. G. (2022). Market mechanisms for local electricity markets: A review of models, solution concepts and algorithmic techniques. *Renewable and Sustainable Energy Reviews*, 156:111890.

[102] Tziovani, L., Hadjidemetriou, L., and Timotheou, S. (2022). Energy scheduling of wind-storage systems using stochastic and robust optimization. In *2022 IEEE Power & Energy Society General Meeting (PESGM)*, pages 1–5. IEEE.

[103] Uryasev, S. (2000). Conditional value-at-risk: Optimization algorithms and applications. In *proceedings of the IEEE/IAFE/INFORMS 2000 conference on computational intelligence for financial engineering (CIFEr)(Cat. No. 00TH8520)*, pages 49–57. IEEE.

[104] van den Berg, W. (2024). GitHub Repository RP-2023-2024. https://github.com/wendyvdberg00/RP-2023-2024.

[105] Wang, Z., Negash, A., and Kirschen, D. S. (2017). Optimal scheduling of energy storage under forecast uncertainties. *IET Generation, Transmission & Distribution*, 11(17):4220–4226.

[106] Wu, L. and Shahidehpour, M. (2010). A hybrid model for day-ahead price forecasting. *IEEE Transactions on Power Systems*, 25(3):1519–1530.

[107] Xie, M., Sandels, C., Zhu, K., and Nordström, L. (2013). A seasonal arima model with exogenous variables for elspot electricity prices in sweden. In *2013 10th International conference on the European energy market (EEM)*, pages 1–4. IEEE.

[108] Xuan, A., Shen, X., Guo, Q., and Sun, H. (2021). A conditional value-at-risk based planning model for integrated energy system with energy storage and renewables. *Applied Energy*, 294:116971.

[109] Yu, D., Wu, J., Wang, W., and Gu, B. (2022). Optimal performance of hybrid energy system in the presence of electrical and heat storage systems under uncertainties using stochastic p-robust optimization technique. *Sustainable Cities and Society*, 83:103935.

[110] Yurdakul, O. and Billimoria, F. (2023). Risk-averse self-scheduling of storage in decentralized markets. In *2023 IEEE Power & Energy Society General Meeting (PESGM)*, pages 1–5. IEEE.

[111] Zheng, Q. P., Wang, J., and Liu, A. L. (2014). Stochastic optimization for unit commitment—a review. *IEEE Transactions on Power Systems*, 30(4):1913–1924.

[112] Zheng, Y., Wang, Y., and Yang, Q. (2023). Bidding strategy design for electric vehicle aggregators in the day-ahead electricity market considering price volatility: A risk-averse approach. *Energy*, 283:129138.